Earth gradients, geodynamics, earthquakes

Carlo Doglioni

In honor of Piero Marcati

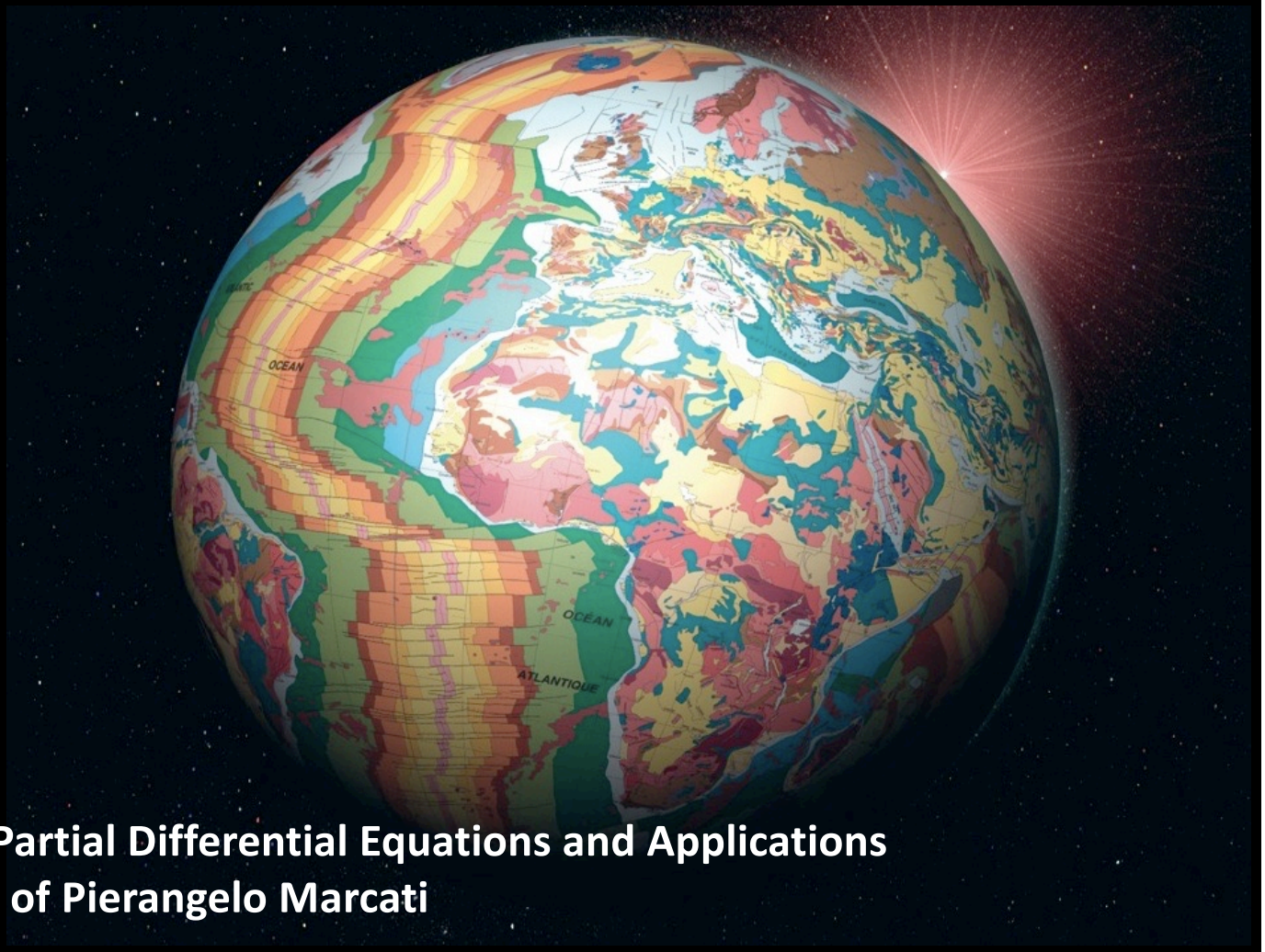

International Conference on Partial Differential Equations and Applications in honor of the 70th birthday of Pierangelo Marcati

L'Aquila, June 19 - 24, 2023

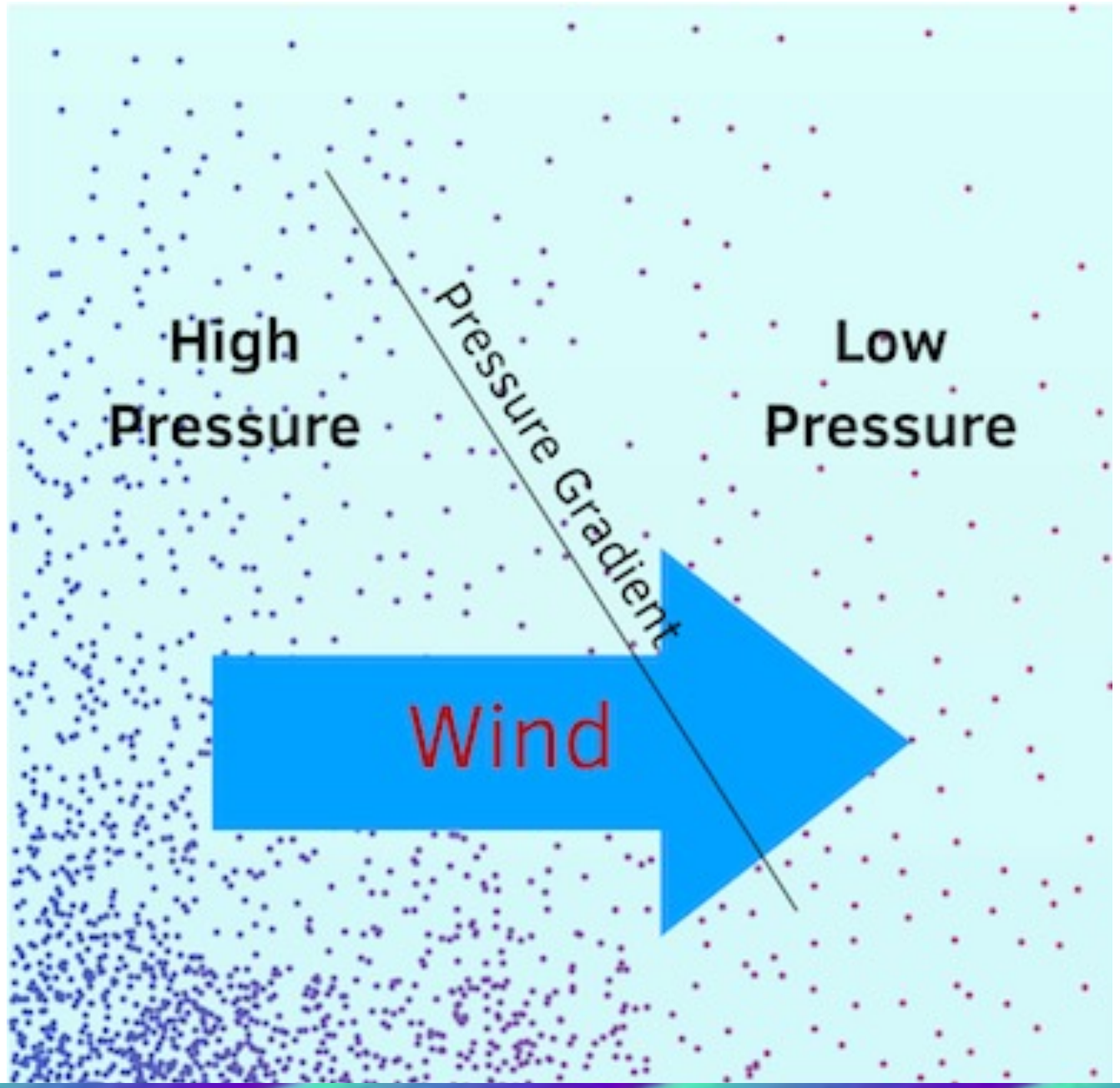

It is the asymmetry that generates the phenomenon

PIERRE CURIE

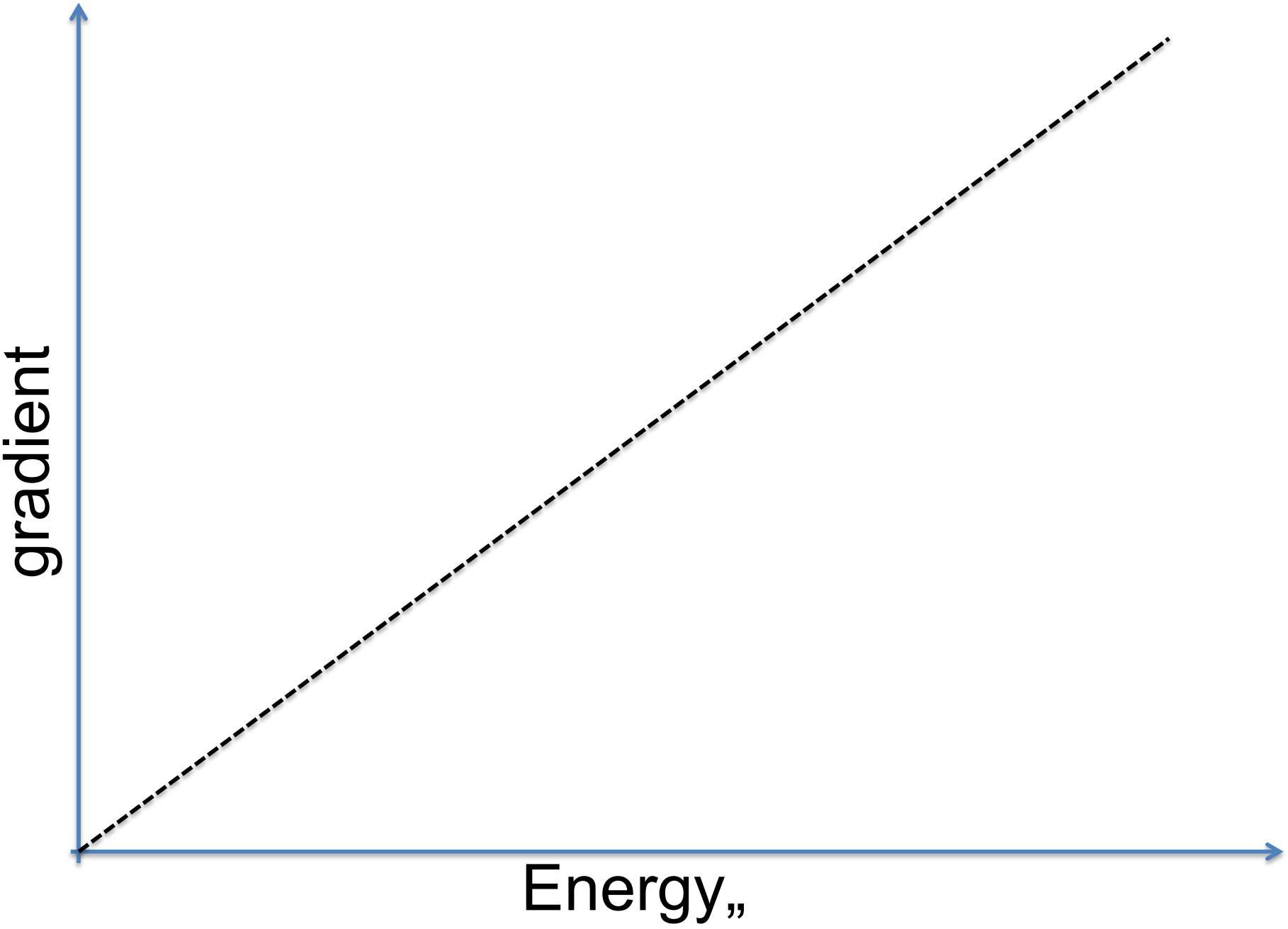
gradient
Energy„

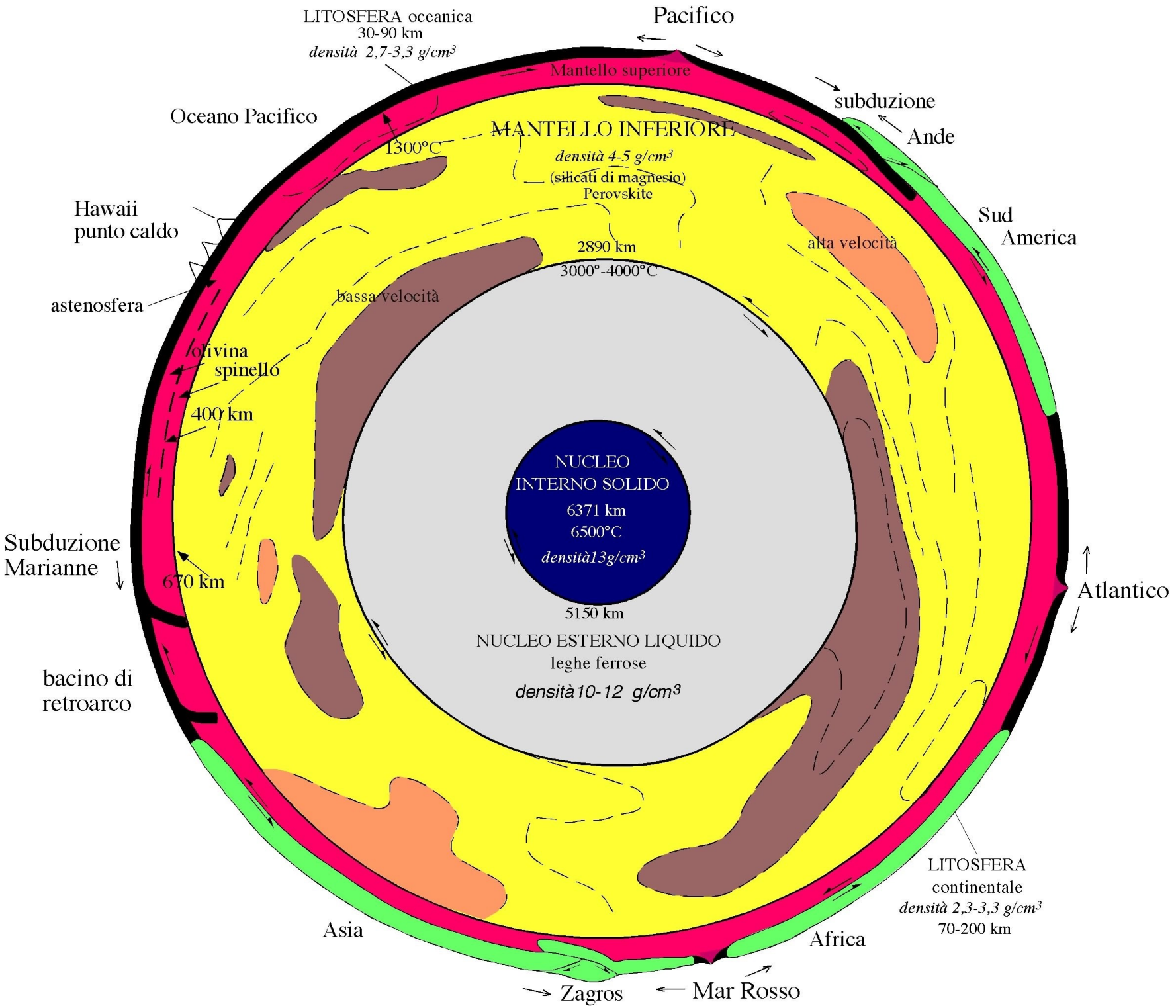
LITOSFERA oceanica
30-90 km
densità 2,7-3,3 g/cm3
Pacifico
Mantello superiore
subduzione
Ande
Oceano Pacifico
MANTELLO INFERIORE
densità 4-5 g/cm3
(silicati di magnesio)
Perovskite
1300°C
Hawaii
punto caldo
Sud
America
alta velocità
2890 km
3000°-4000°C
astenosfera
bassa velocità
olivina
spinello
400 km
NUCLEO
INTERNO SOLIDO
6371 km
6500°C
densità13g/cm3
Subduzione
Marianne
670 km
Atlantico
5150 km
NUCLEO ESTERNO LIQUIDO
leghe ferrose
densità10-12 g/cm3
bacino di
retroarco
LITOSFERA
continentale
densità 2,3-3,3 g/cm3
70-200 km
Asia
Africa
Zagros
Mar Rosso

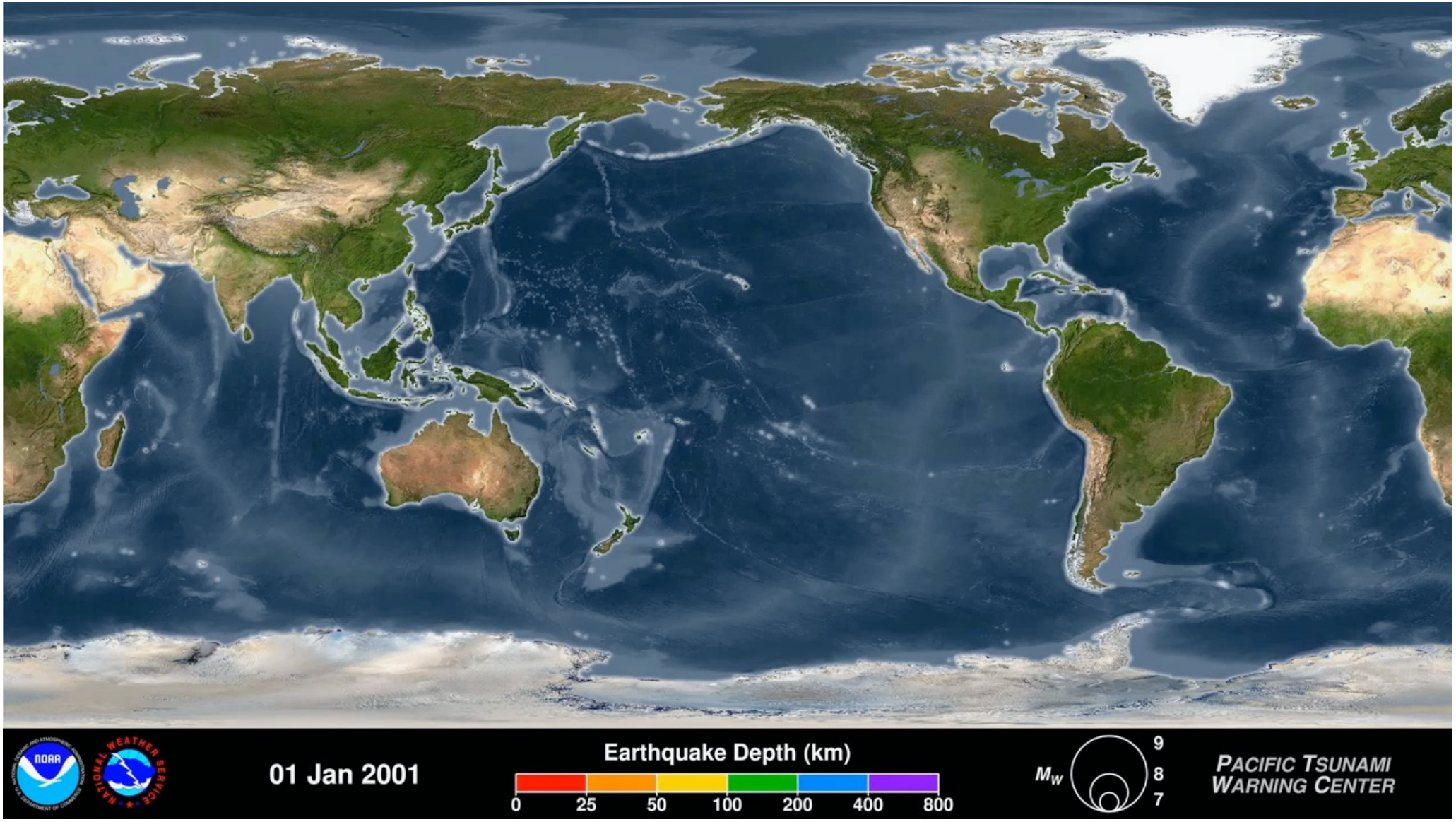
01 Jan 2001
Earthquake Depth (km)
0
25
50
100
200
400
800
M_W
9
8
7
PACIFIC TSUNAMI WARNING CENTER

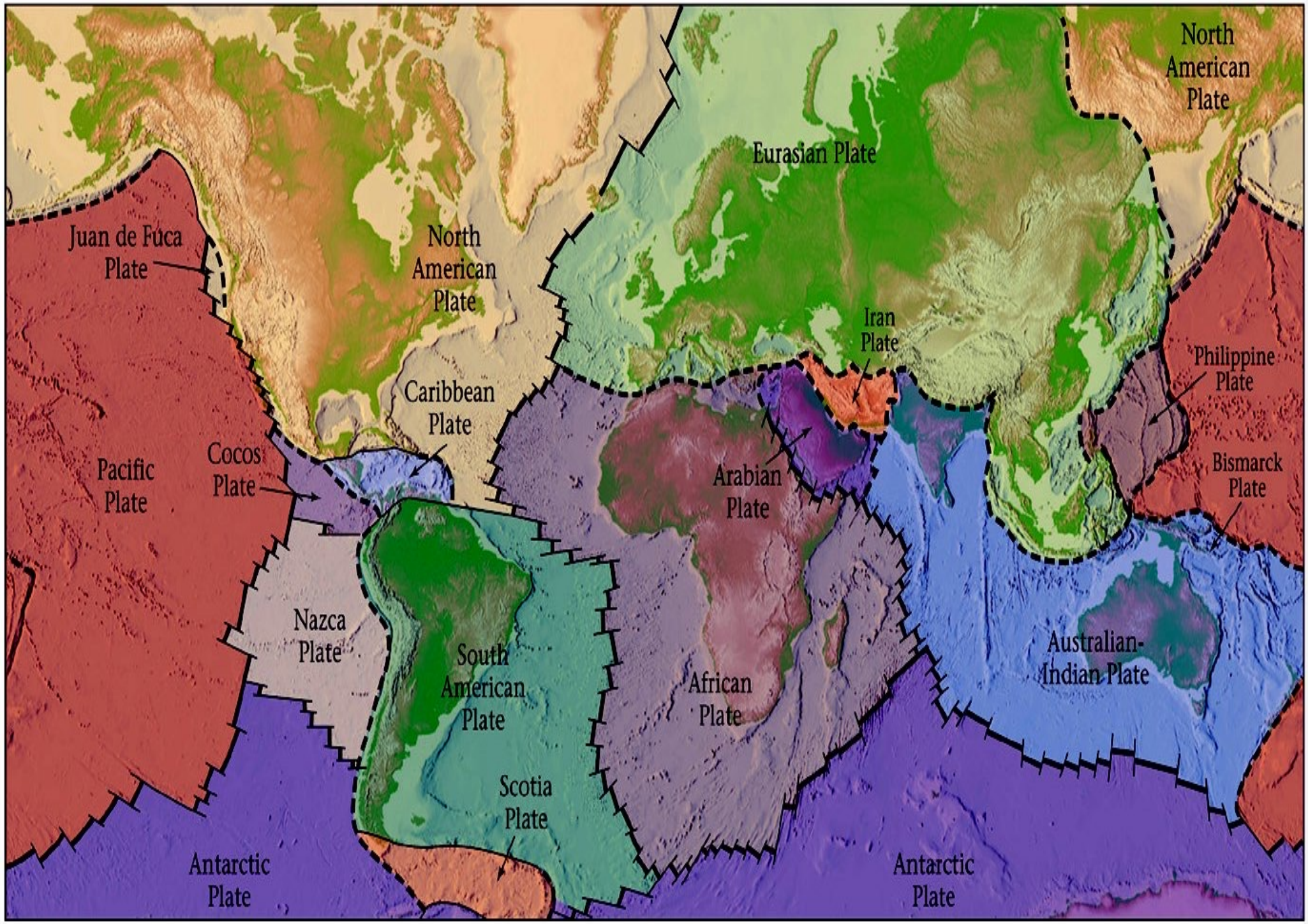
North American Plate
Eurasian Plate
Juan de Fuca Plate
North American Plate
Iran Plate
Philippine Plate
Caribbean Plate
Pacific Plate
Cocos Plate
Arabian Plate
Bismarck Plate
Nazca Plate
South American Plate
African Plate
Australian-Indian Plate
Scotia Plate
Antarctic Plate
Antarctic Plate
Trench or collision zone
Ridge
Transform boundary

RIFTING

Time 1

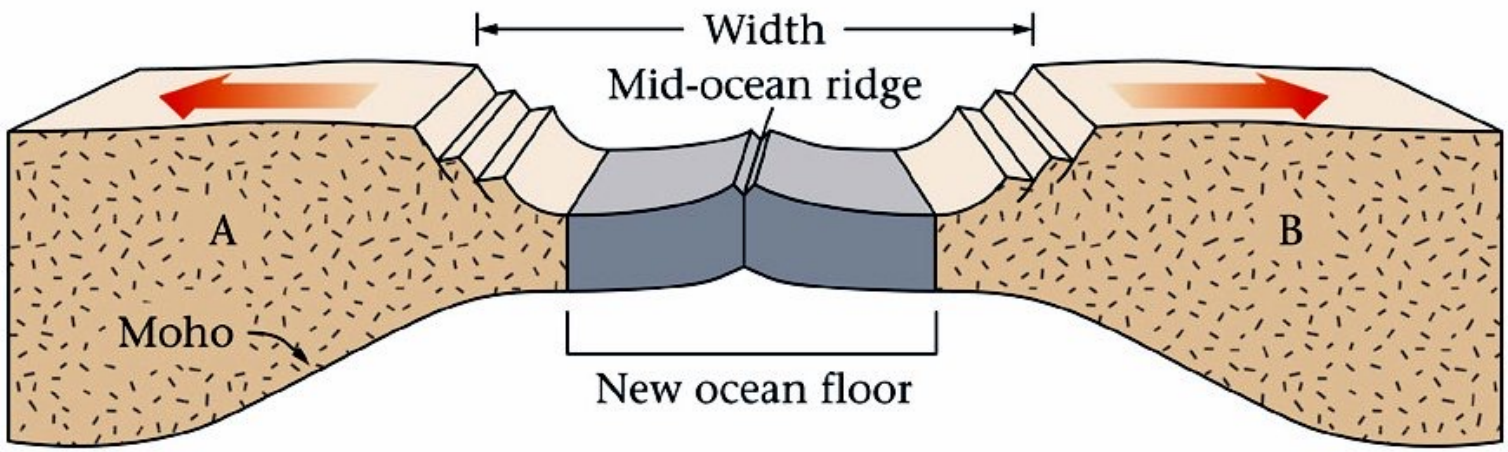

RIFTING

Time 2

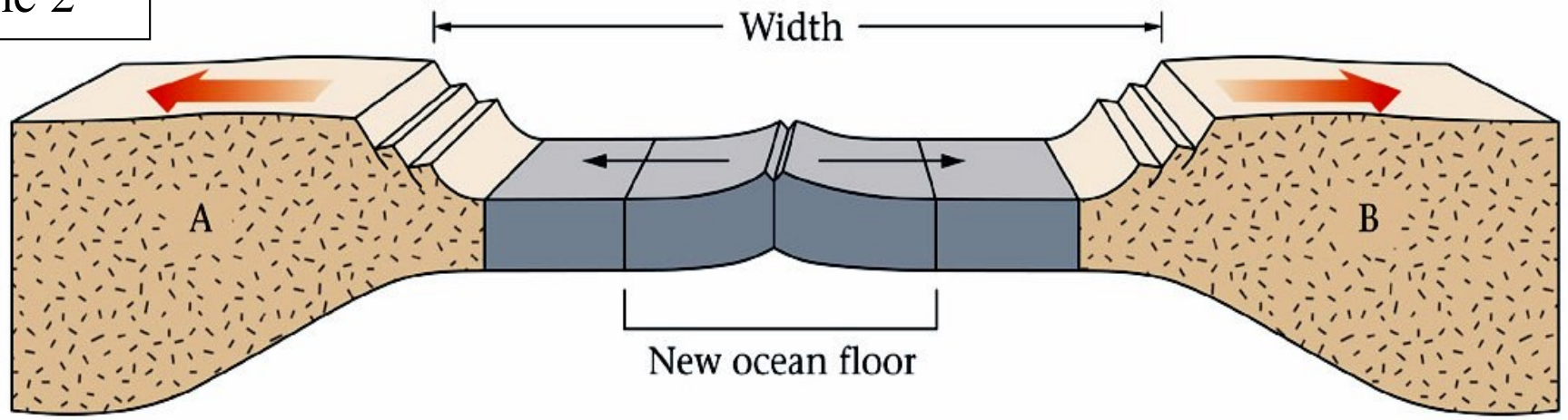

RIFTING

Time 3

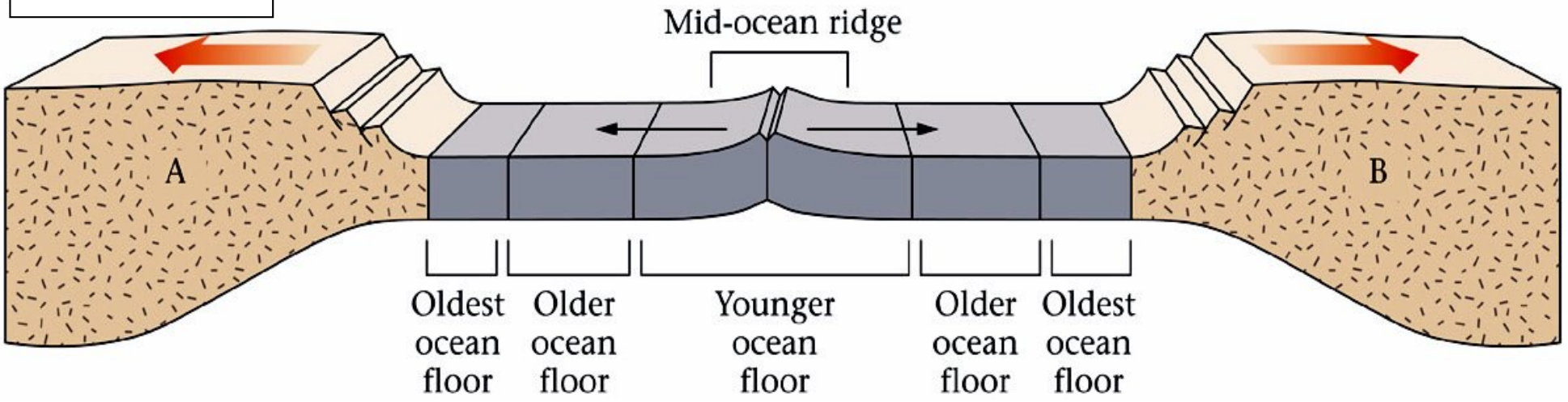

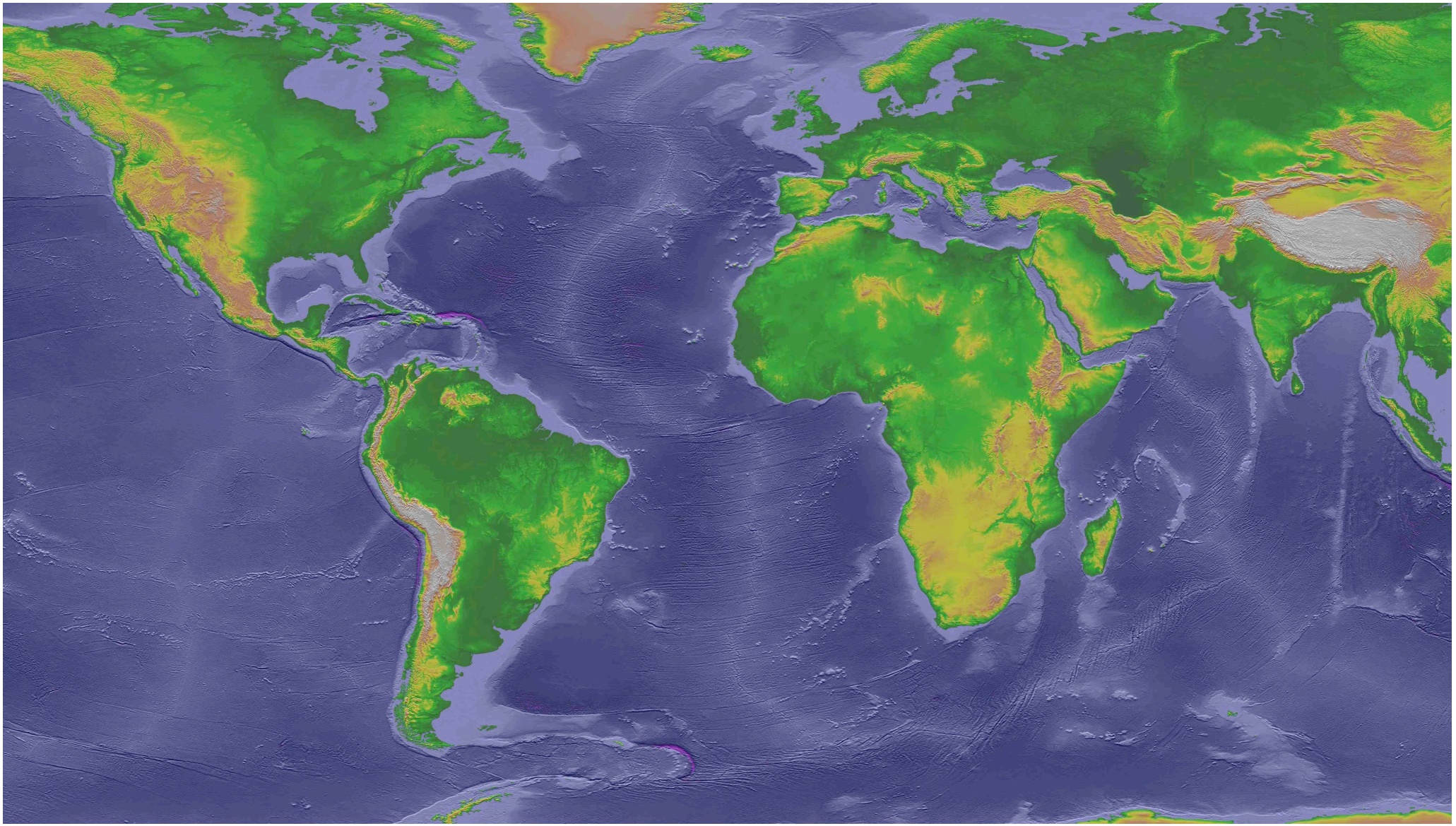

SUBDUCTION

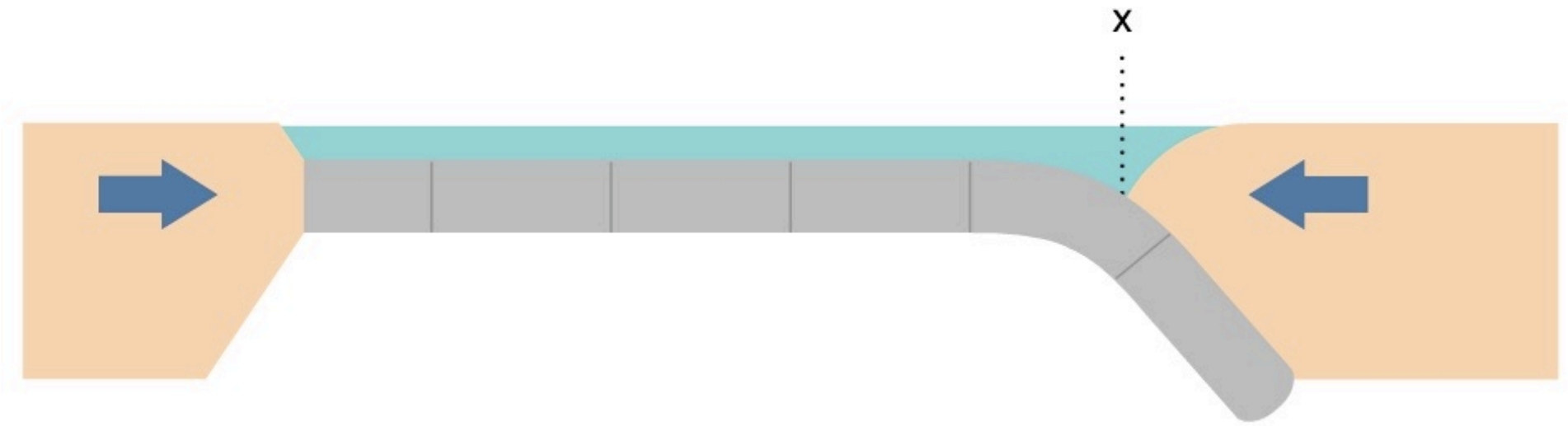

SUBDUCTION

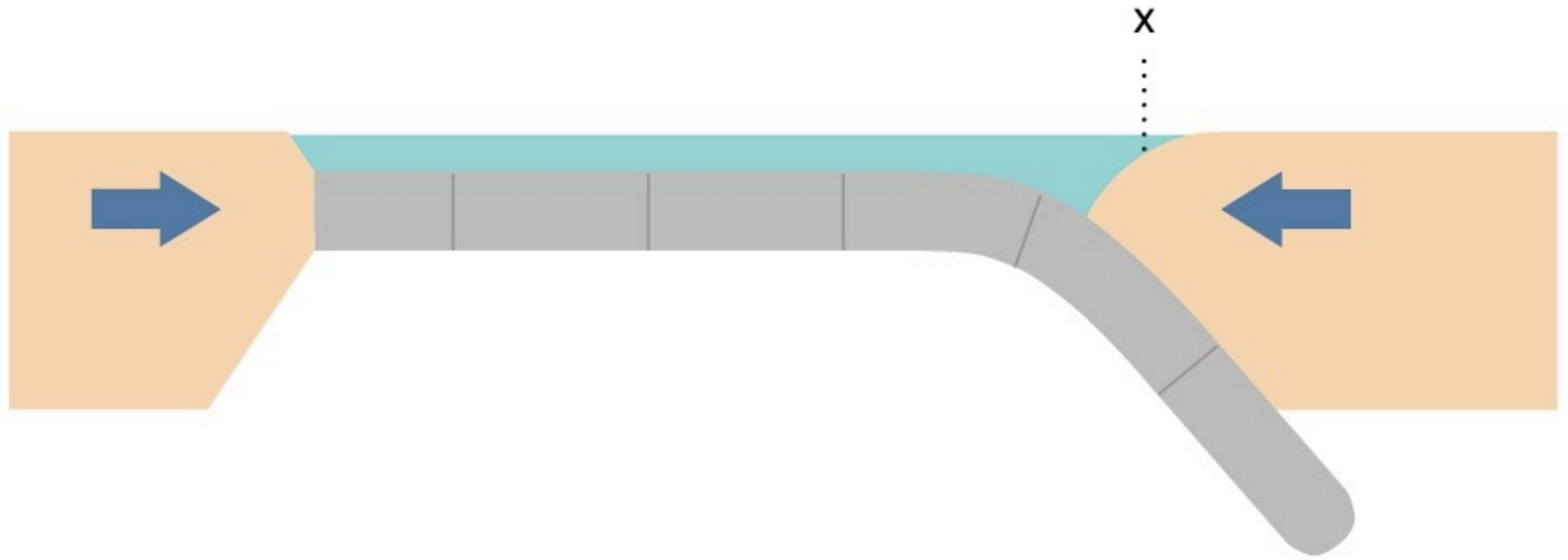

SUBDUCTION

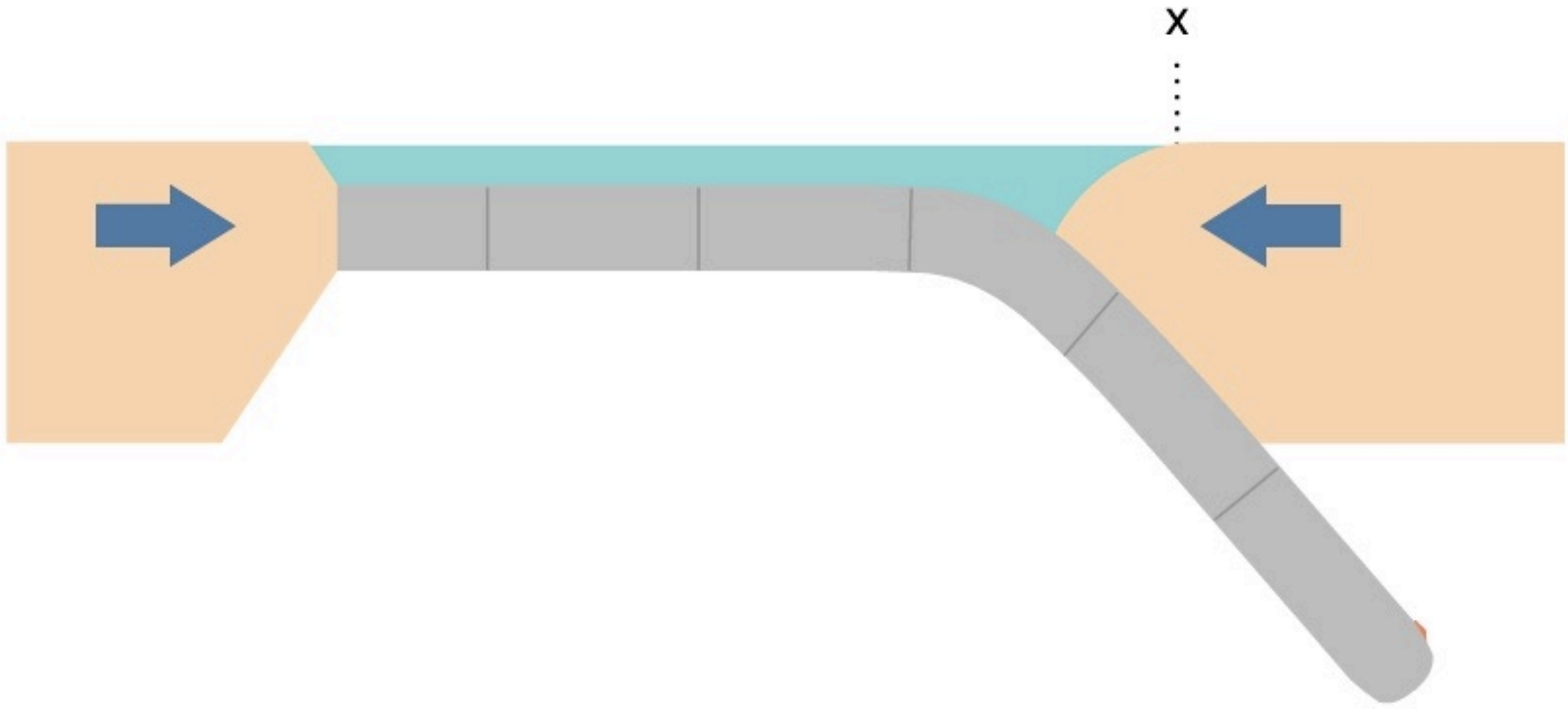

SUBDUCTION

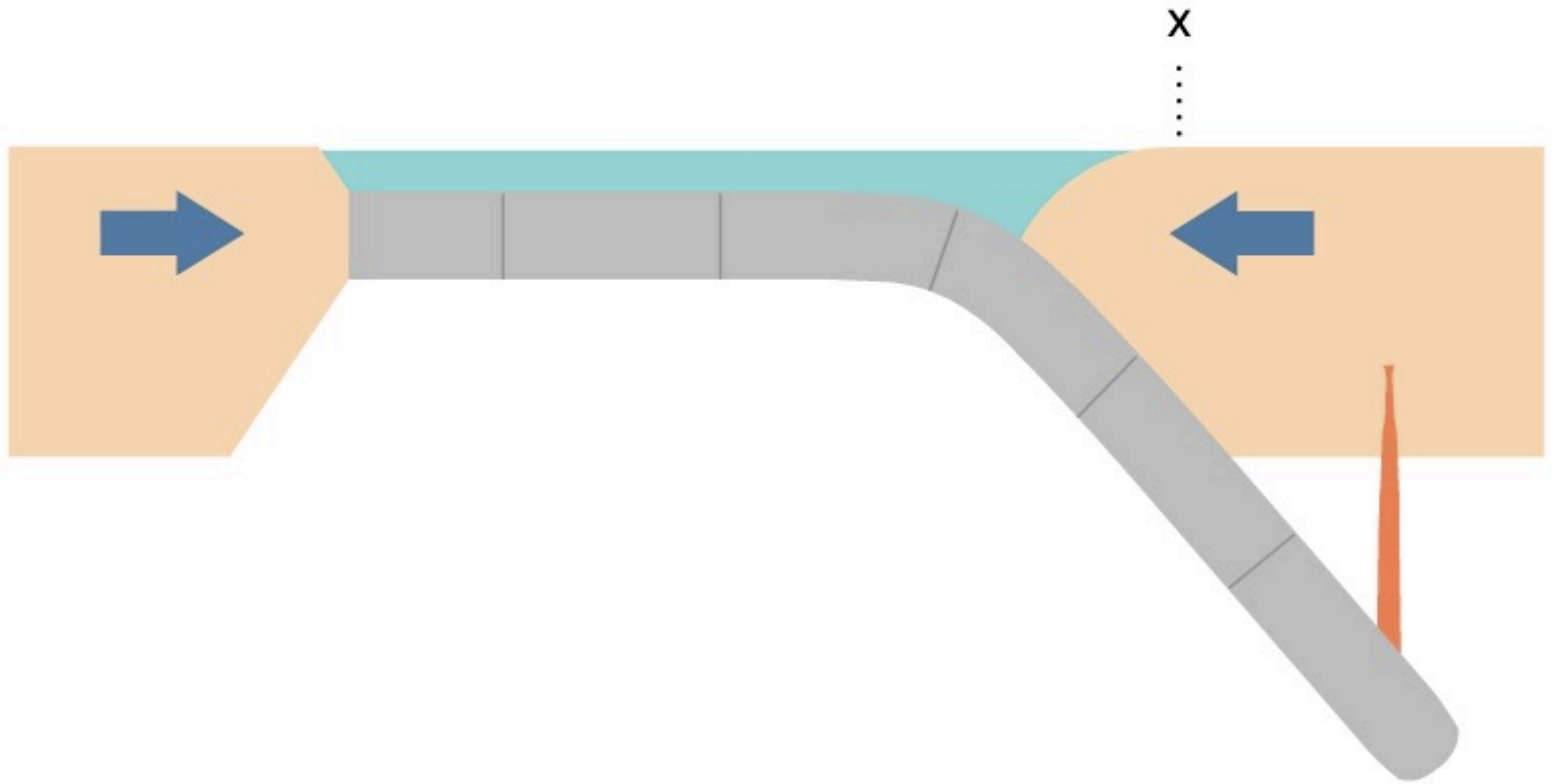

SUBDUCTION

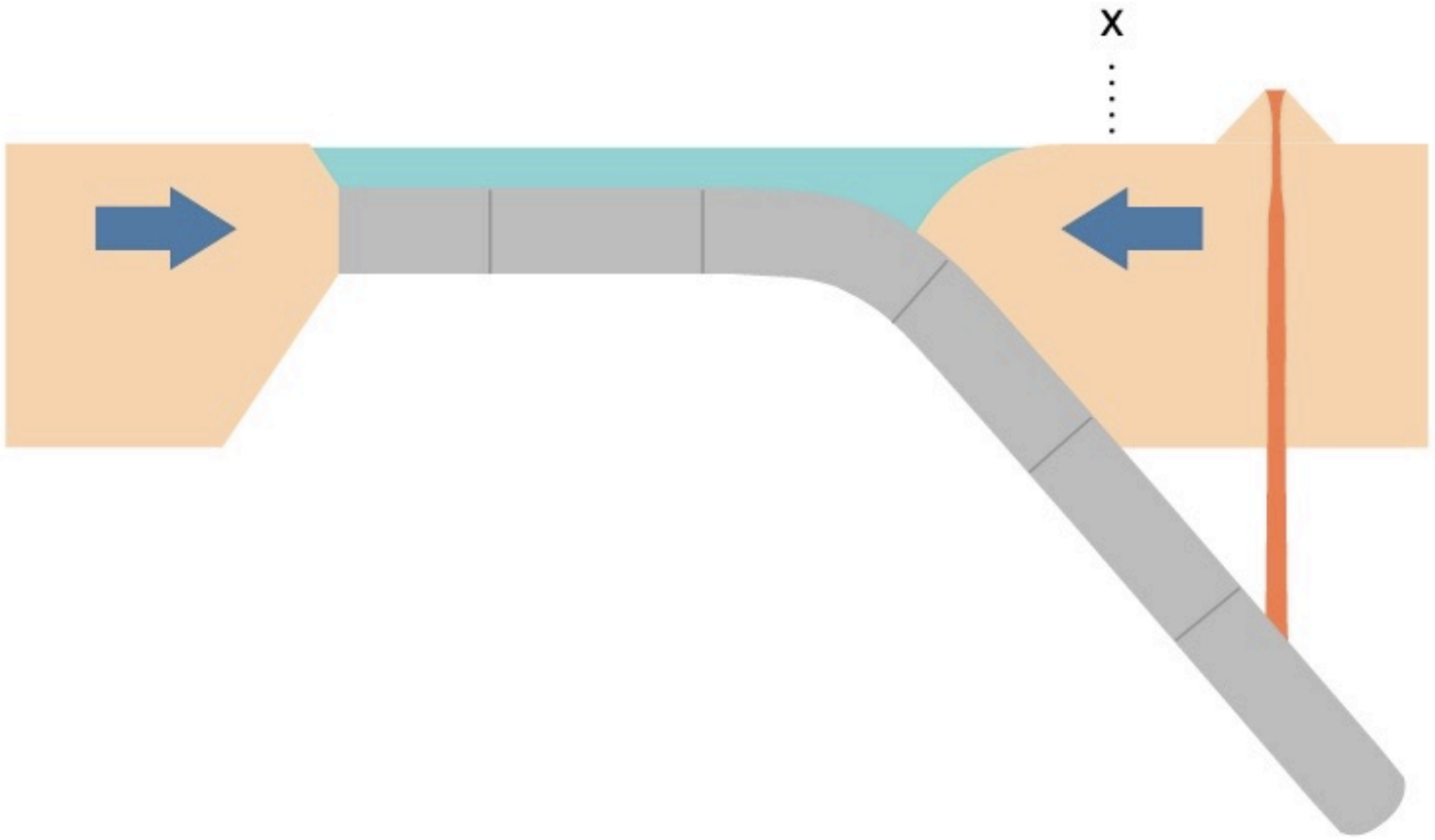

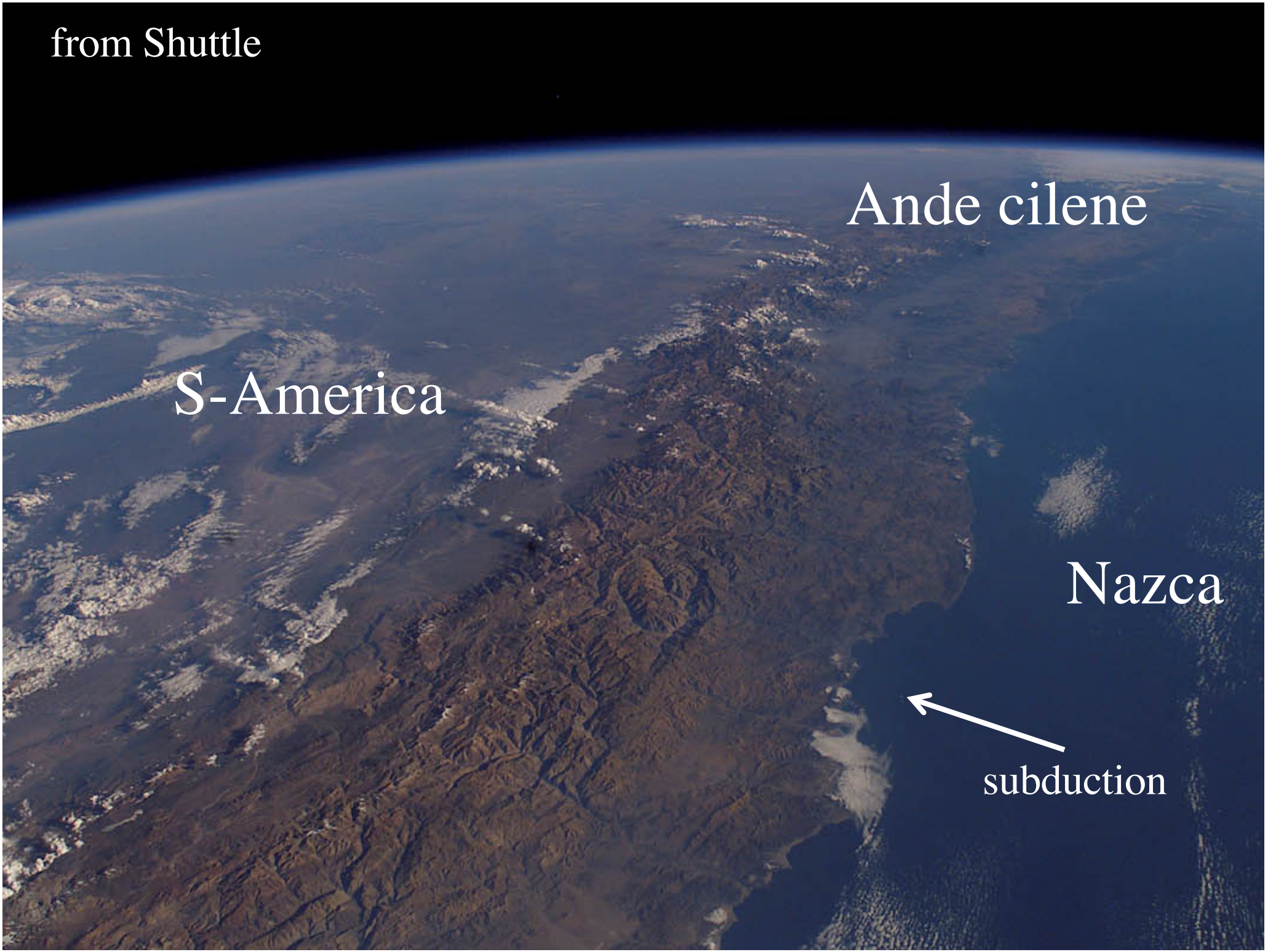
from Shuttle
Ande cilene
S-America
Nazca
subduction

Past 100 Ma movements

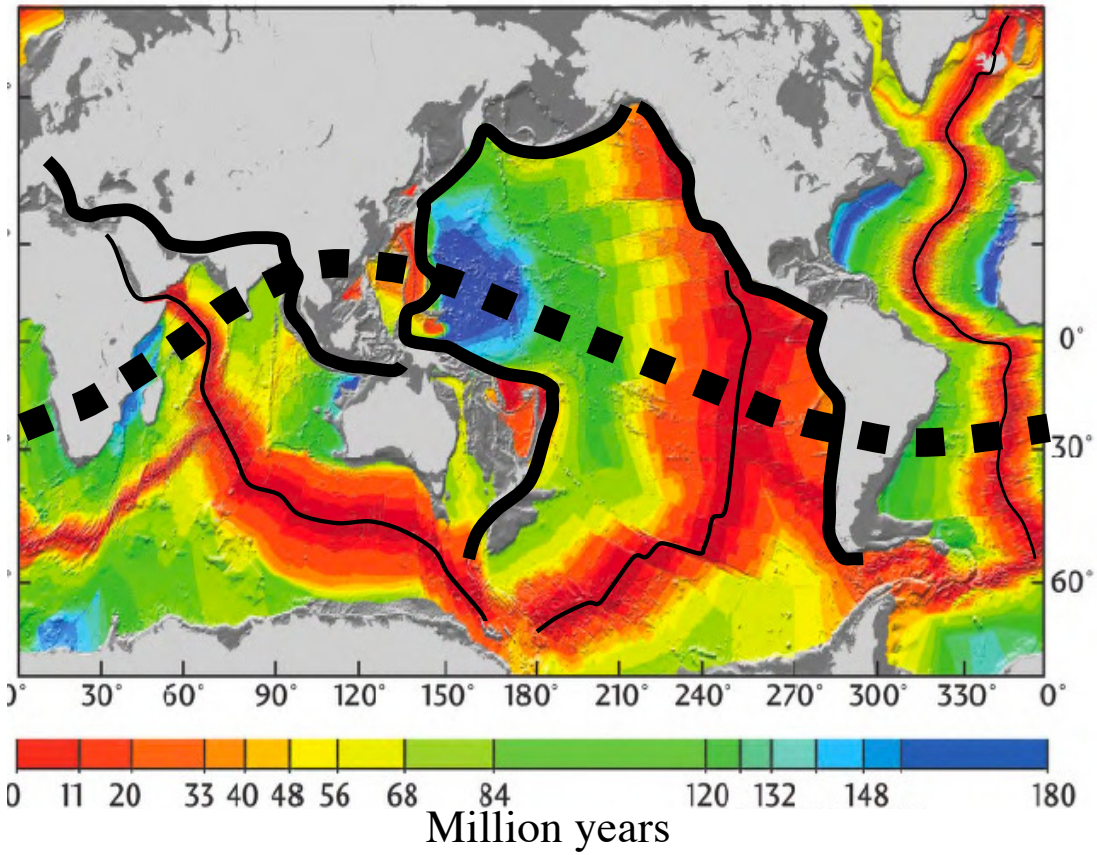

Present movements

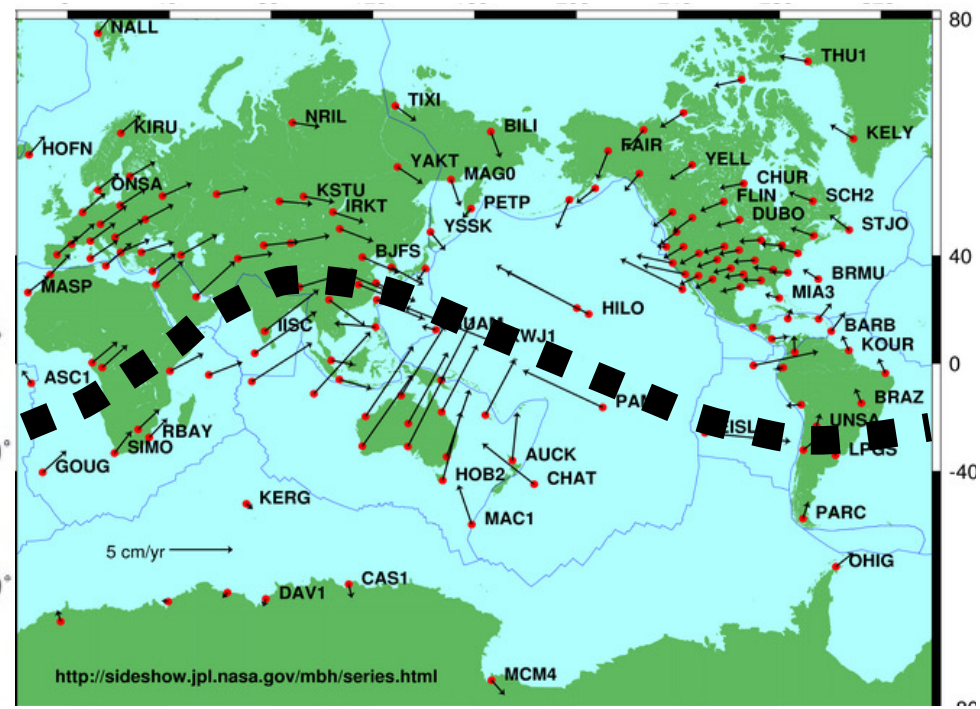

Doglioni & Panza 2015 Advances Geophys.

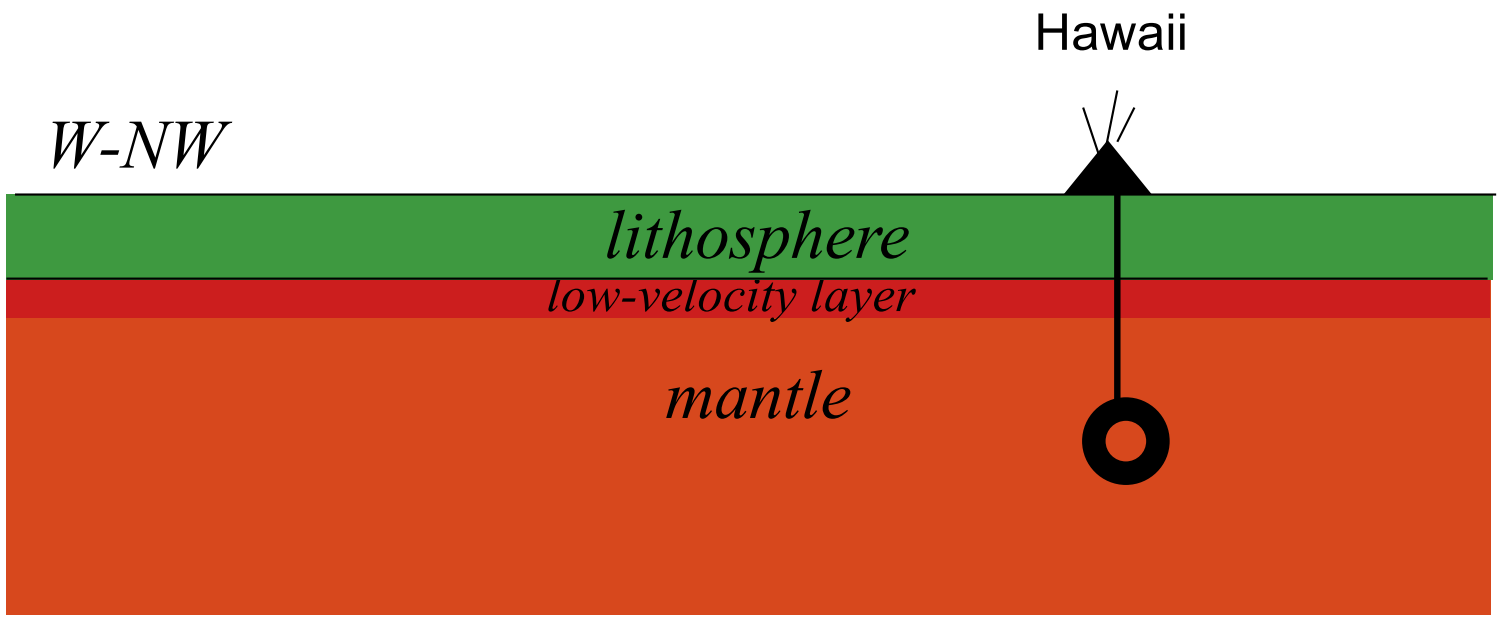
Hawaii
W-NW
lithosphere
low-velocity layer
mantle

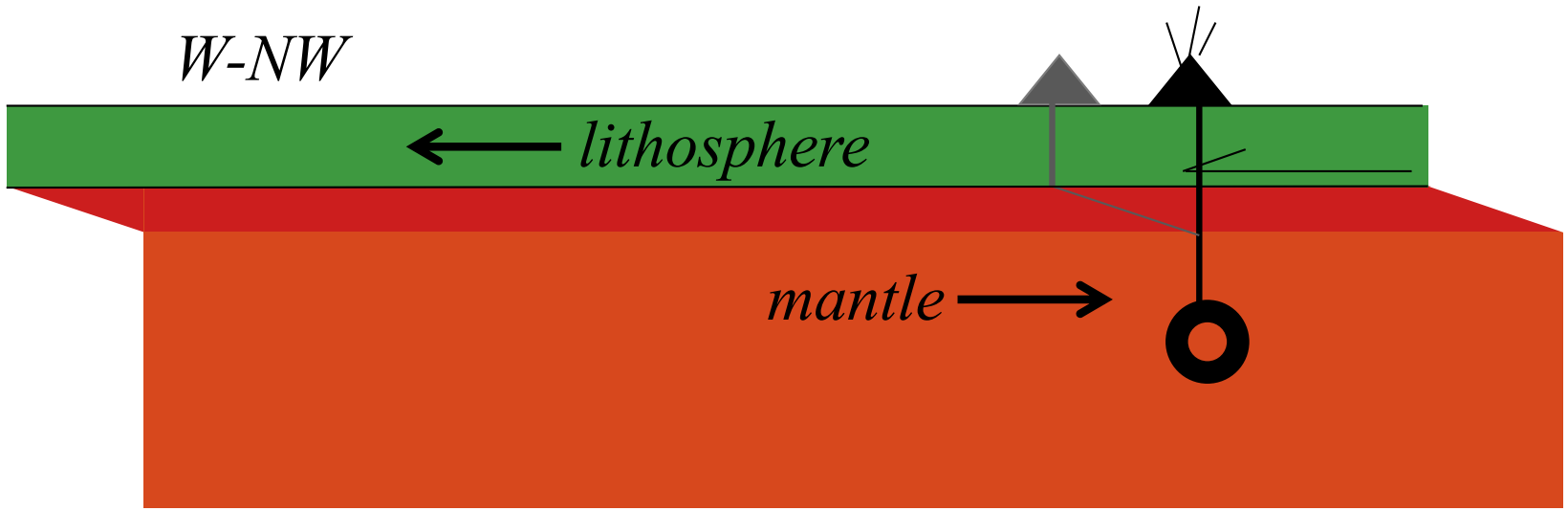
W-NW
lithosphere
mantle

decoupling of the lithosphere

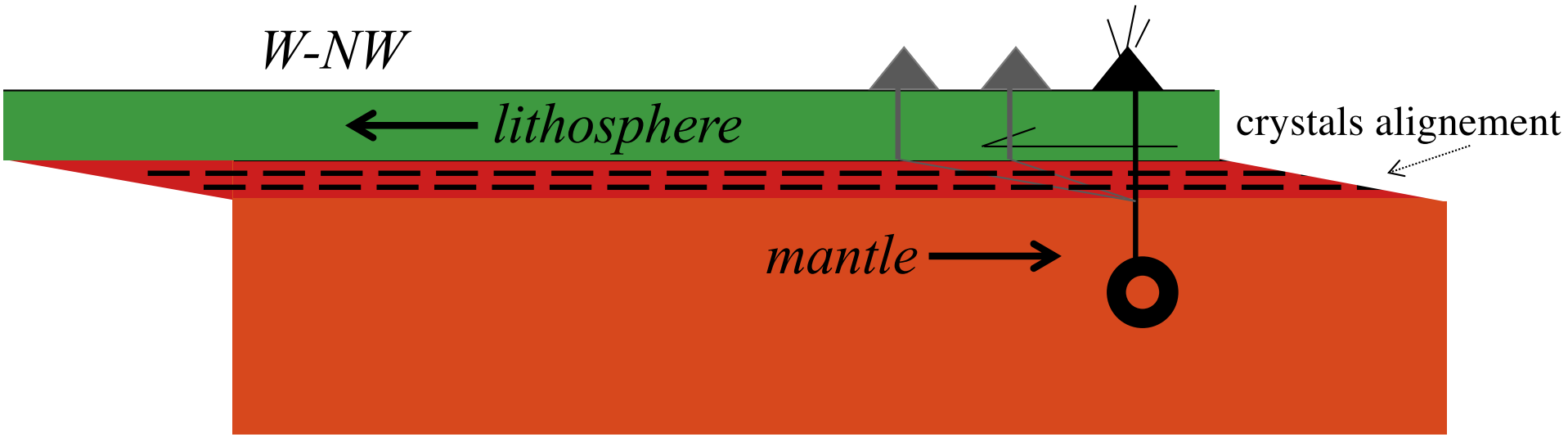

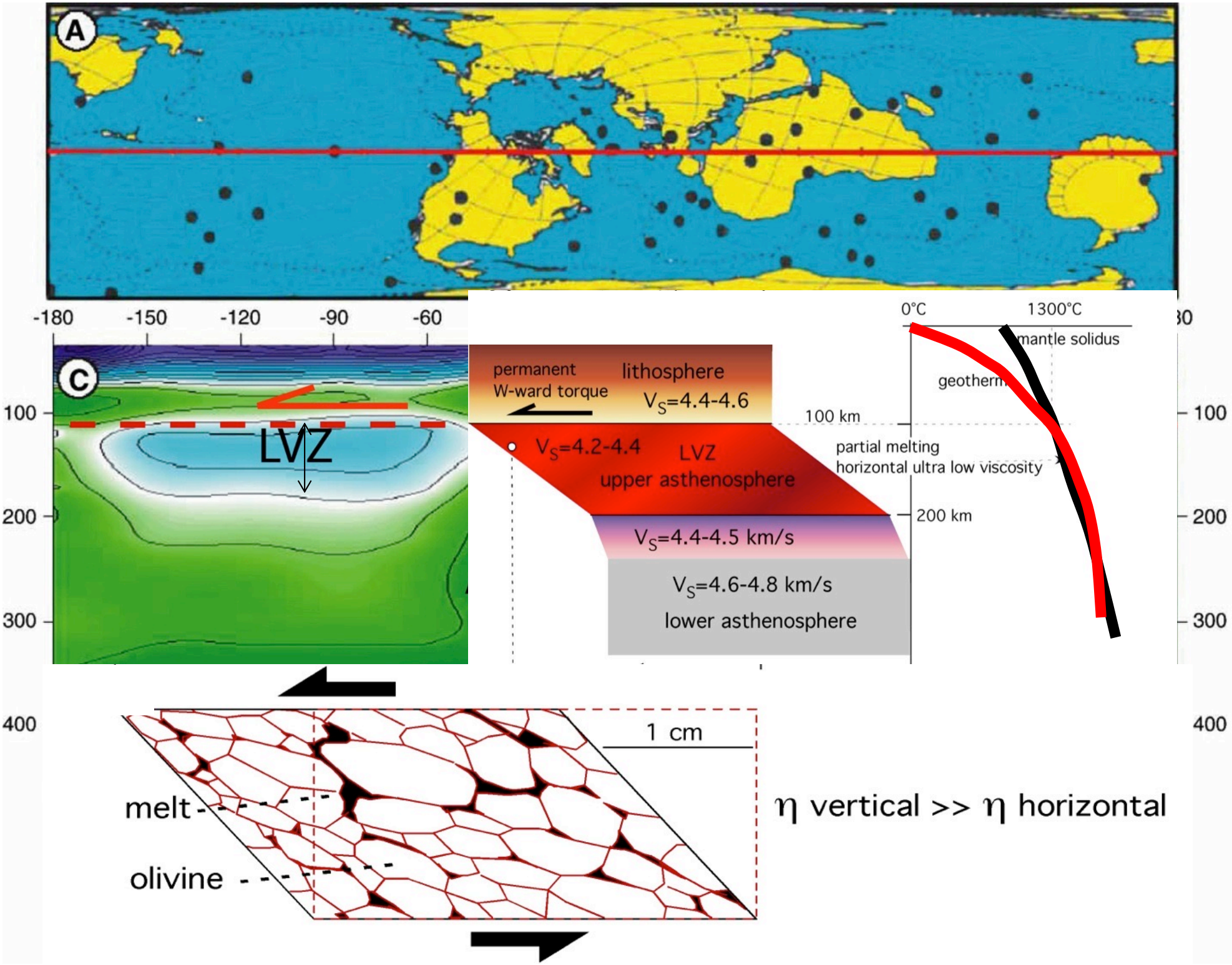
A
-180
-150
-120
-90
-60
C
LVZ
100
200
300
400
permanent
W-ward torque
lithosphere
V_S=4.4-4.6
V_S=4.2-4.4
LVZ
upper asthenosphere
V_S=4.4-4.5 km/s
V_S=4.6-4.8 km/s
lower asthenosphere
0°C
1300°C
mantle solidus
geotherm
100 km
partial melting
horizontal ultra low viscosity
200 km
1 cm
melt
olivine
η vertical >> η horizontal

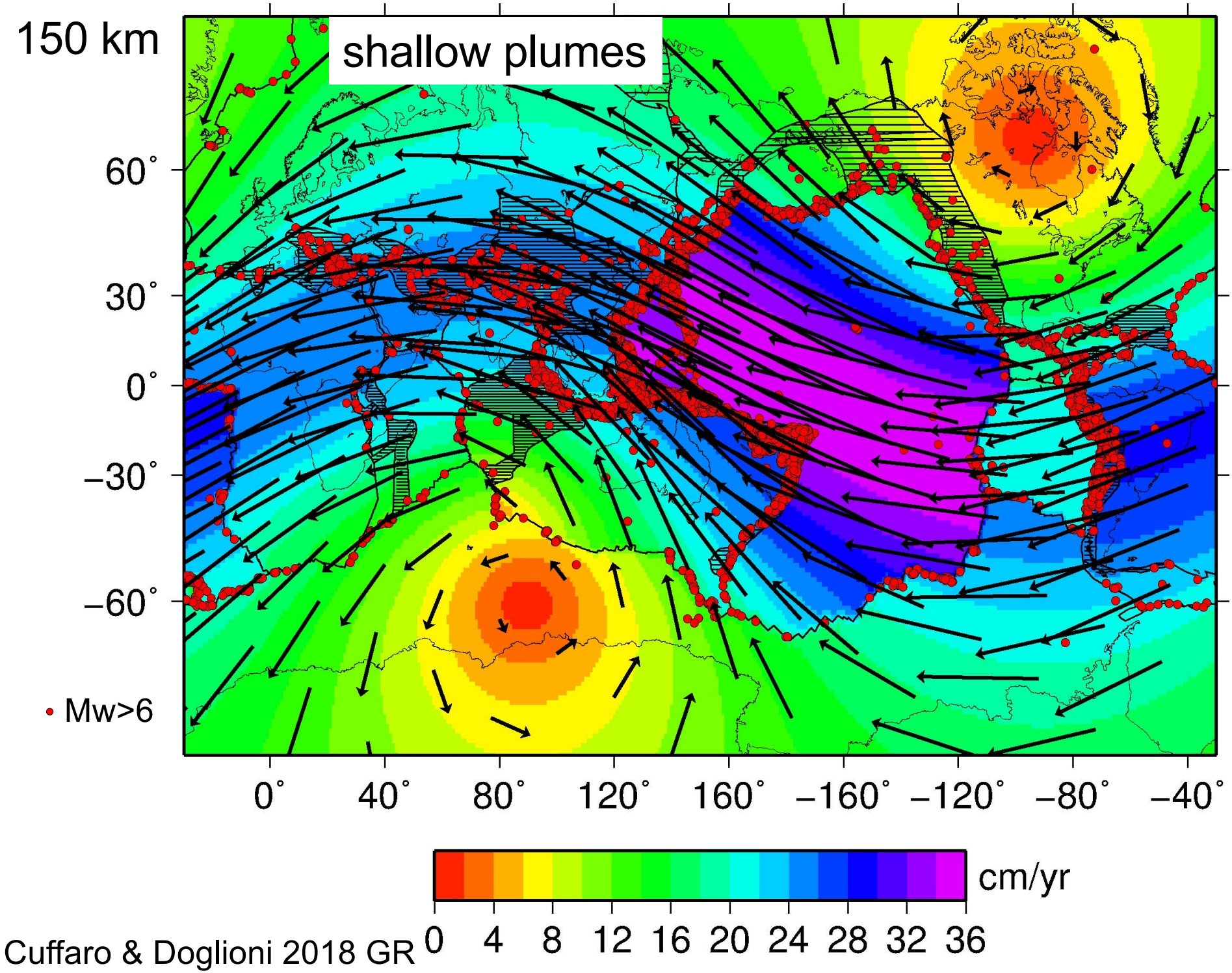

Cuffaro & Doglioni 2018 GR

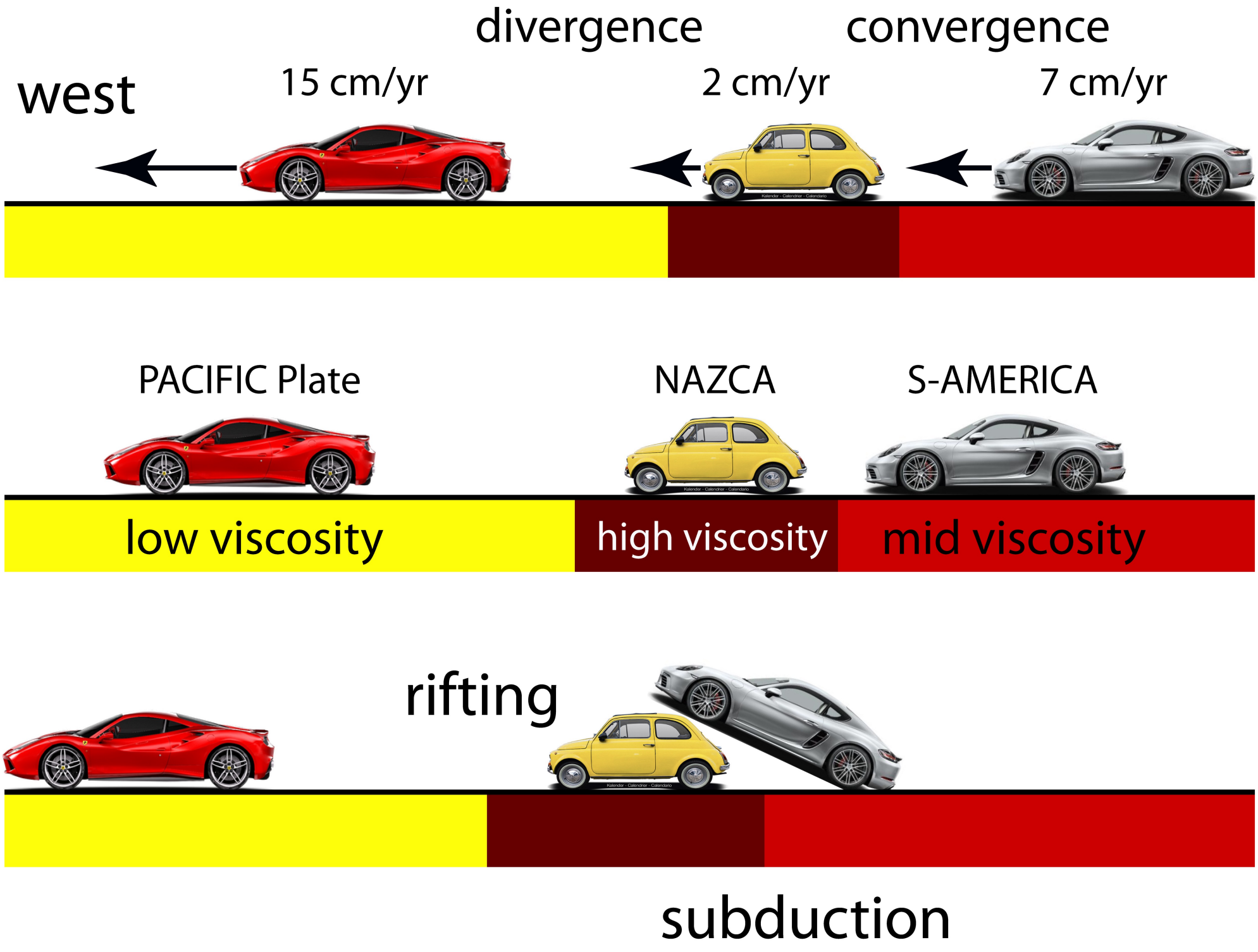
divergence
convergence
west
15 cm/yr
2 cm/yr
7 cm/yr
PACIFIC Plate
NAZCA
S-AMERICA
low viscosity
high viscosity
mid viscosity
rifting
subduction

Deep hotspot source

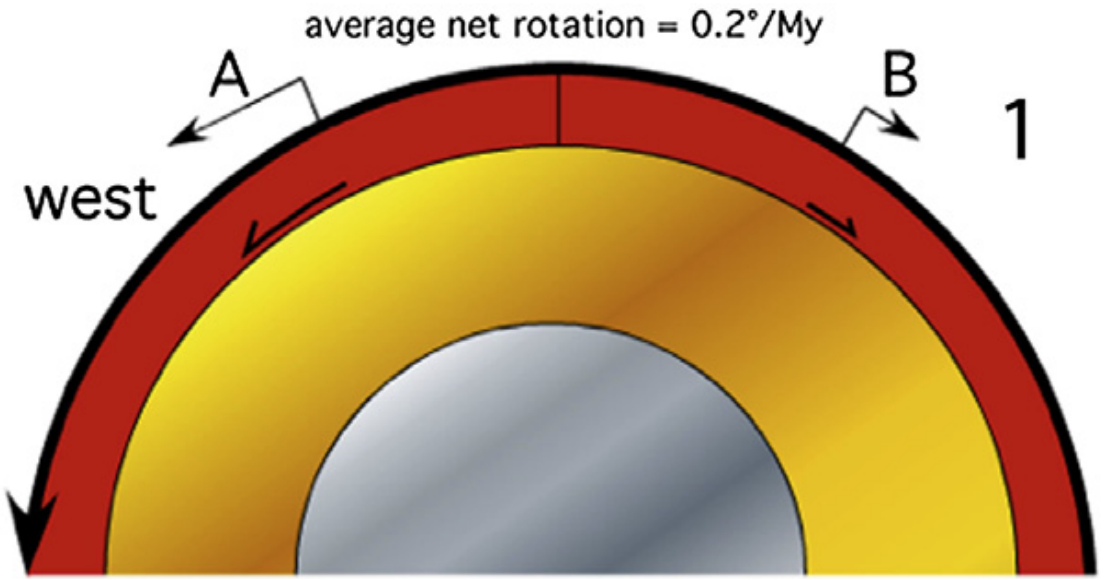

Shallow hotspot source

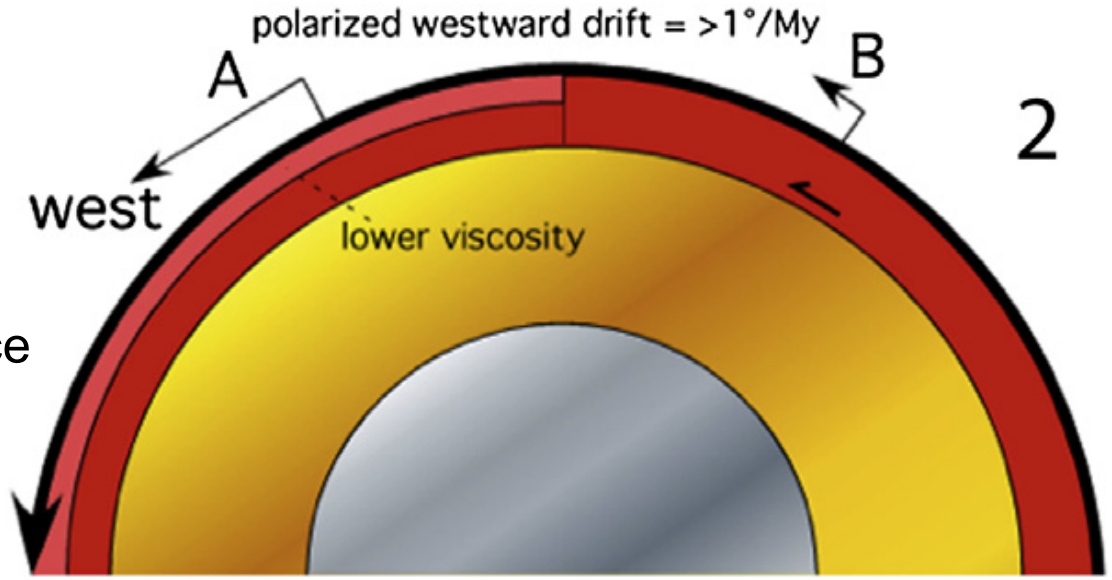

Doglioni & Panza 2015 Advances Geophys.

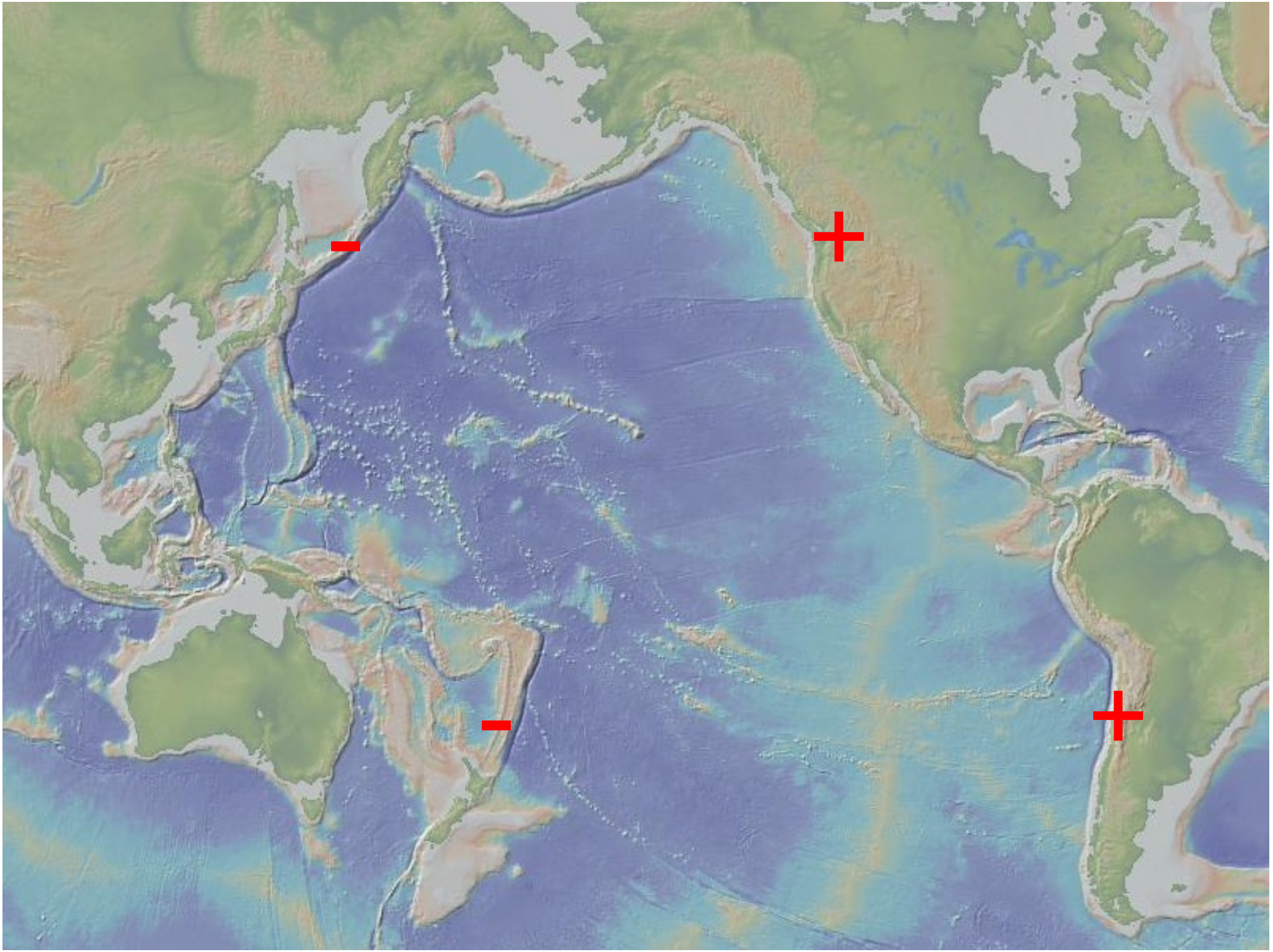

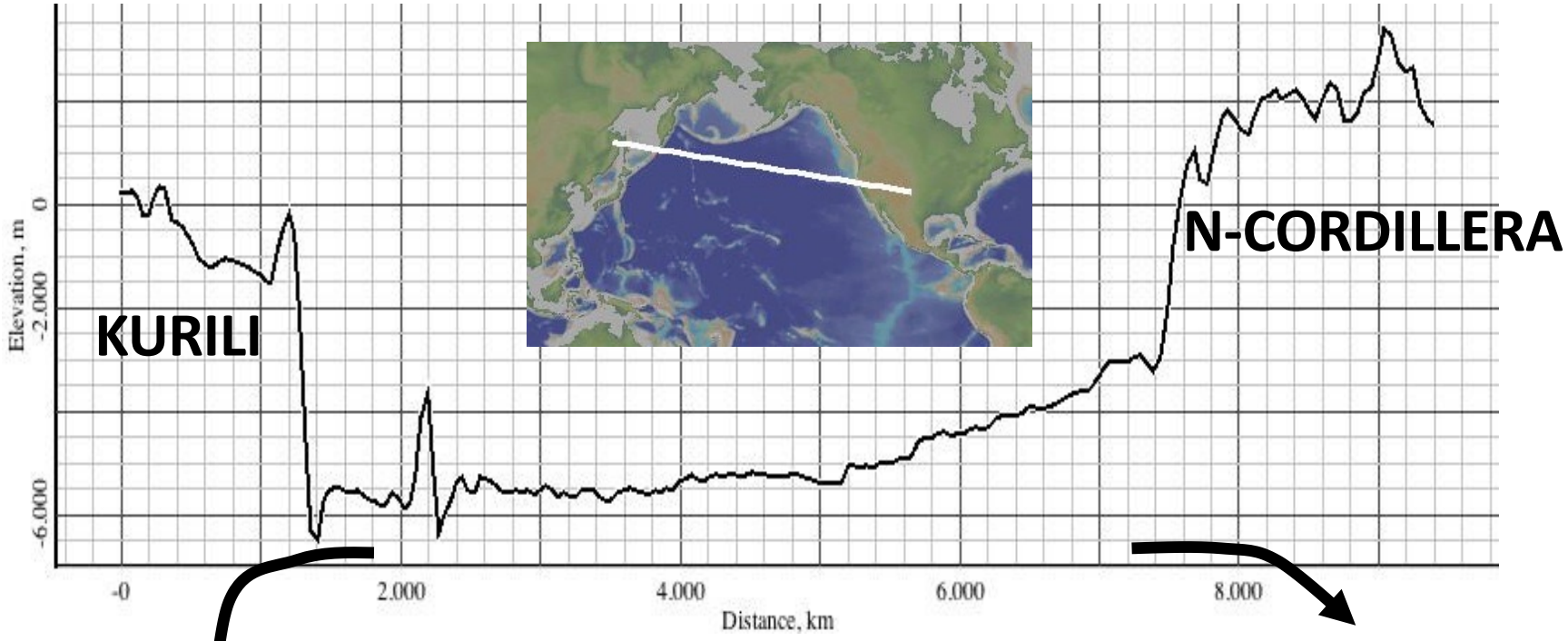

mean values across subduction zones

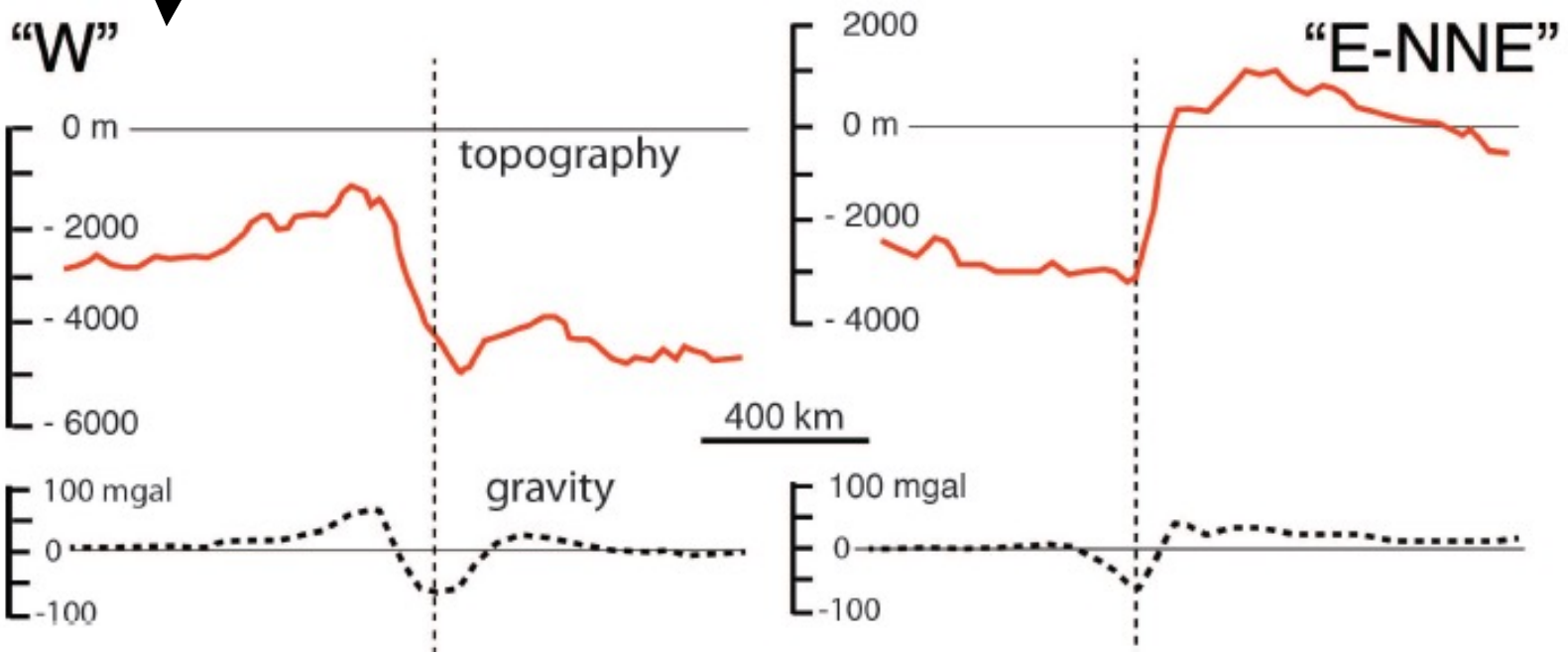

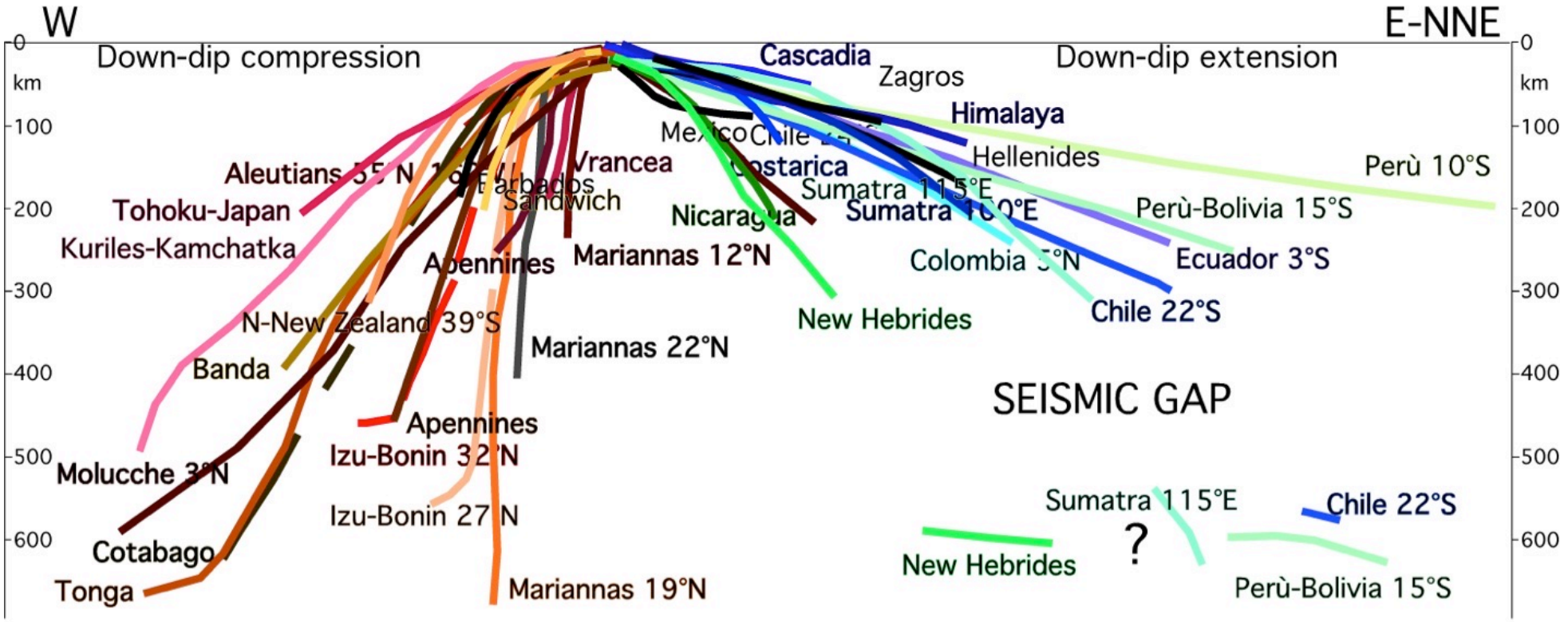

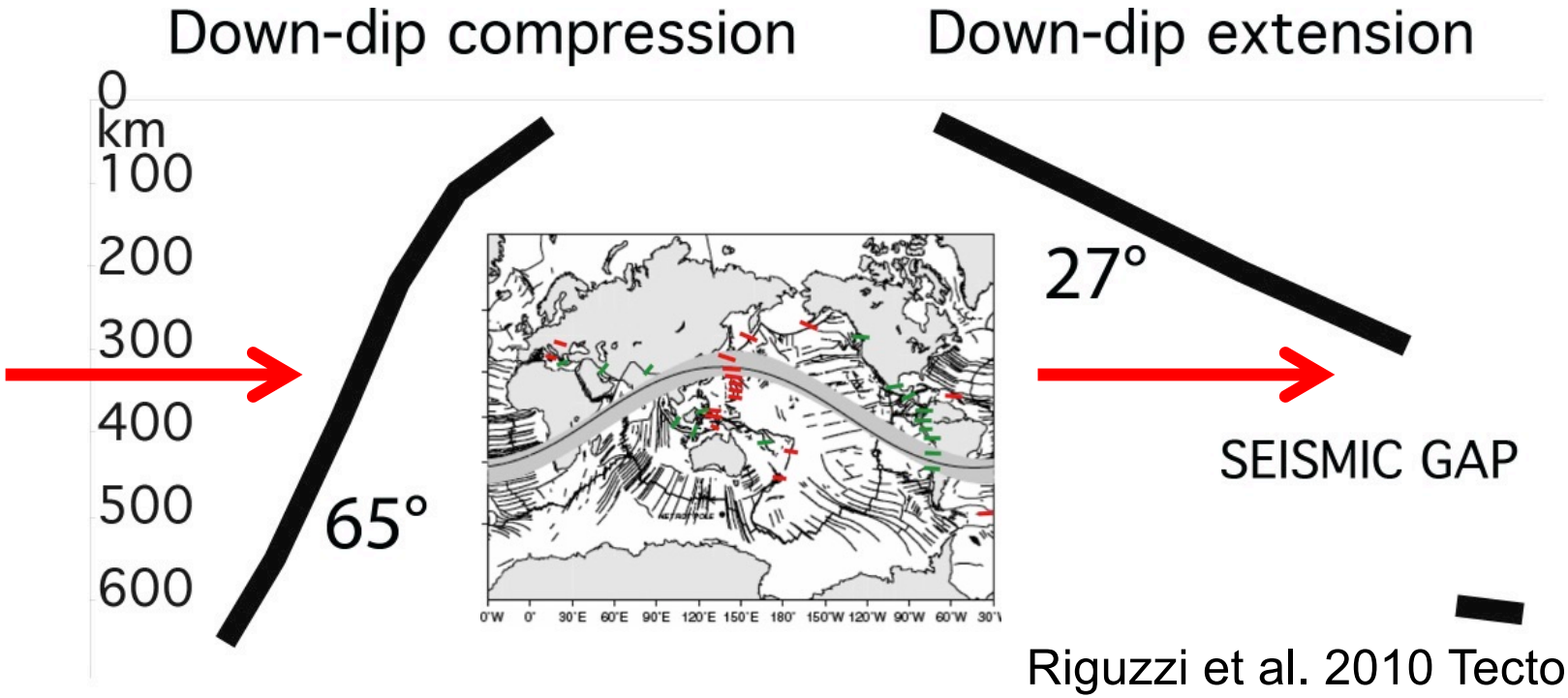

Riguzzi et al. 2010 Tectonophysics

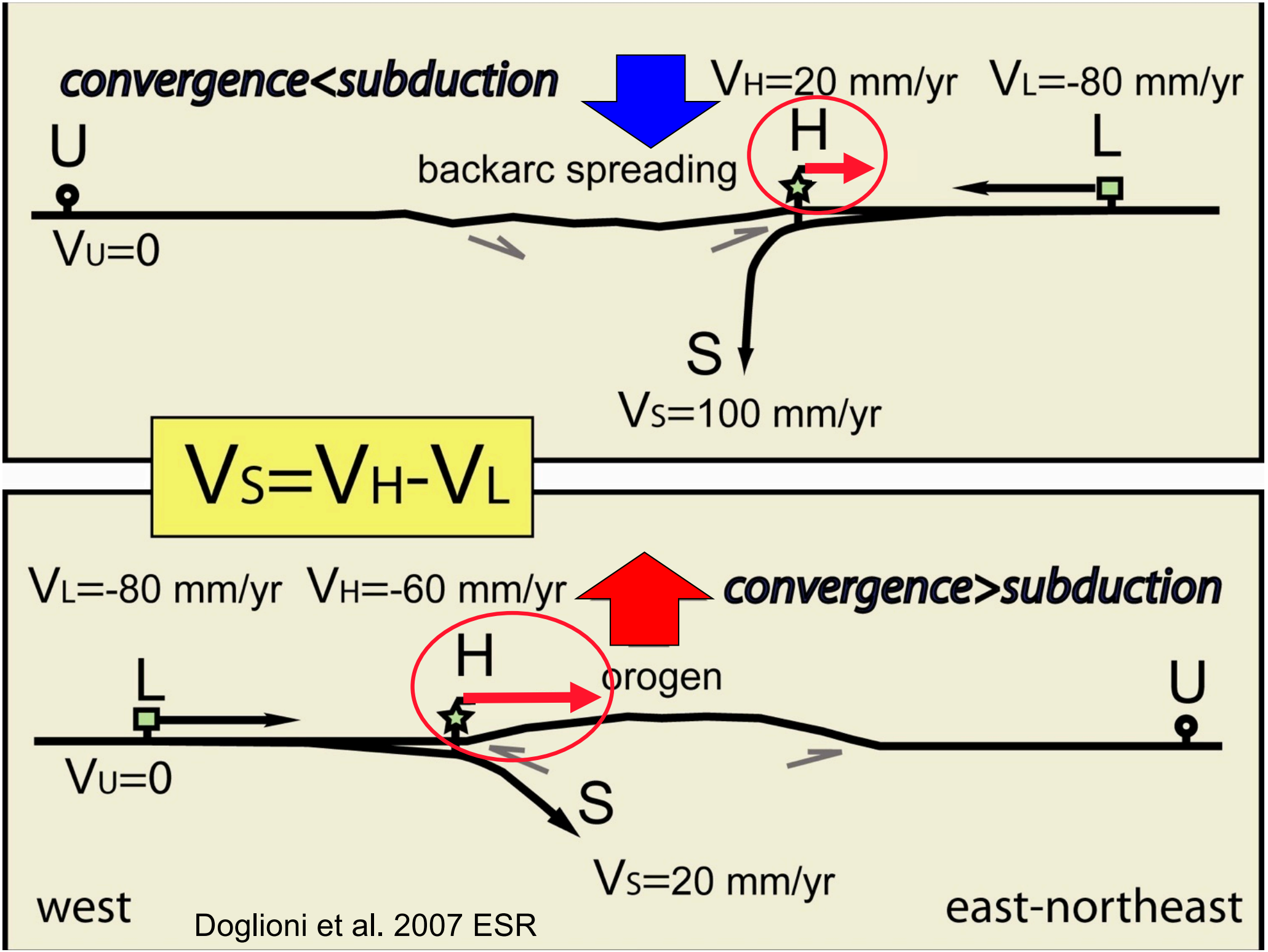

Doglioni et al. 2007 ESR

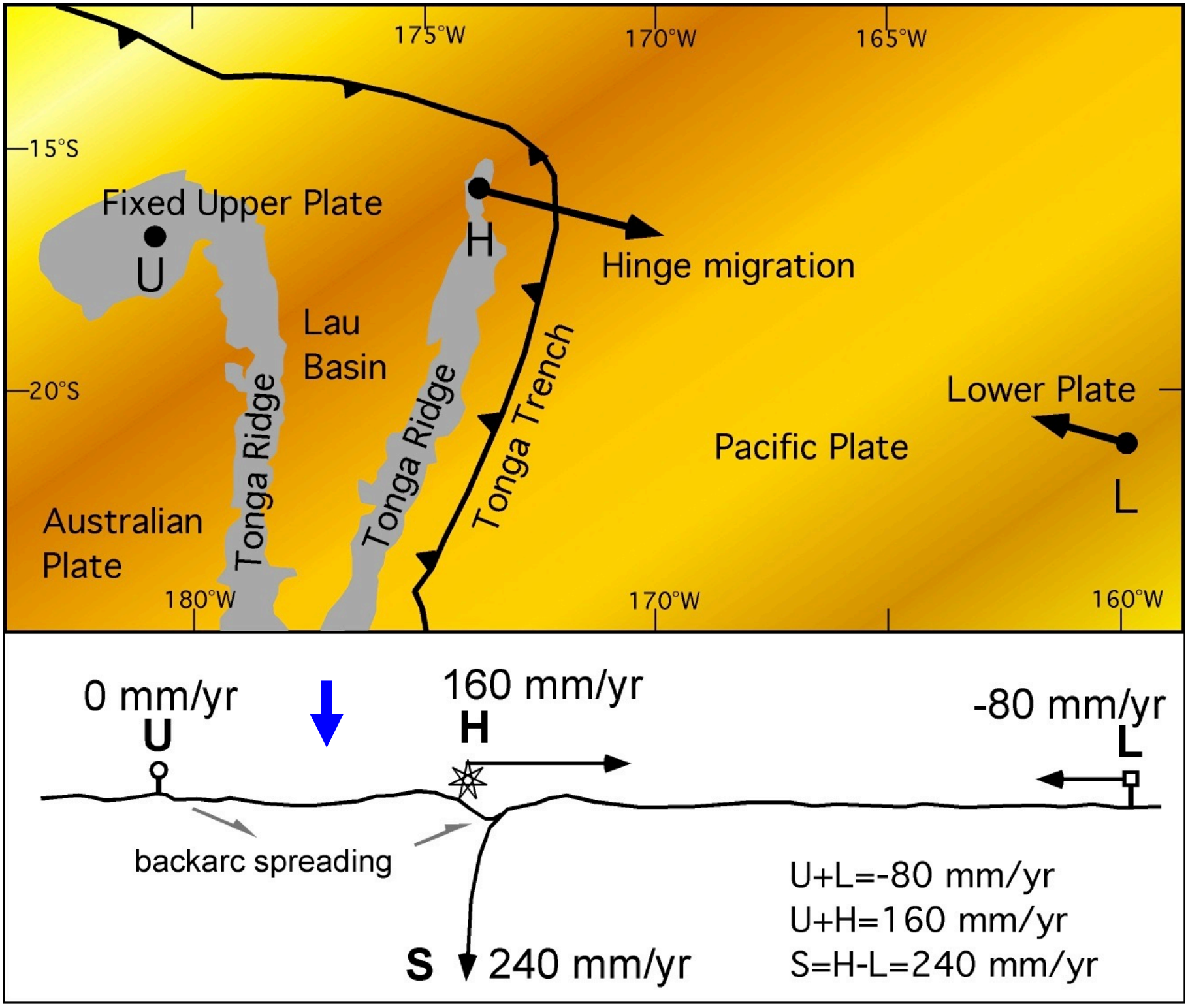
175°W
170°W
165°W
15°S
20°S
Fixed Upper Plate
U
H
Hinge migration
Lau
Basin
Tonga Ridge
Tonga Ridge
Tonga Trench
Lower Plate
Pacific Plate
L
Australian
Plate
180°W
170°W
160°W
0 mm/yr
U
160 mm/yr
H
-80 mm/yr
L
backarc spreading
S
240 mm/yr
U+L=-80 mm/yr
U+H=160 mm/yr
S=H-L=240 mm/yr

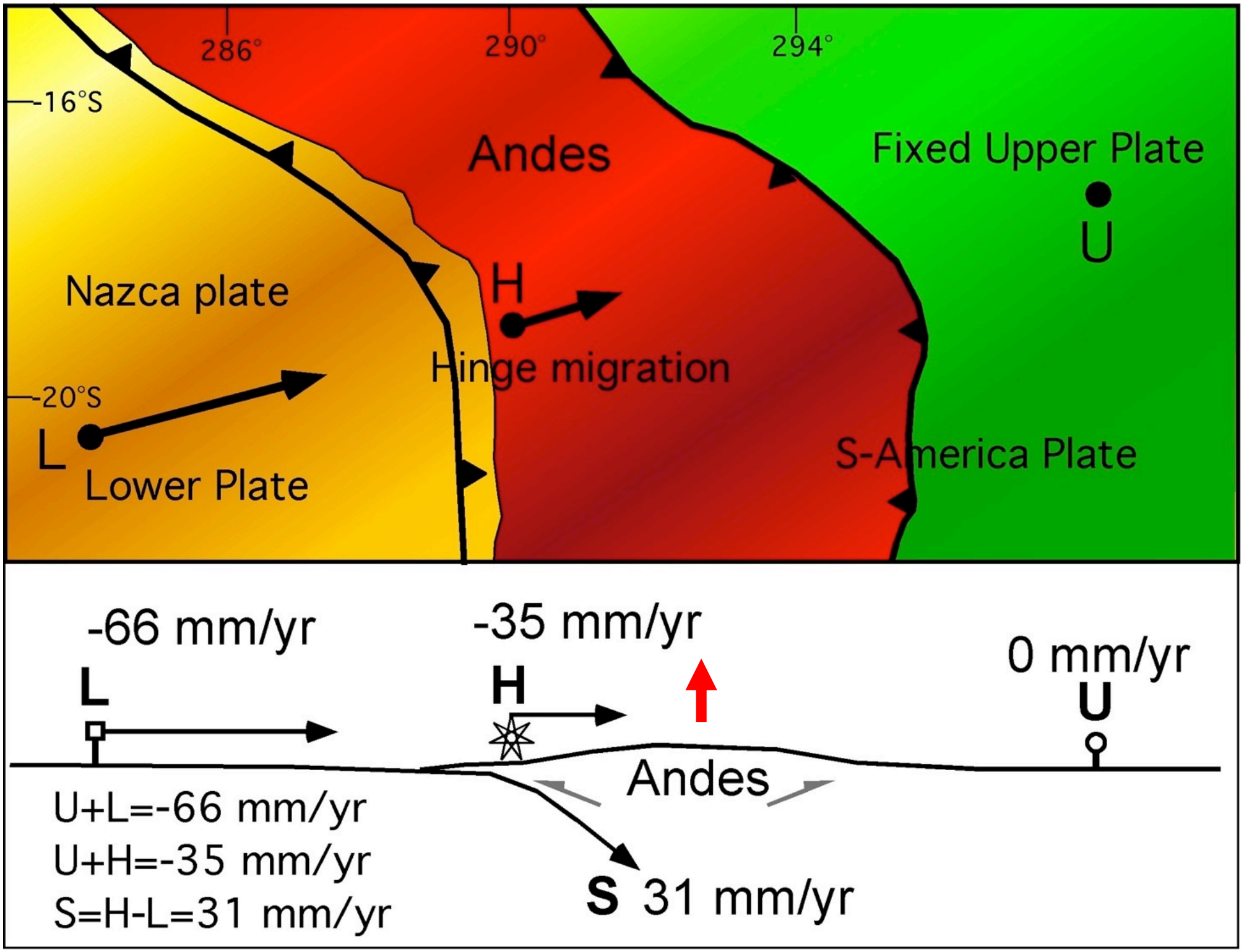
286°
290°
294°
16°S
20°S
Andes
Fixed Upper Plate
U
Nazca plate
H
Hinge migration
L
Lower Plate
S-America Plate
-66 mm/yr
-35 mm/yr
0 mm/yr
L
H
U
Andes
U+L=-66 mm/yr
U+H=-35 mm/yr
S=H-L=31 mm/yr
S 31 mm/yr

Slab recycling volumes ≈ 306 km³/yr (180 Ma)

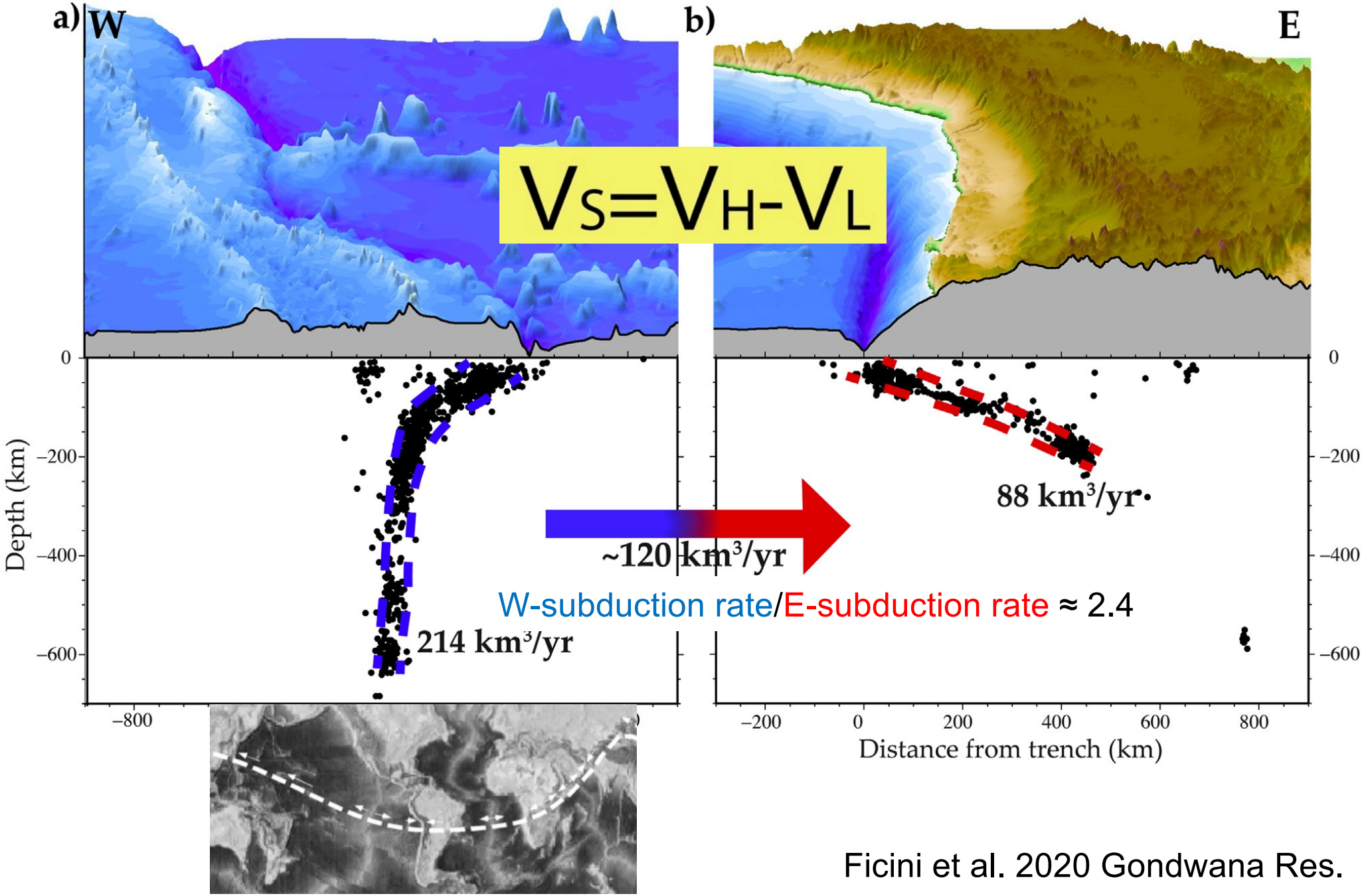

Ficini et al. 2020 Gondwana Res.

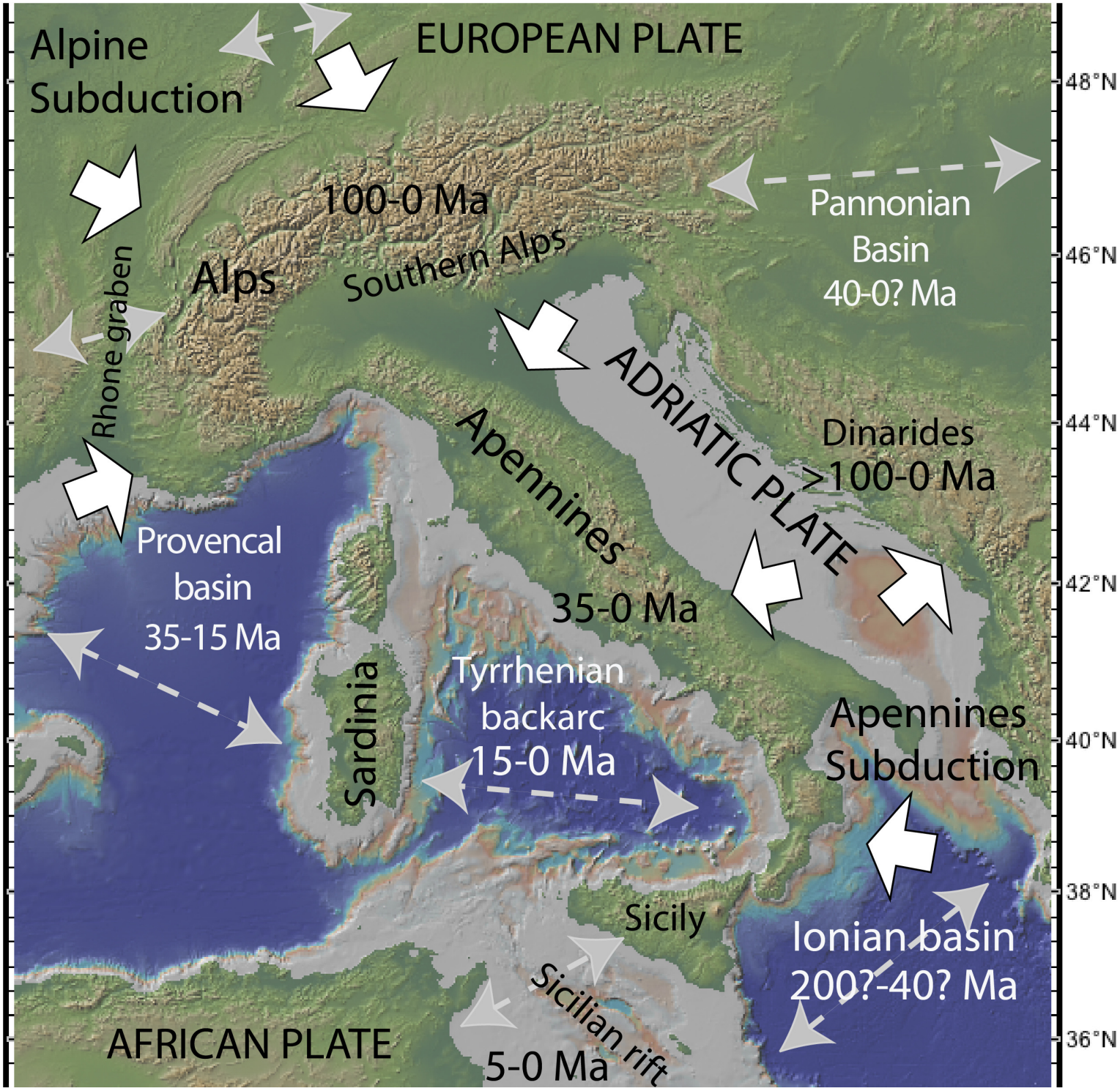
Alpine
Subduction
EUROPEAN PLATE
100-0 Ma
Alps
Southern Alps
Pannonian
Basin
40-0? Ma
Rhone graben
ADRIATIC PLATE
Apennines
Dinarides
>100-0 Ma
35-0 Ma
Provencal
basin
35-15 Ma
Sardinia
Tyrrhenian
backarc
15-0 Ma
Apennines
Subduction
Sicily
Ionian basin
200?-40? Ma
Sicilian rift
AFRICAN PLATE
5-0 Ma
48°N
46°N
44°N
42°N
40°N
38°N
36°N

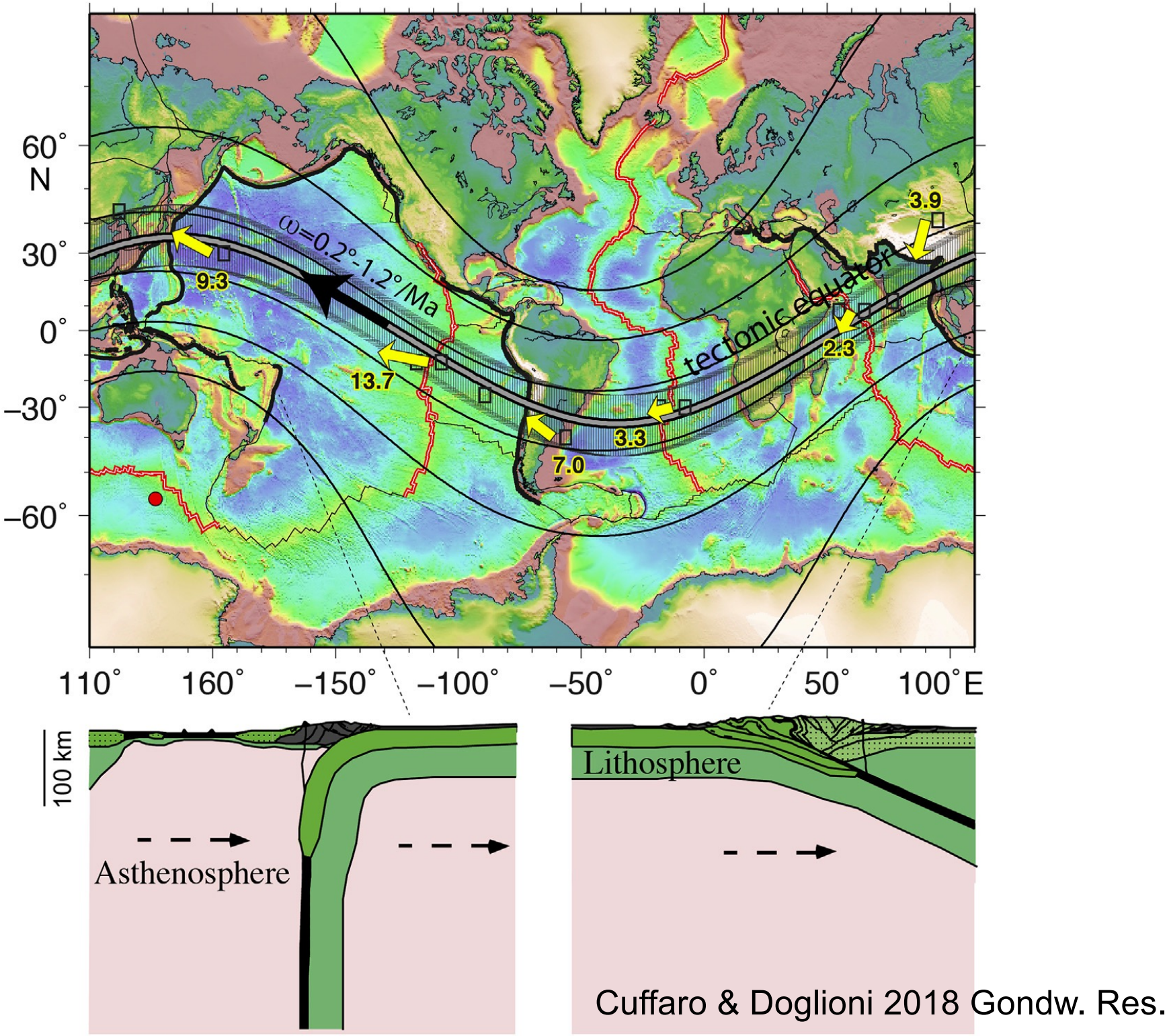

Cuffaro & Doglioni 2018 Gondw. Res.

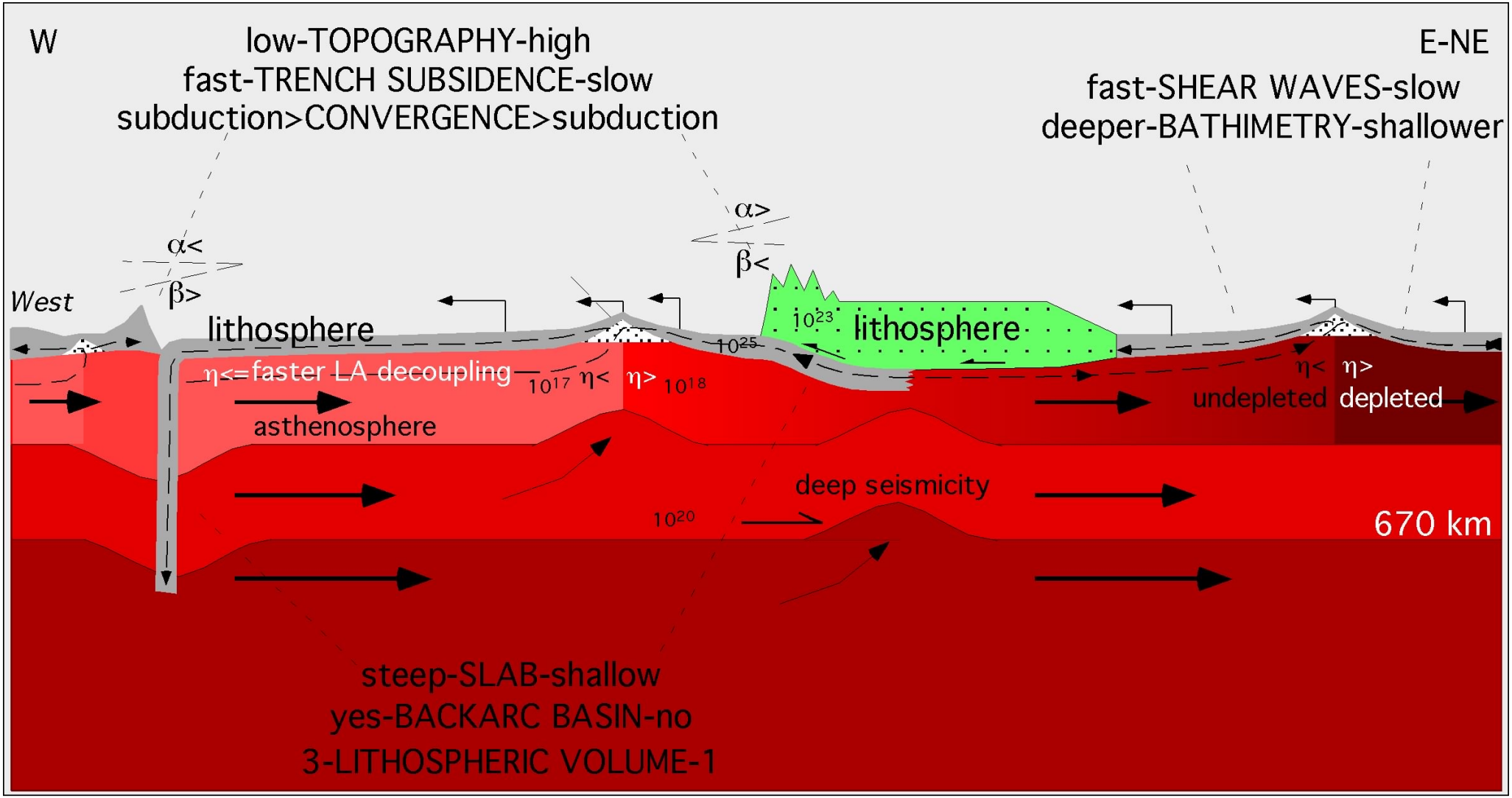

Doglioni & Panza 2015 Advances Geophys.


PLATES MOVE: WHO IS PUSHING THEM??!!

Forces acting on the lithosphere

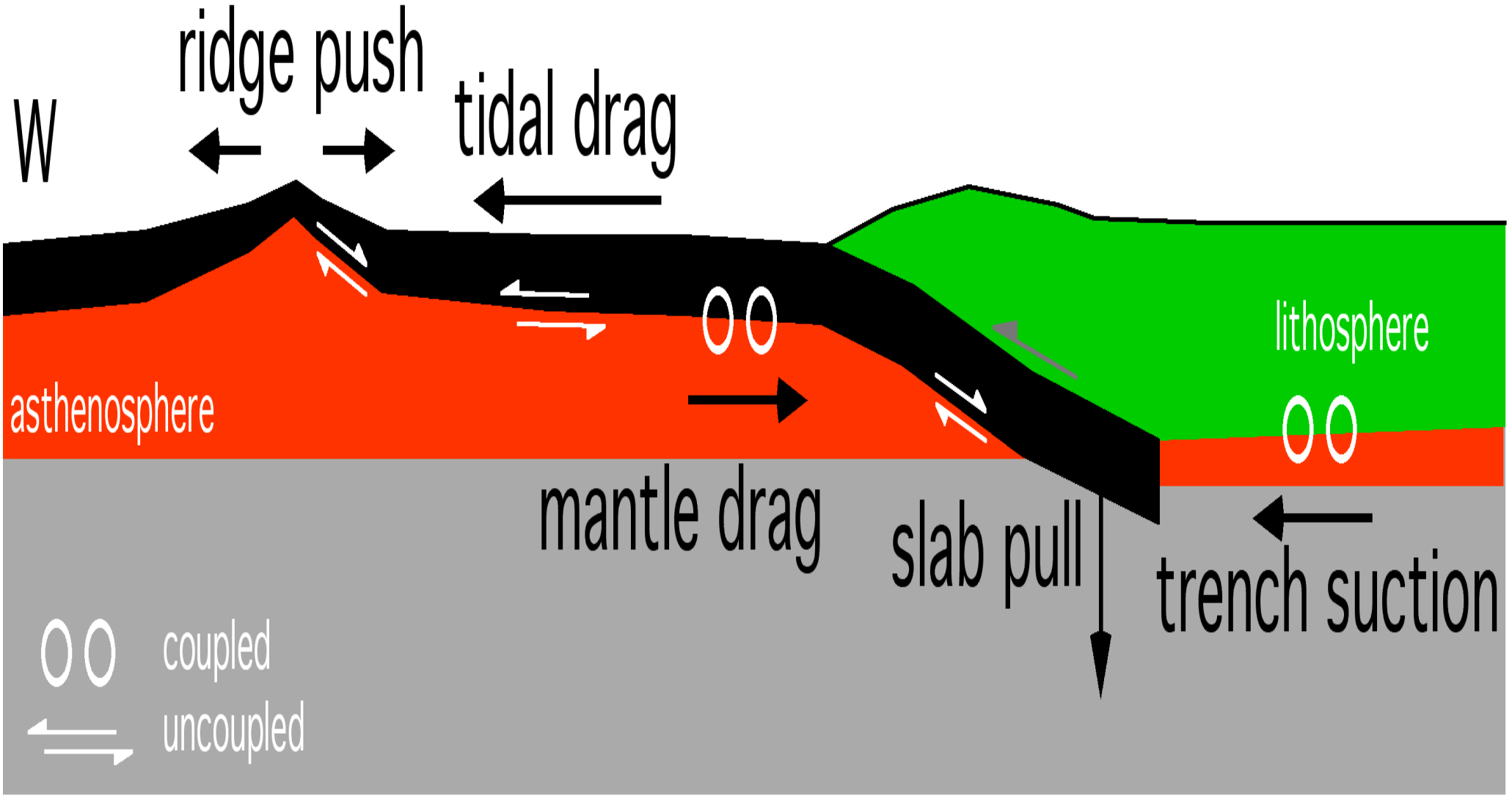

Doglioni et al., 2007, ESR

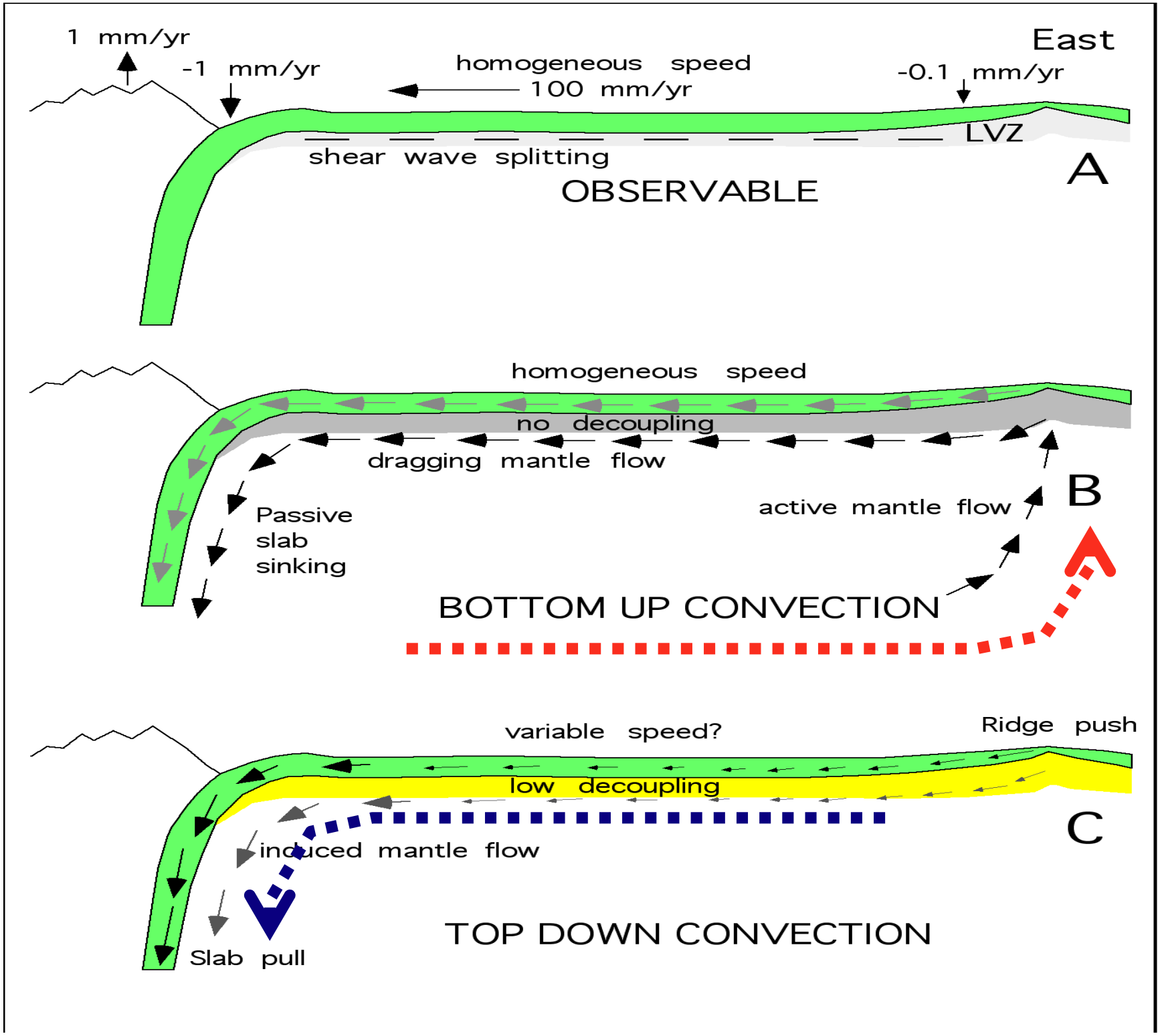
1 mm/yr
-1 mm/yr
homogeneous speed
100 mm/yr
East
-0.1 mm/yr
LVZ
shear wave splitting
A
OBSERVABLE
homogeneous speed
no decoupling
dragging mantle flow
Passive
slab
sinking
active mantle flow
B
BOTTOM UP CONVECTION
variable speed?
Ridge push
low decoupling
C
induced mantle flow
Slab pull
TOP DOWN CONVECTION

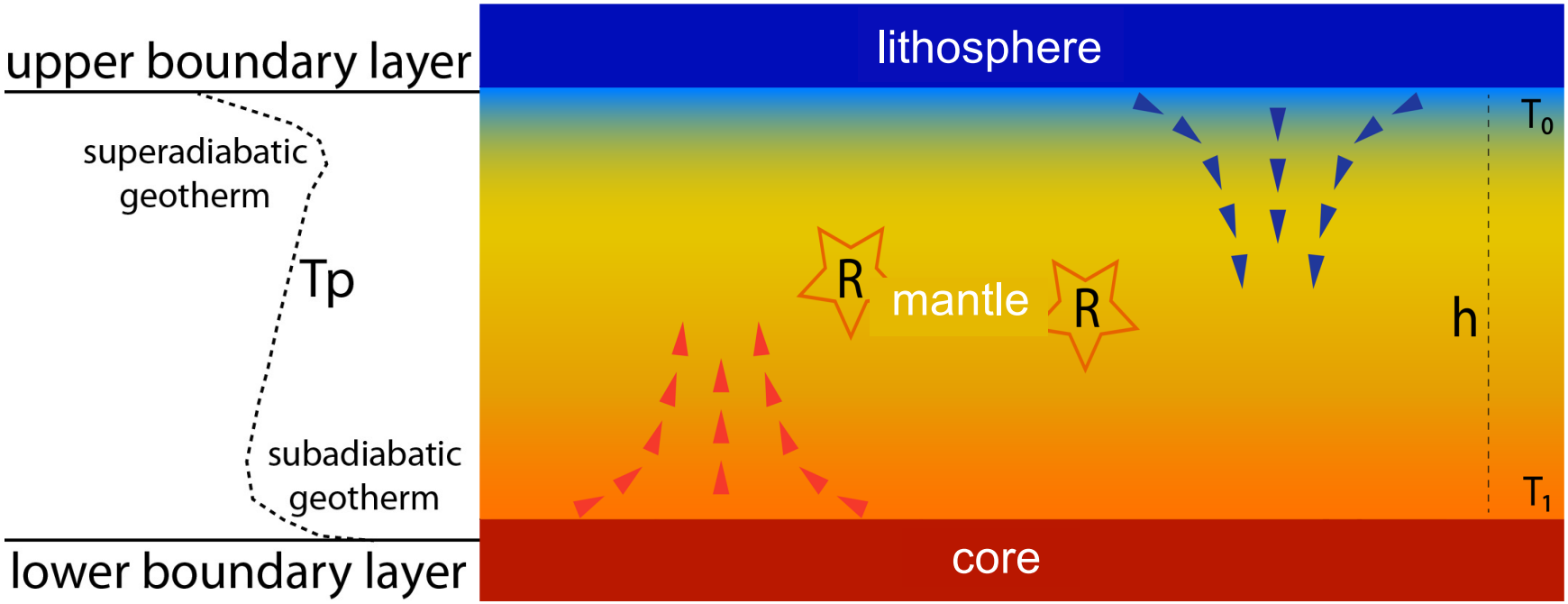

$$Ra = \frac{\rho^2 g \alpha (T_1 - T_0) h^3}{\eta \kappa} \cdot \frac{Q h + R h^2}{\kappa}$$

basal heat internal heat

Ra Rayleigh number
ρ density
g gravity
α thermal expansion
T temperature
h thickness
η viscosity
κ conductivity
Q heat flow at the base
R internal radiogenic heat

Doglioni & Panza 2015

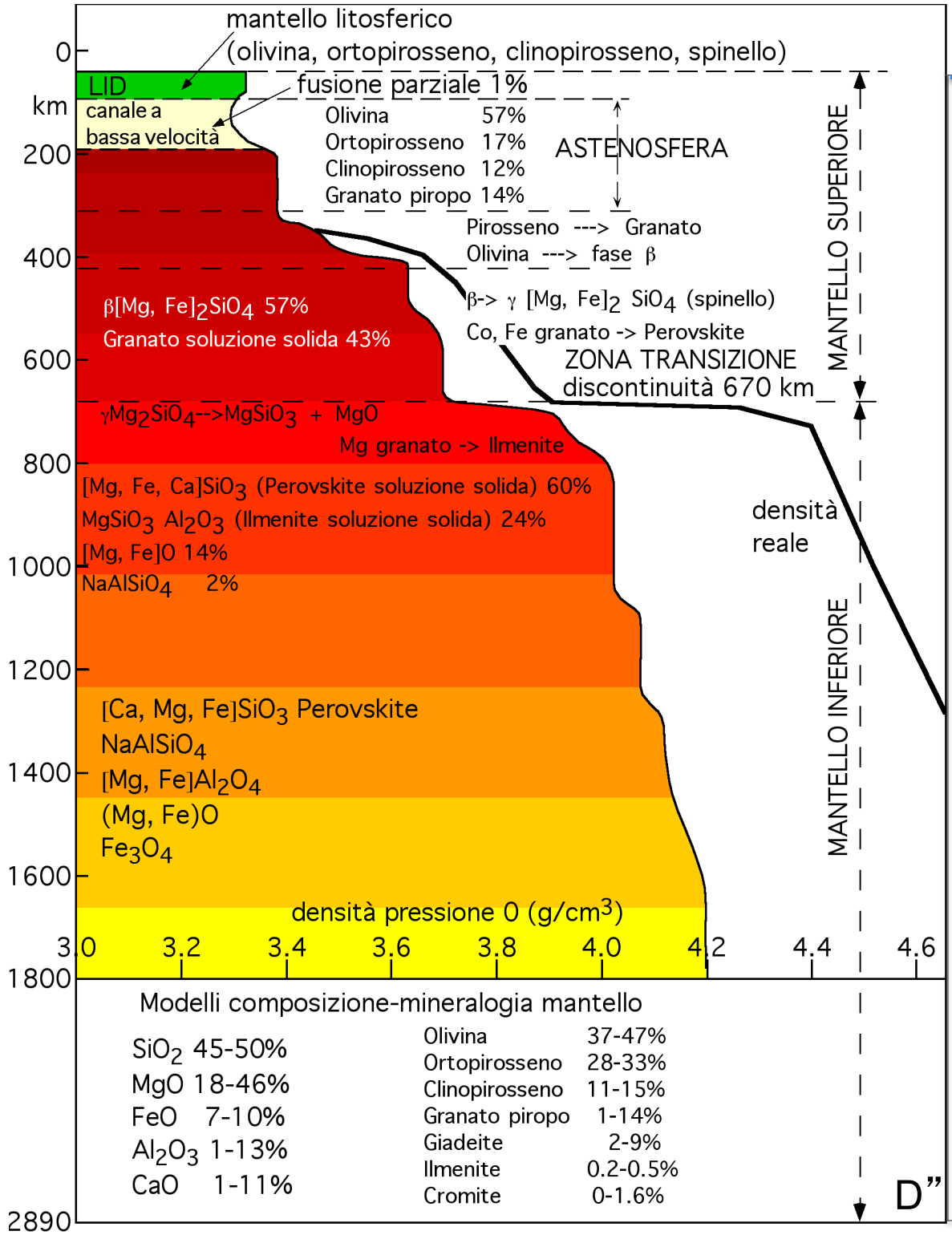
mantello litosferico
(olivina, ortopirosseno, clinopirosseno, spinello)
LID
canale a
bassa velocità
fusione parziale 1%
Olivina 57%
Ortopirosseno 17%
Clinopirosseno 12%
Granato piropo 14%
ASTENOSFERA
Pirosseno ---> Granato
Olivina ---> fase β
β-> γ [Mg, Fe]2 SiO4 (spinello)
Co, Fe granato -> Perovskite
ZONA TRANSIZIONE
discontinuità 670 km
MANTELLO SUPERIORE
β[Mg, Fe]2SiO4 57%
Granato soluzione solida 43%
γMg2SiO4-->MgSiO3 + MgO
Mg granato -> Ilmenite
[Mg, Fe, Ca]SiO3 (Perovskite soluzione solida) 60%
MgSiO3 Al2O3 (Ilmenite soluzione solida) 24%
[Mg, Fe]O 14%
NaAlSiO4 2%
densità
reale
[Ca, Mg, Fe]SiO3 Perovskite
NaAlSiO4
[Mg, Fe]Al2O4
(Mg, Fe)O
Fe3O4
MANTELLO INFERIORE
densità pressione 0 (g/cm3)
km
0
200
400
600
800
1000
1200
1400
1600
1800
2890
3.0
3.2
3.4
3.6
3.8
4.0
4.2
4.4
4.6
Modelli composizione-mineralogia mantello
SiO2 45-50%
MgO 18-46%
FeO 7-10%
Al2O3 1-13%
CaO 1-11%
Olivina 37-47%
Ortopirosseno 28-33%
Clinopirosseno 11-15%
Granato piropo 1-14%
Giadeite 2-9%
Ilmenite 0.2-0.5%
Cromite 0-1.6%
D”

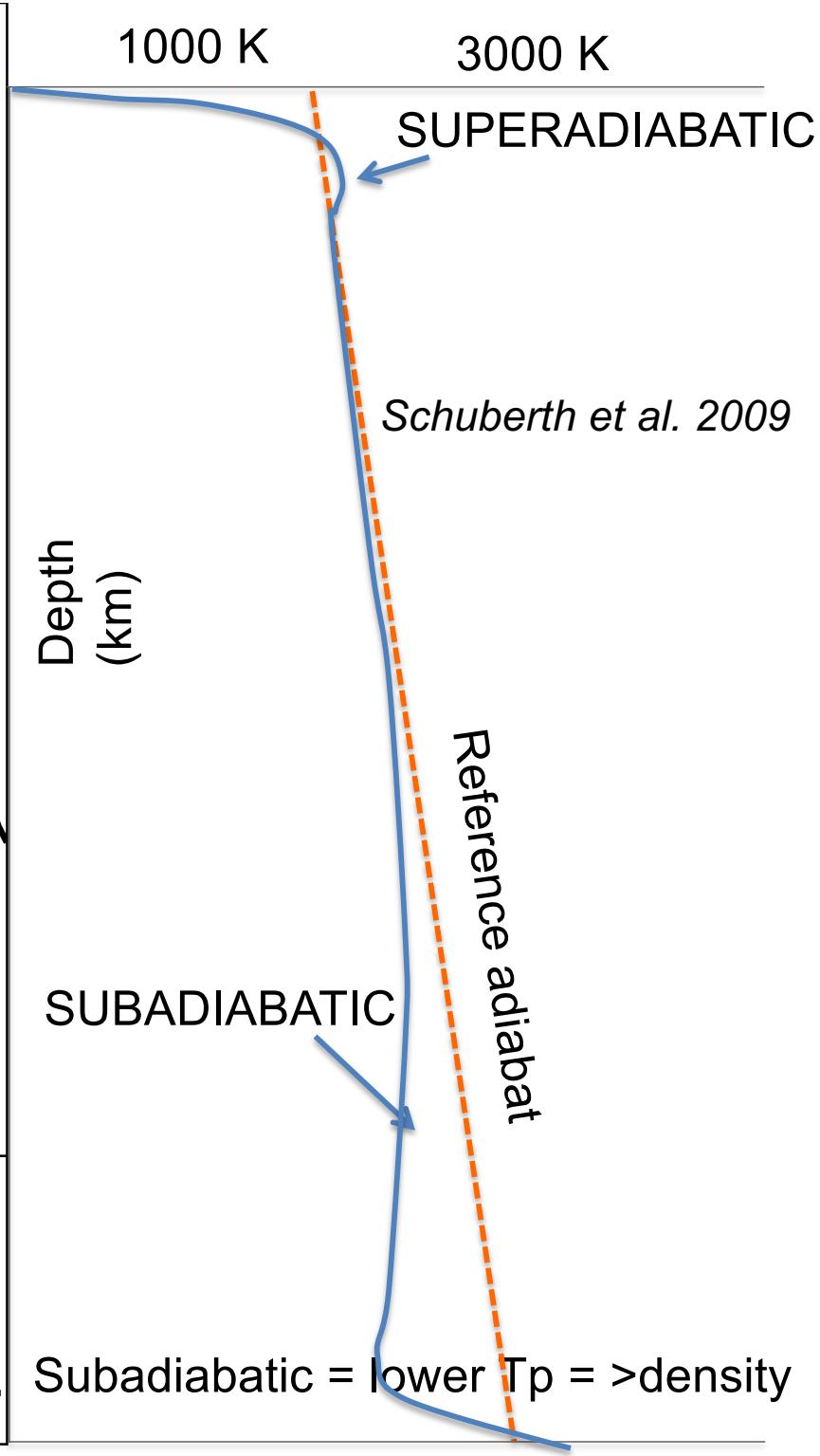
1000 K
3000 K
SUPERADIABATIC
Schuberth et al. 2009
Depth
(km)
Reference adiabat
SUBADIABATIC
Subadiabatic = lower Tp = >density

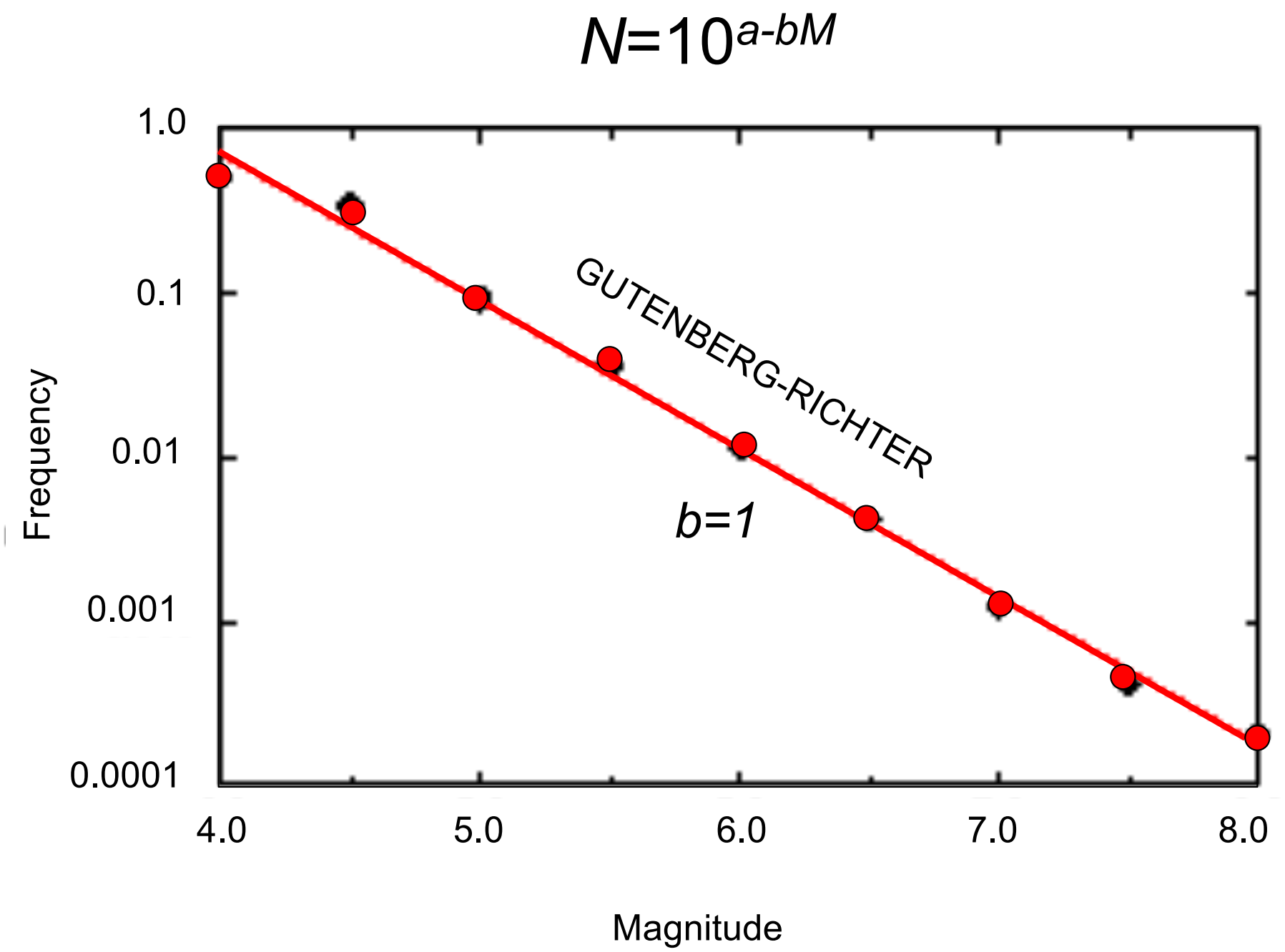
$N=10^{a-bM}$
1.0
0.1
0.01
0.001
0.0001
Frequency
GUTENBERG-RICHTER
b=1
4.0
5.0
6.0
7.0
8.0
Magnitude

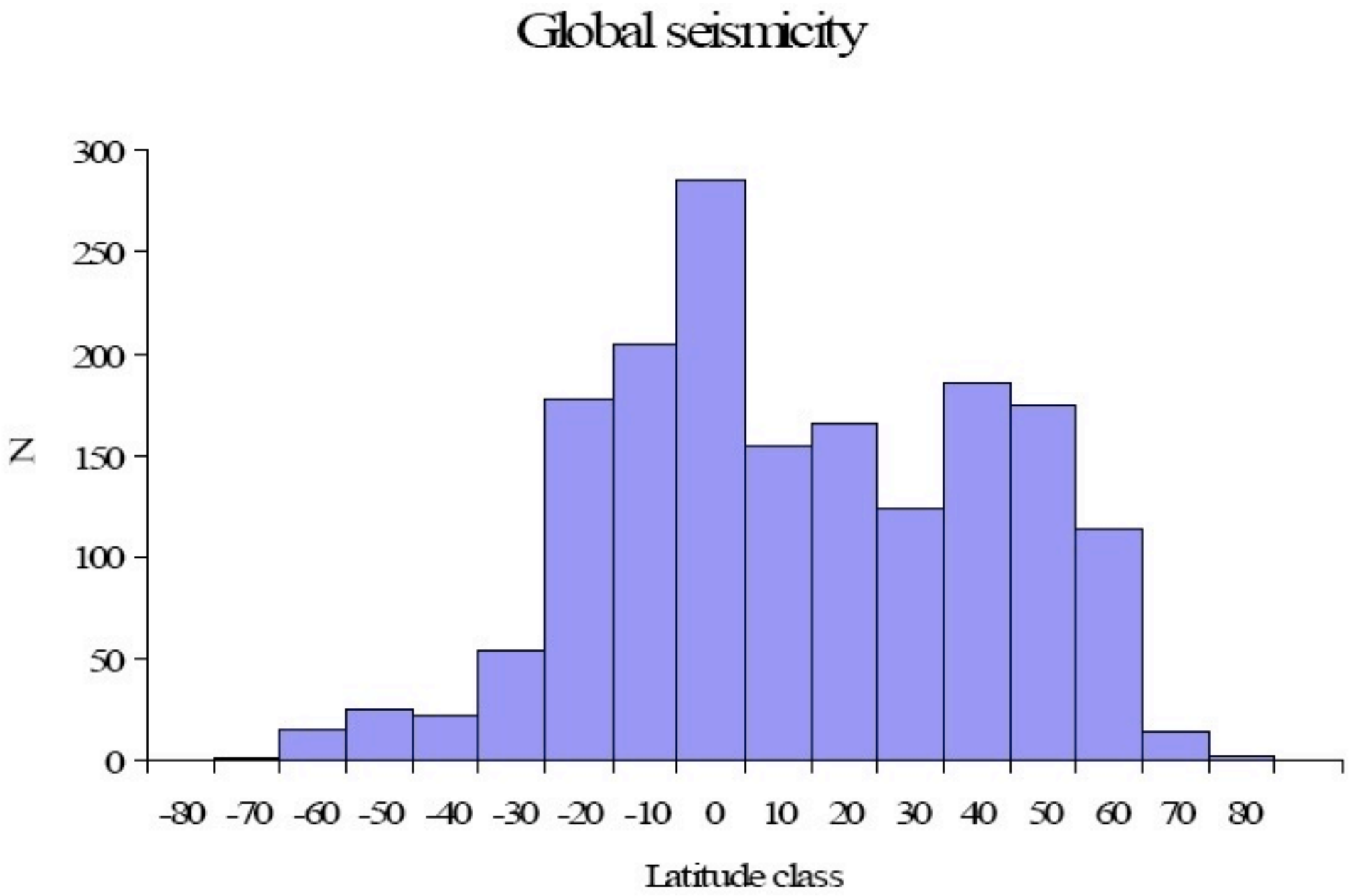

Riguzzi et al., 2010 Tectonophysics

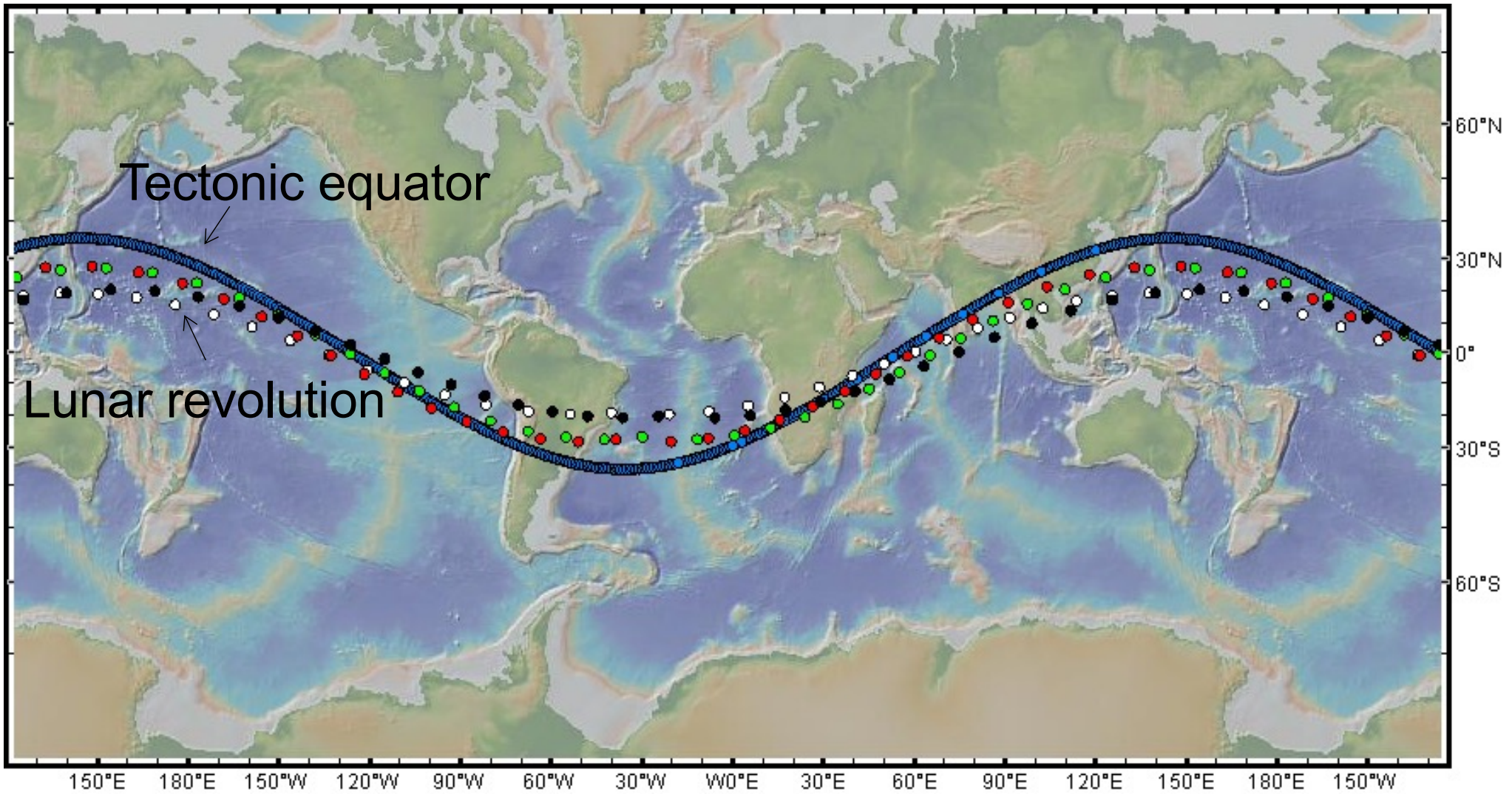

Adinolfi et al. in prep.

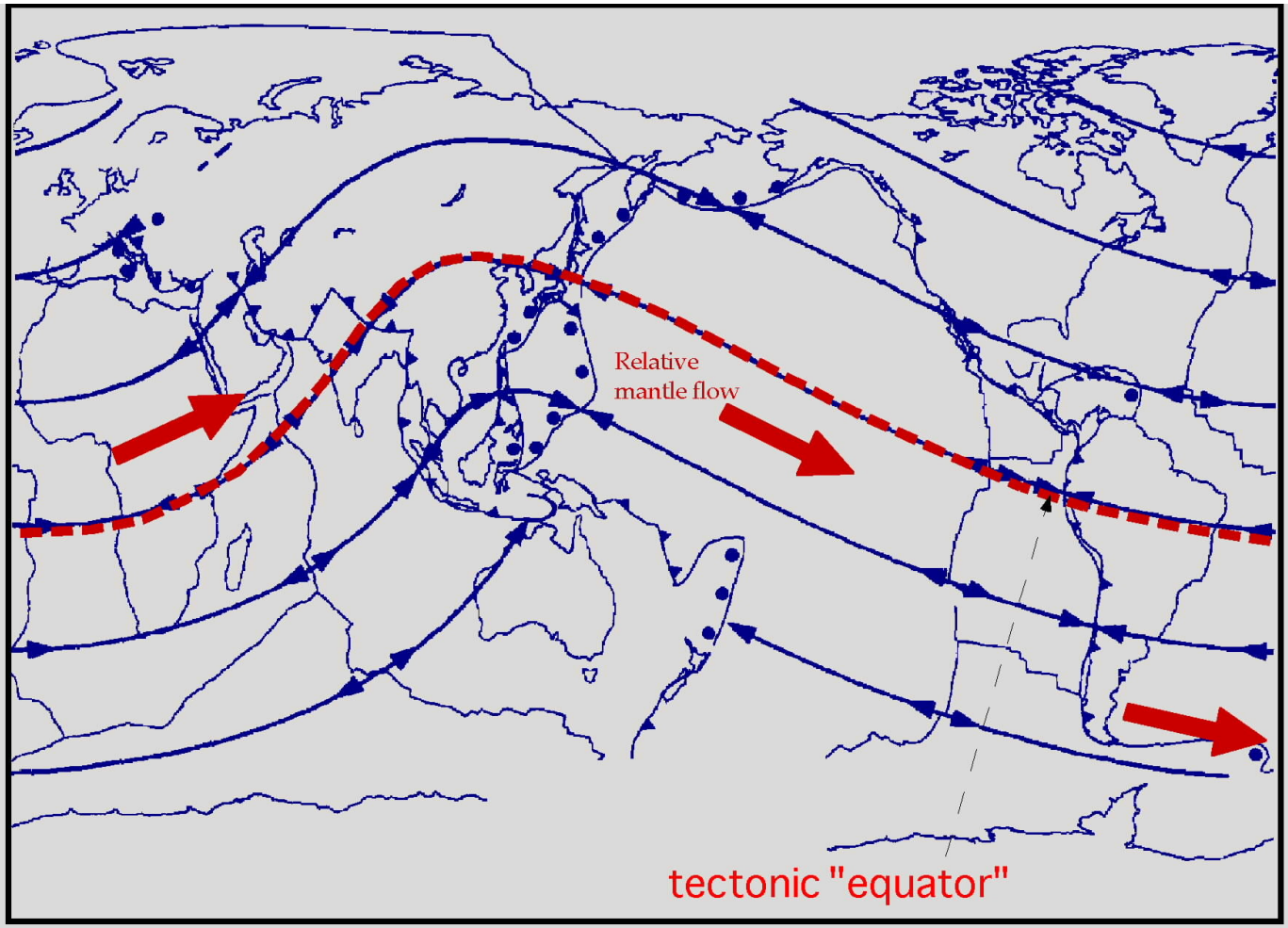

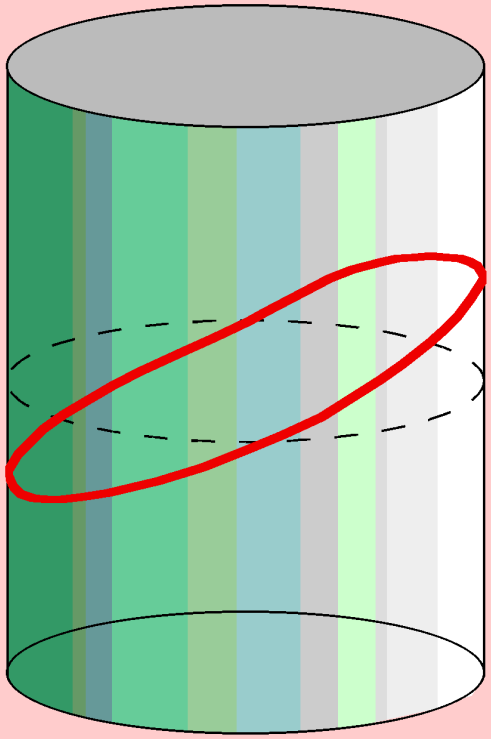

Tectonic equator

Geographic equator

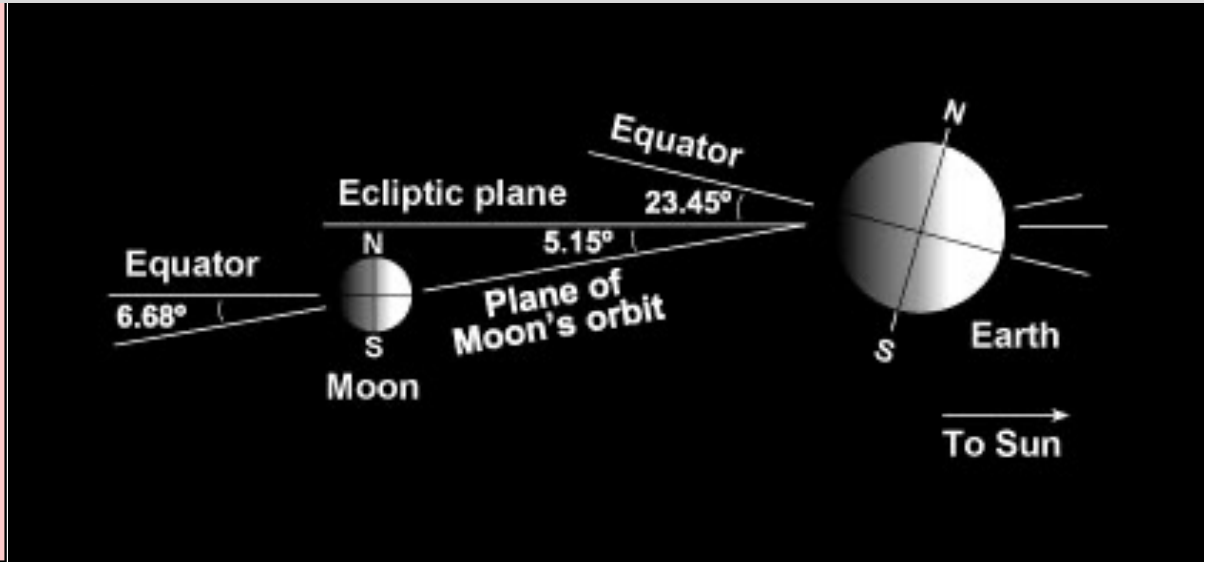

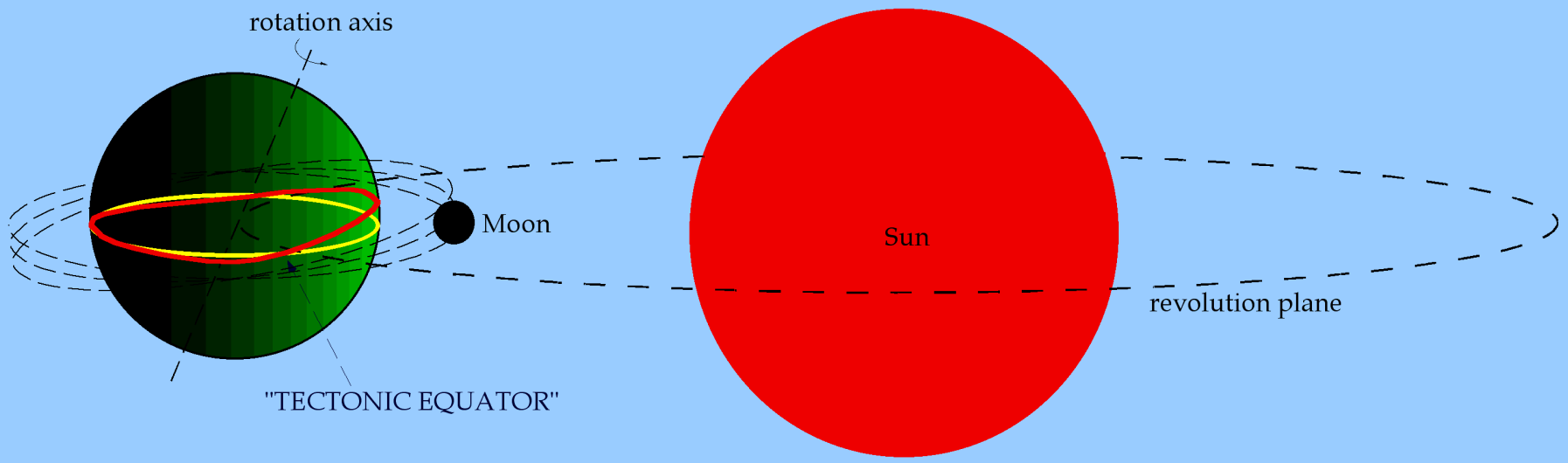
rotation axis
Moon
Sun
revolution plane
"TECTONIC EQUATOR"

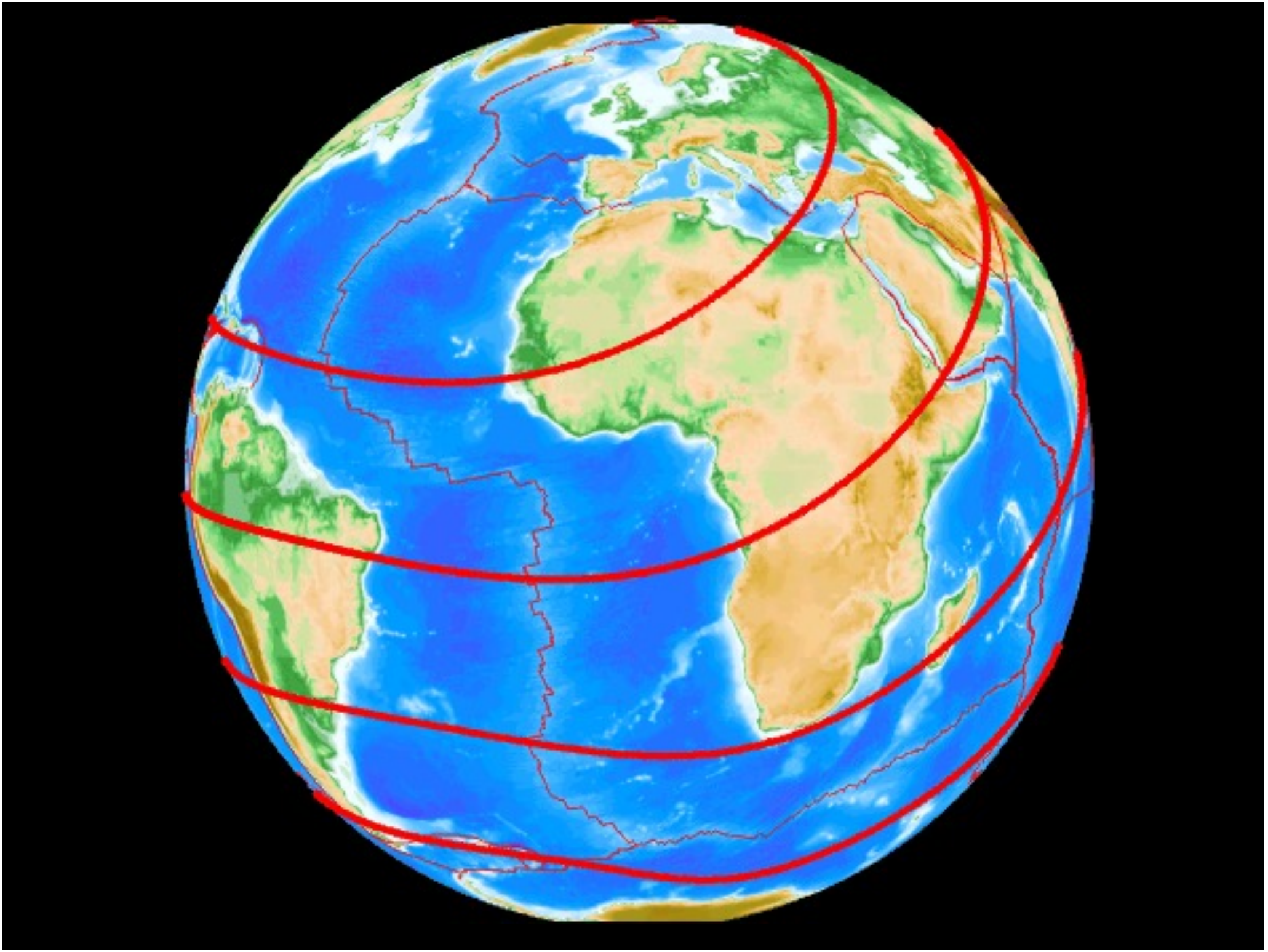

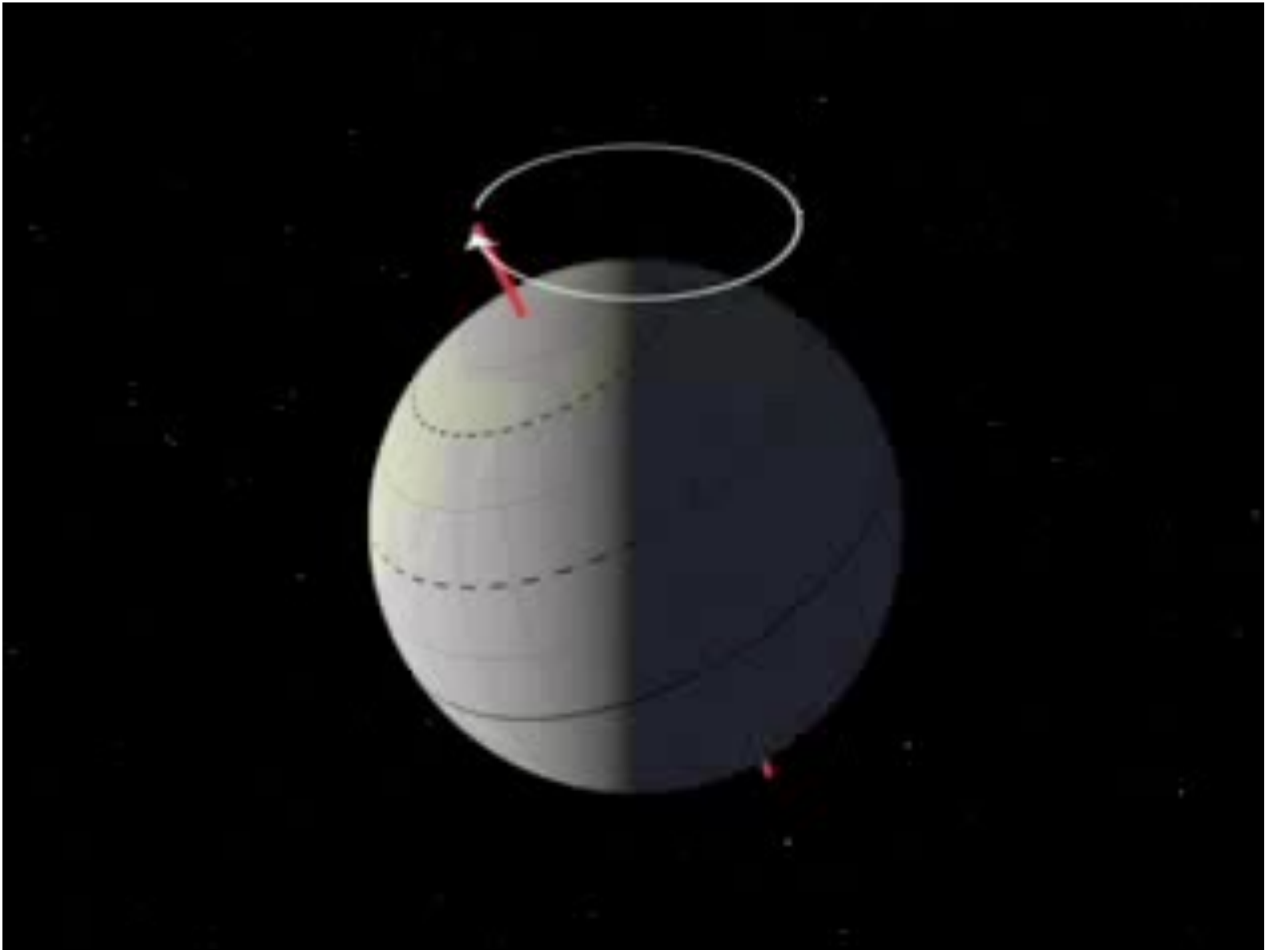

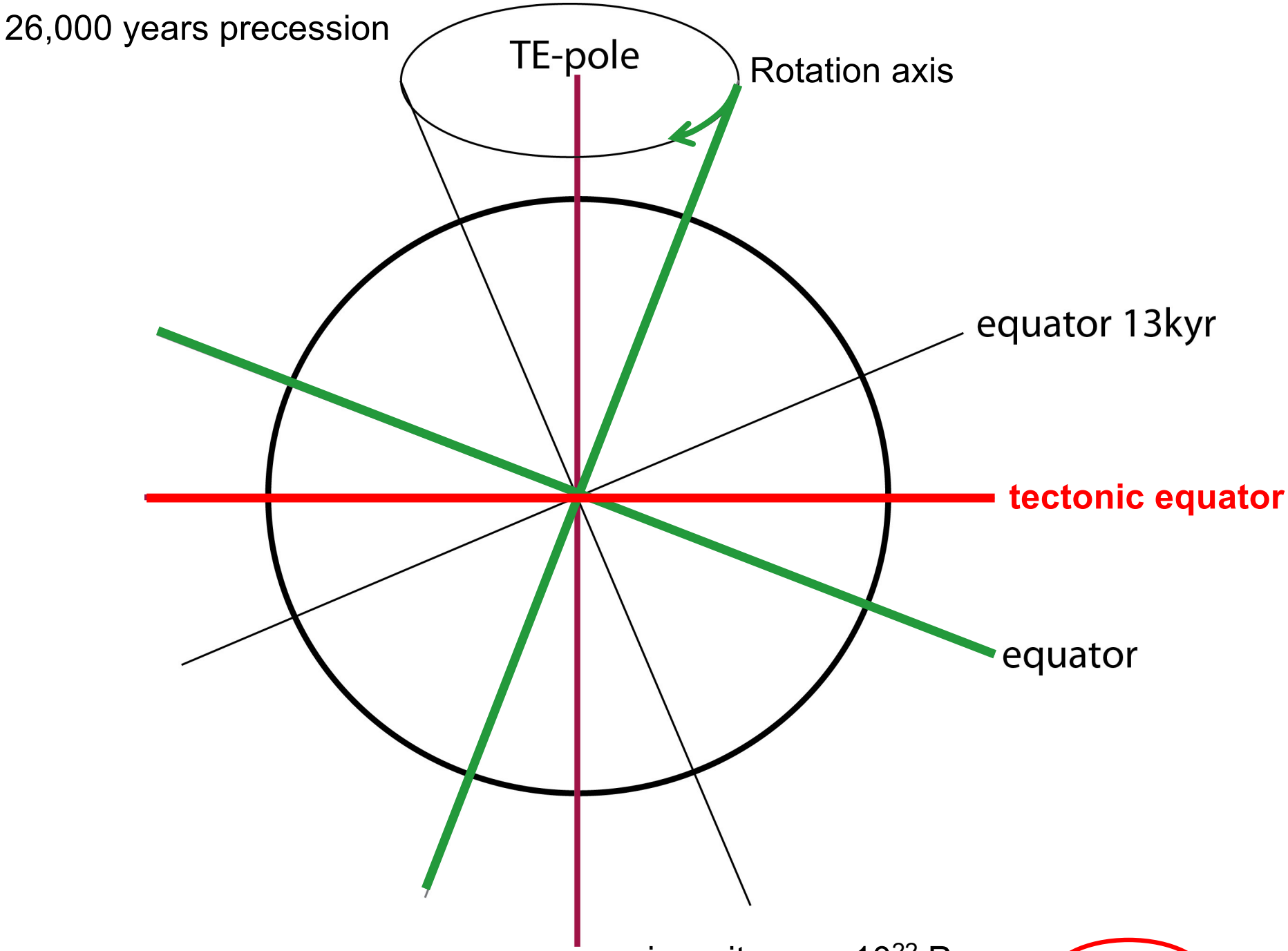

$$\text{Maxwell relaxation time} = \frac{\text{viscosity}}{\text{rigidity}} = \frac{10^{22}\ \text{Pa s}}{10^{11}\ \text{Pa}} = 10^{11}\ \text{s}$$

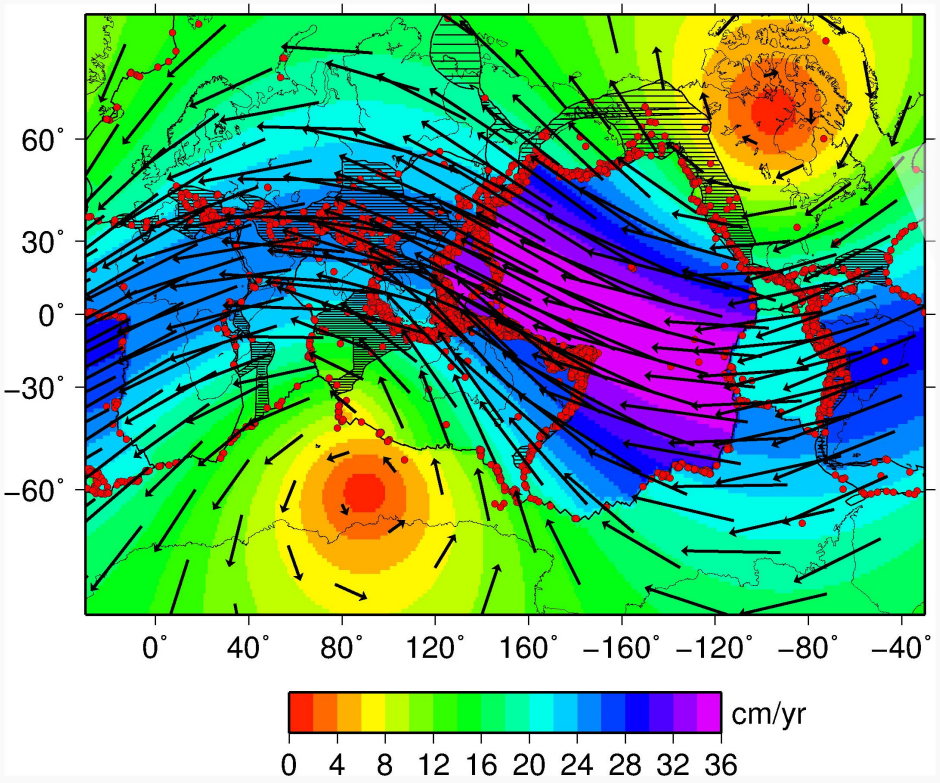

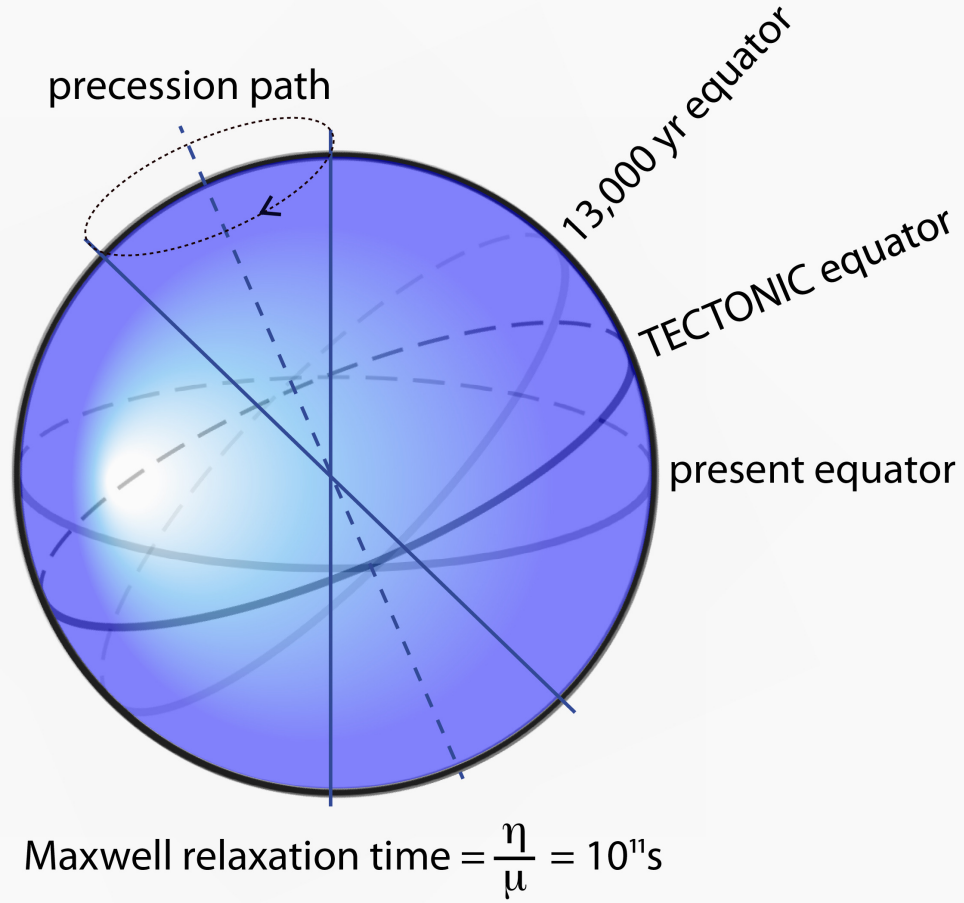

Zaccagnino et al. 2020

TIDAL FRICTION

- Earth's rotation is slowing: with dinosaurs the day was of 22h
- Moon receding at 38 mm/year
- Tidal friction $10^{20\text{-}21}$ J/yr
- Tectonic moment 10^{21} J/yr

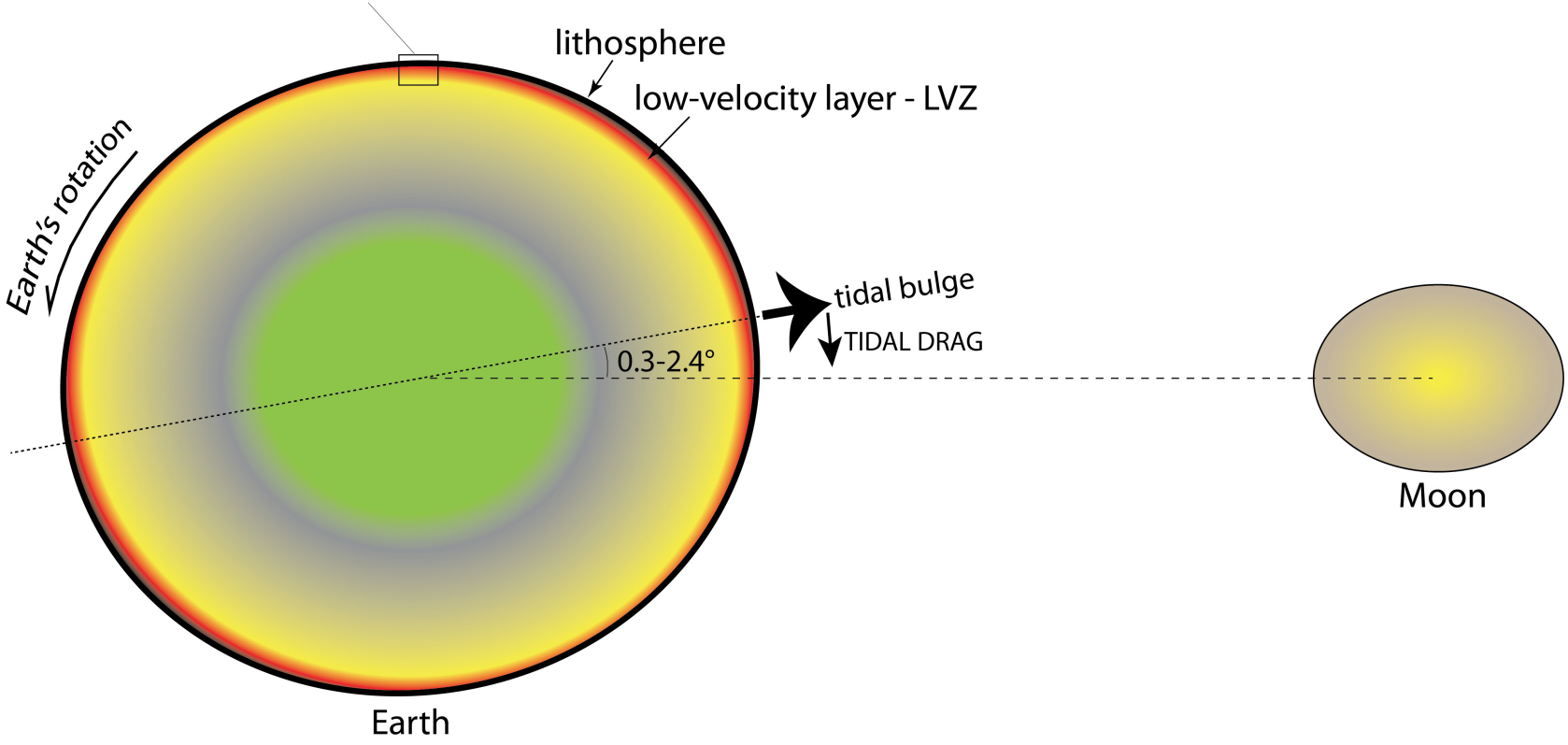

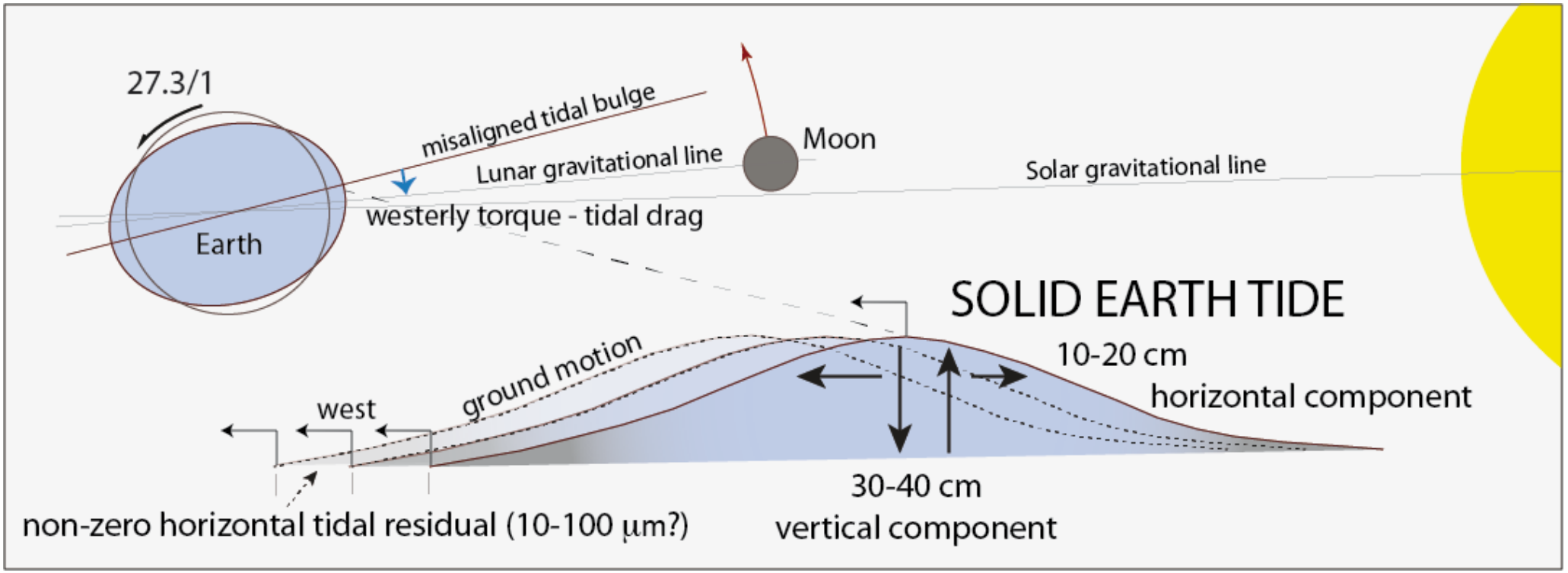

Zaccagnino et al. 2020

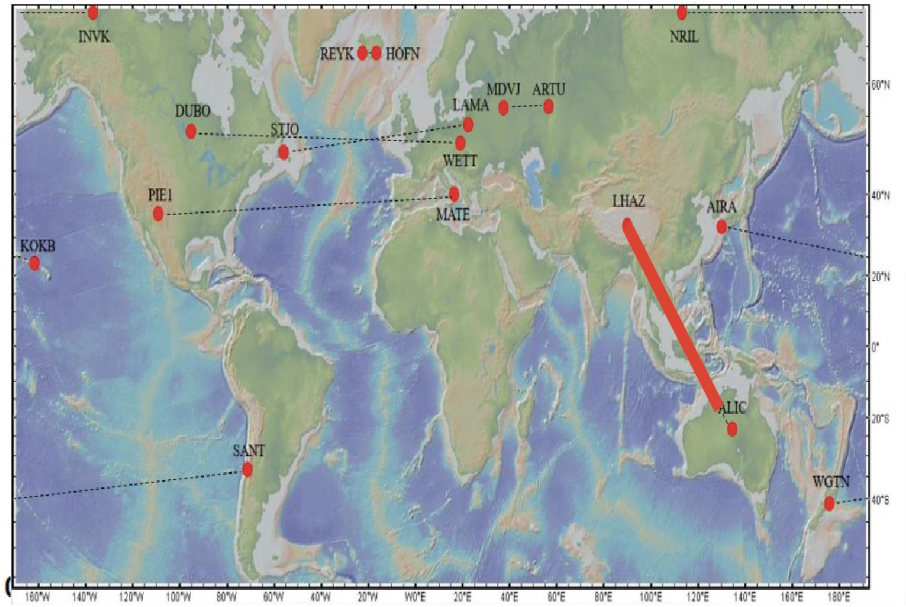

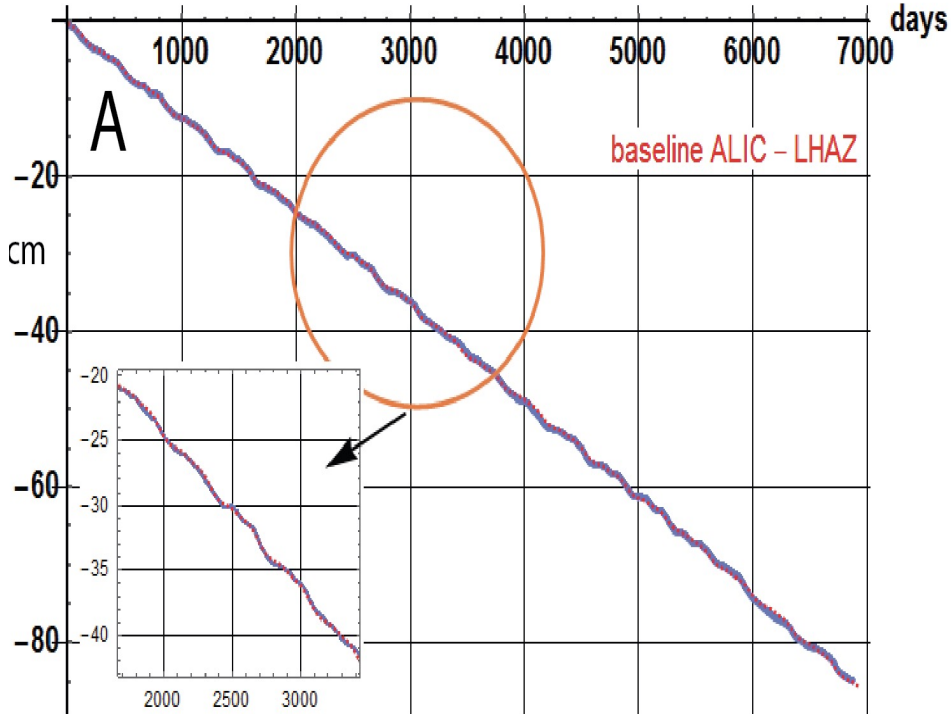

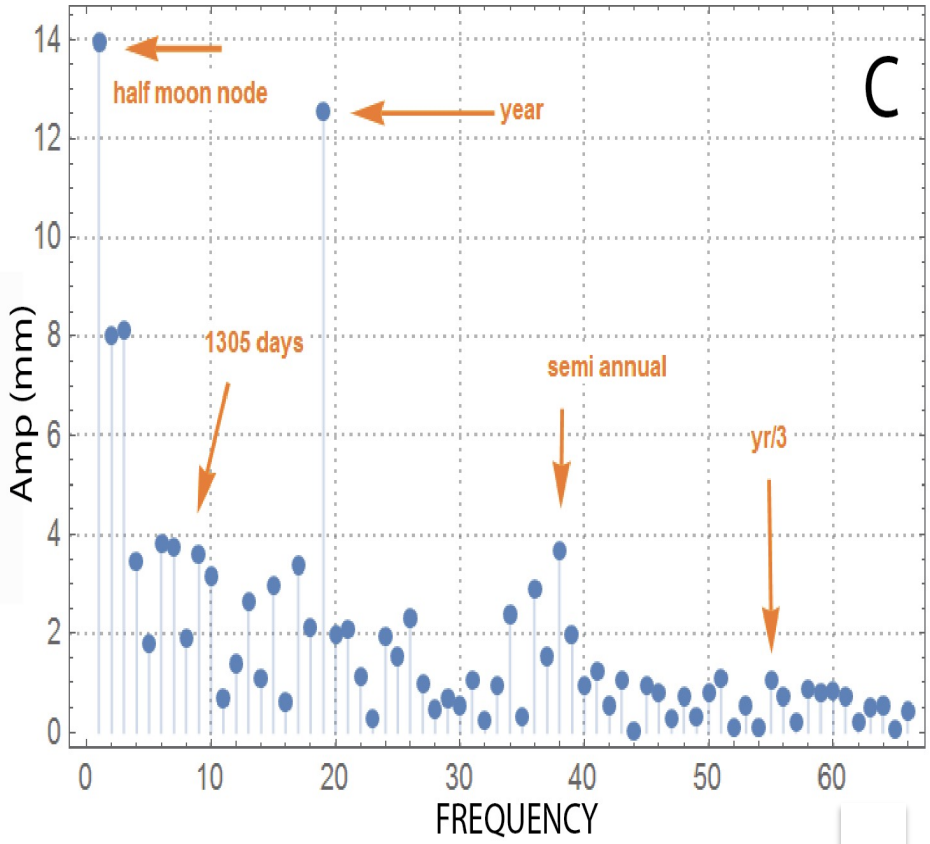

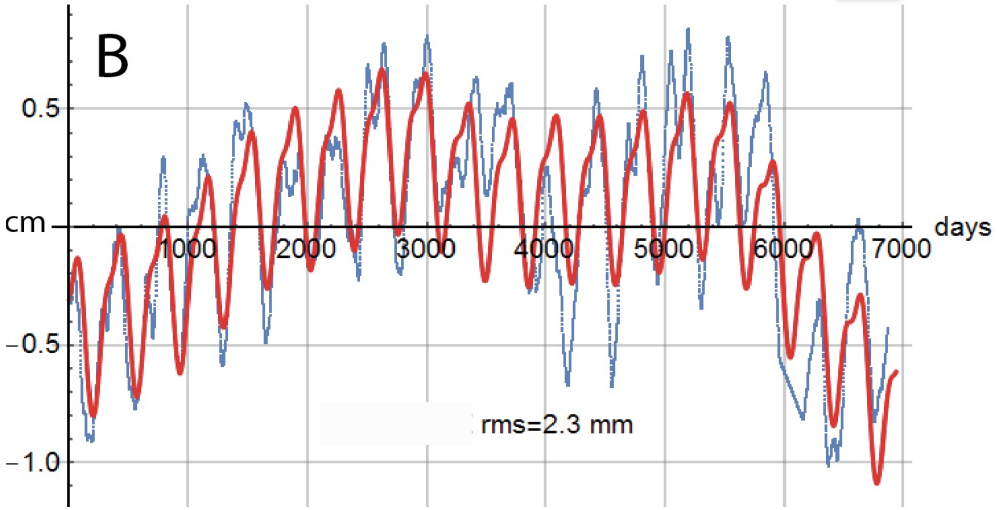

Zaccagnino et al. 2020 ESR

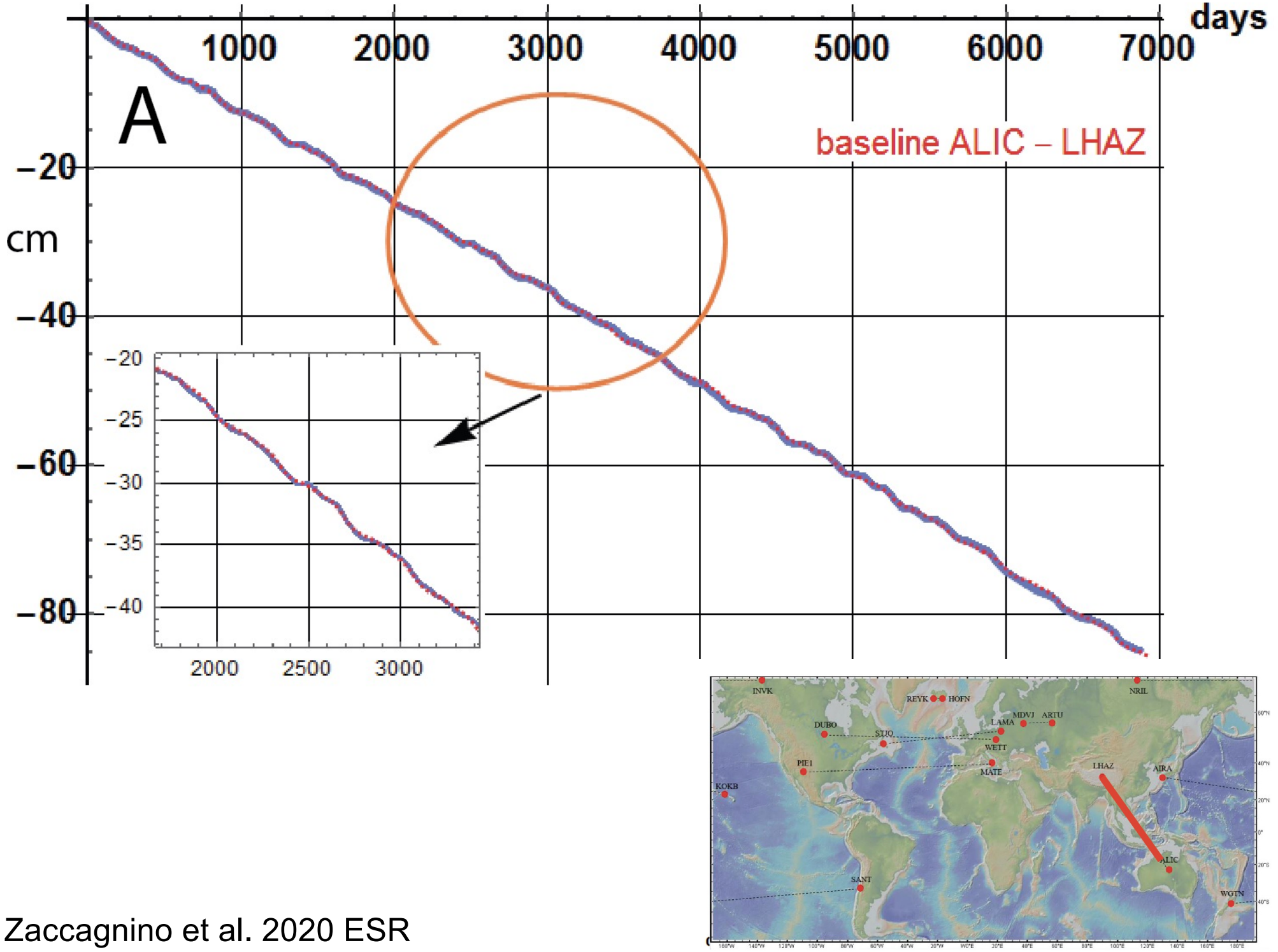

Zaccagnino et al. 2020 ESR

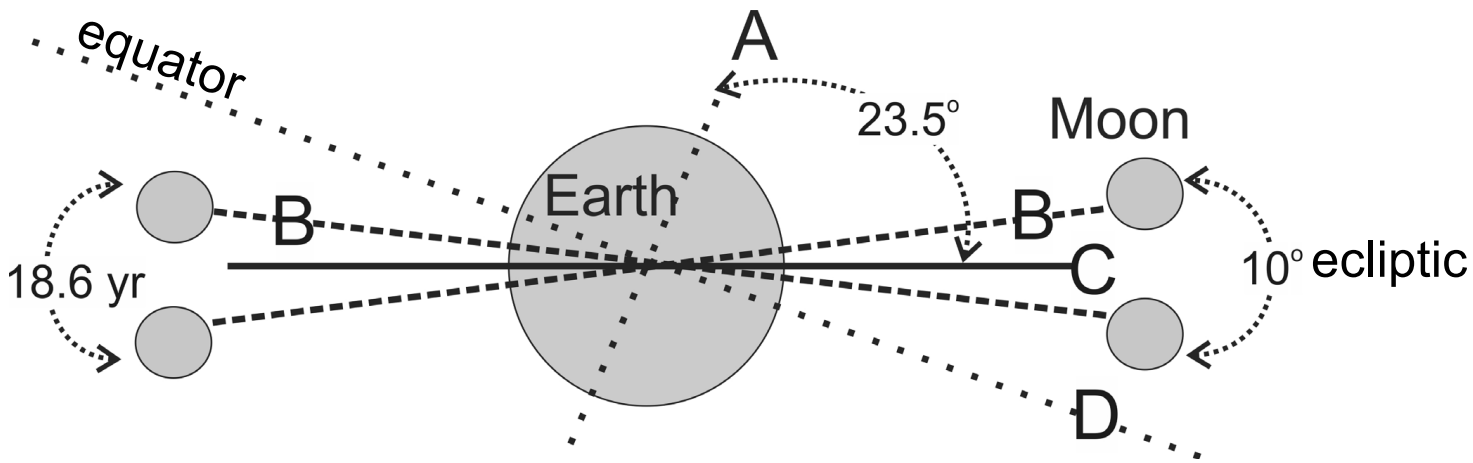
equator
A
23.5°
Moon
Earth
B
B
18.6 yr
C
10° ecliptic
D

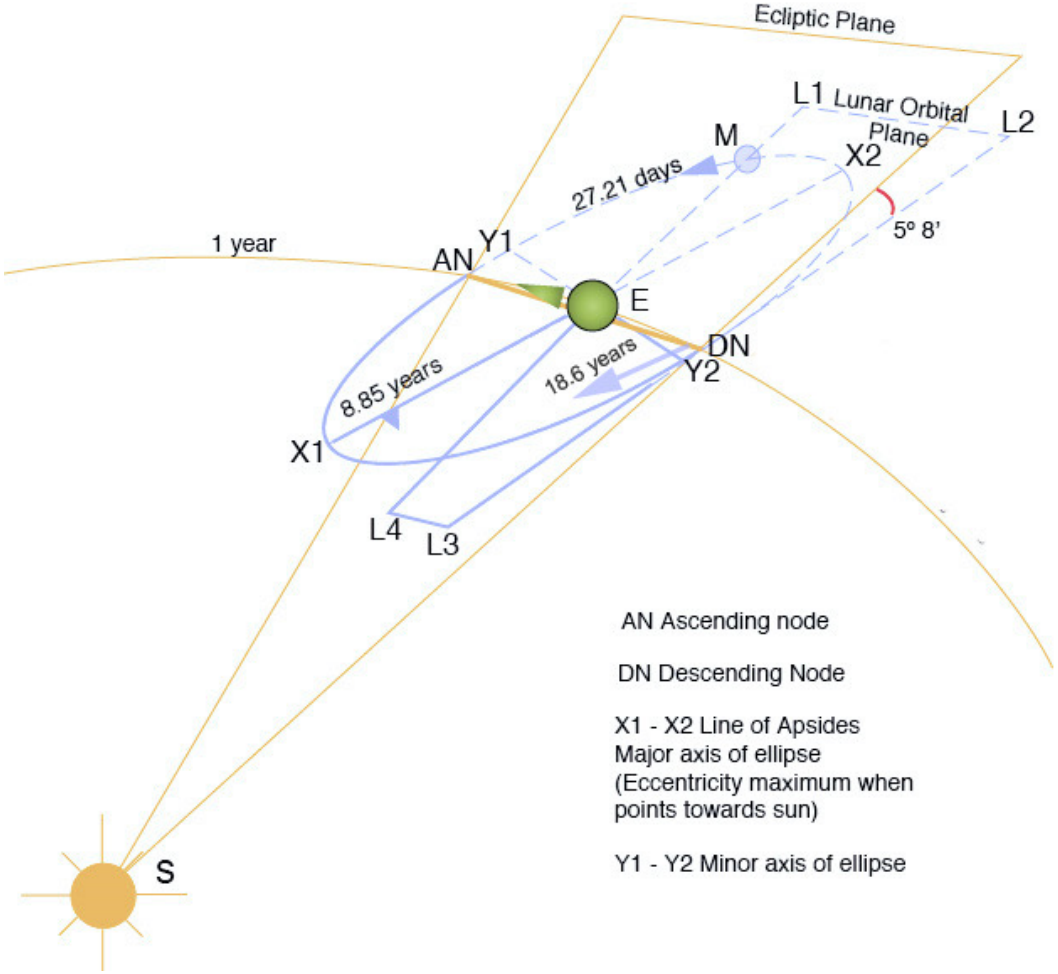
Ecliptic Plane
L1
Lunar Orbital Plane
L2
M
X2
27.21 days
5° 8'
1 year
AN
Y1
E
DN
Y2
8.85 years
18.6 years
X1
L4
L3
S
AN Ascending node
DN Descending Node
X1 - X2 Line of Apsides
Major axis of ellipse
(Eccentricity maximum when points towards sun)
Y1 - Y2 Minor axis of ellipse

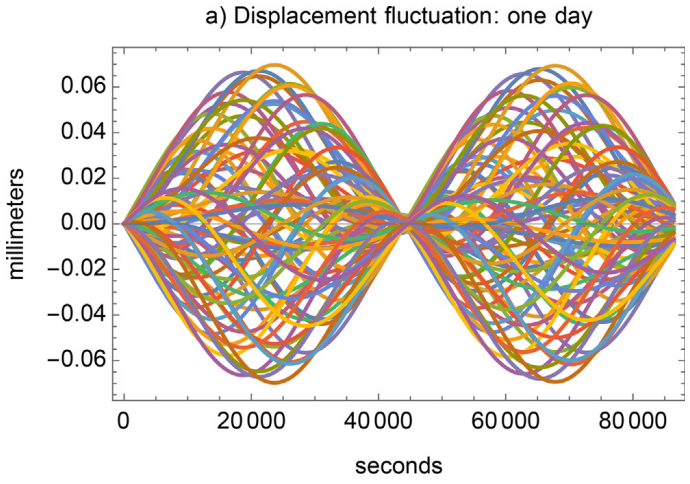

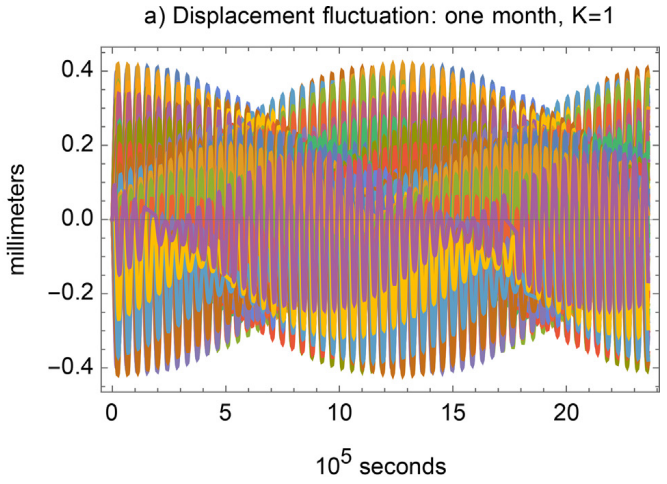

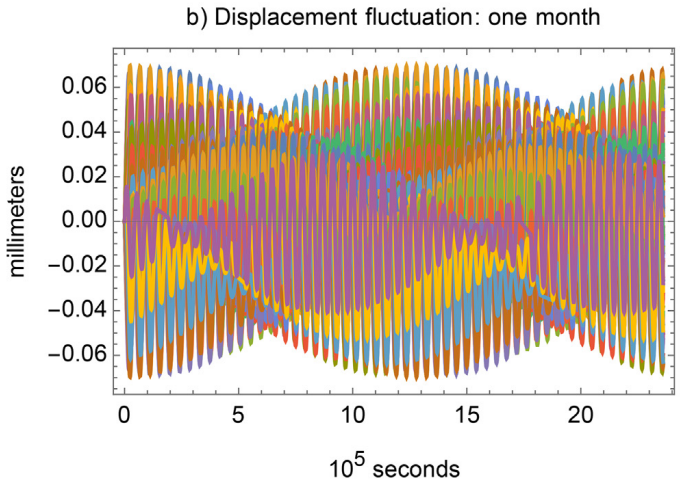

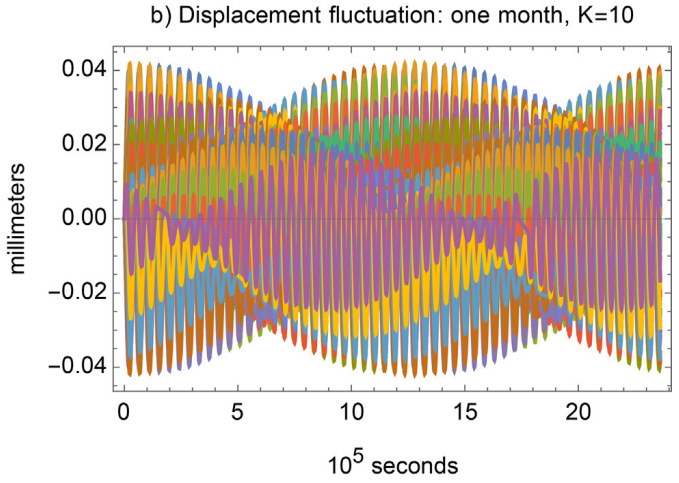

K=frictional coefficient

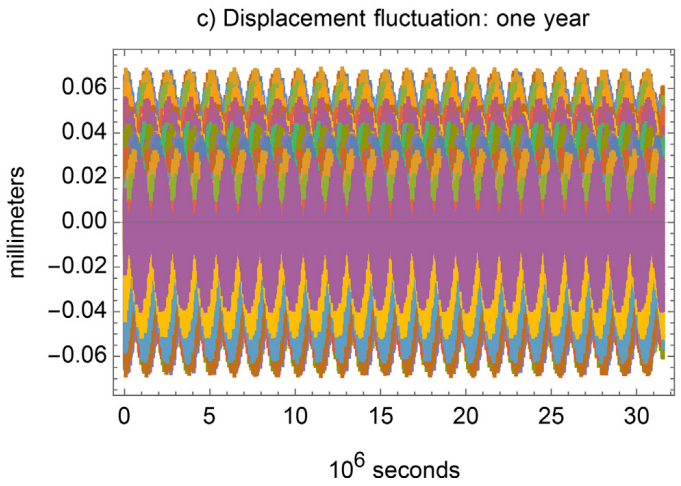

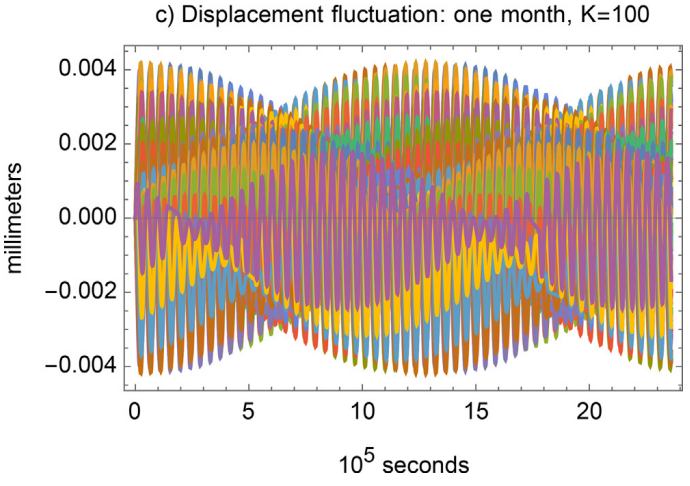

Nesi et al. 2023 GSF

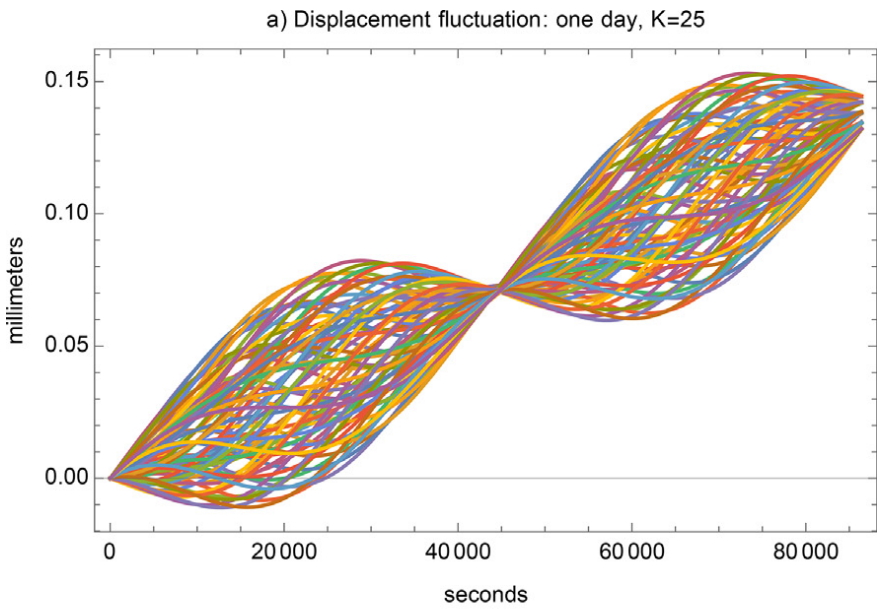

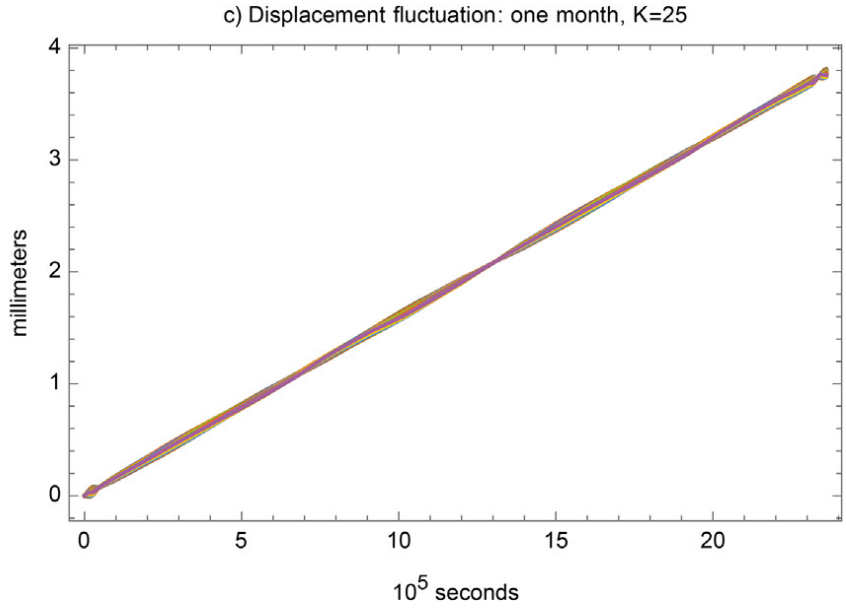

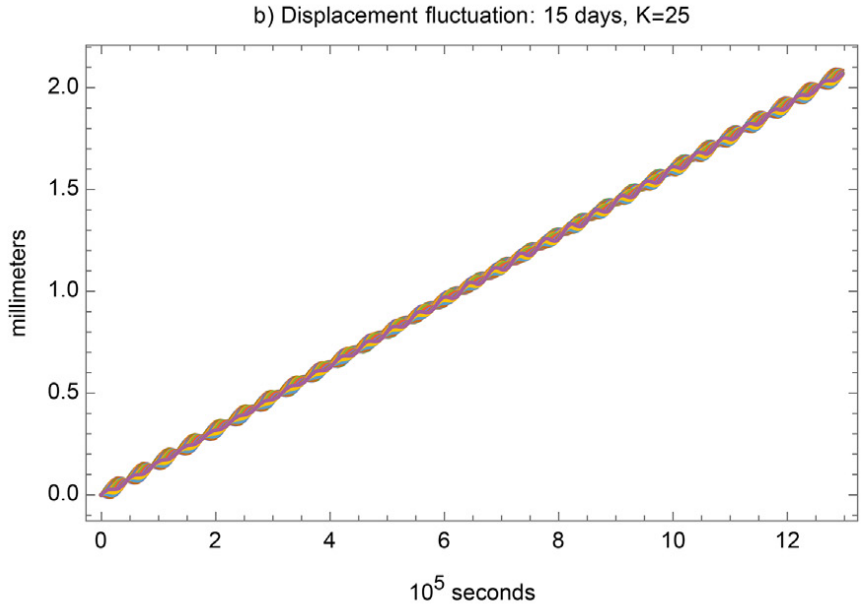

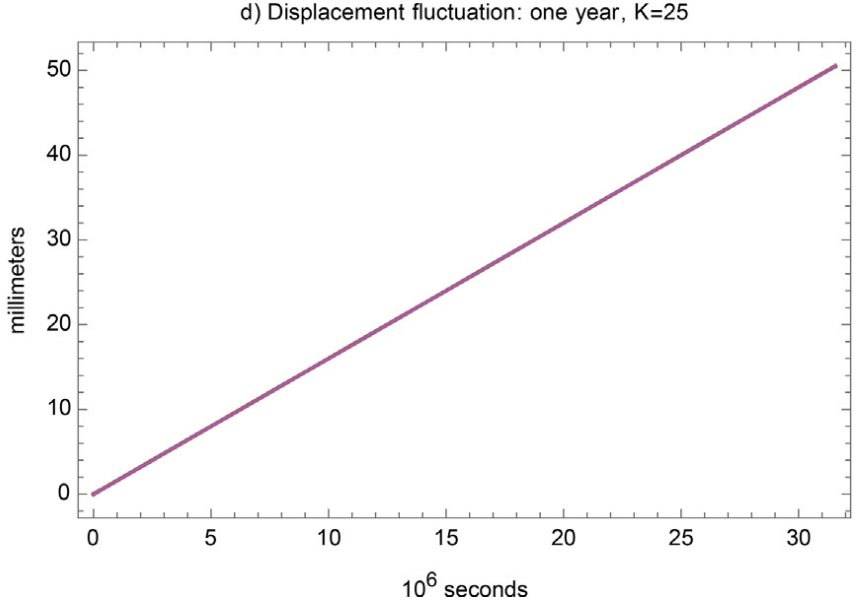

Nesi et al. 2023 GSF

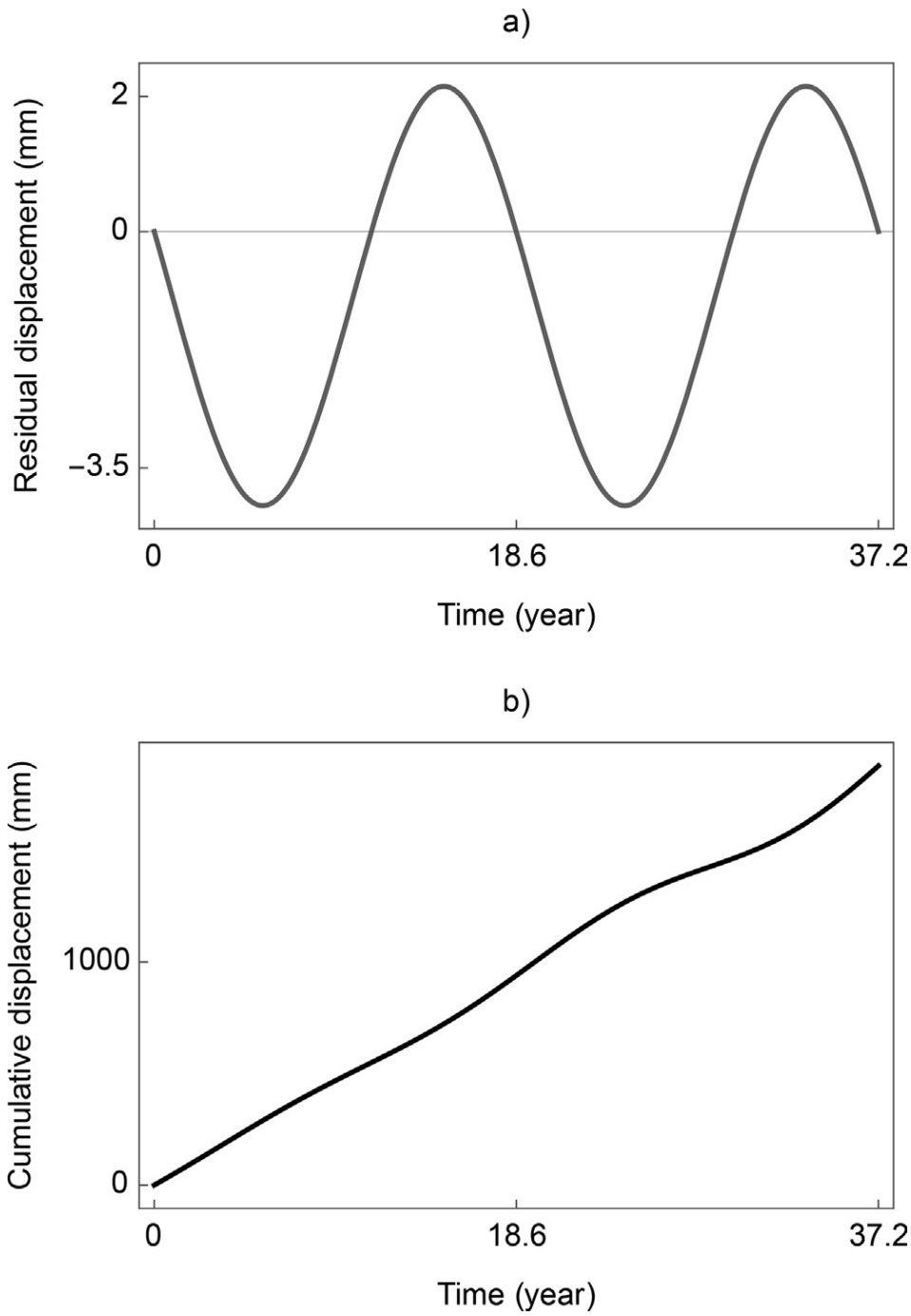

Fig. 7. Tidal modulations of plate motions around the linear long-term trend for $K = 50\ s^{-1}$ (corresponding to $\eta \approx 2.5 \times 10^{15}$ Pa·s) produced by the 18.6-years-long

Nesi et al. 2023 GSF

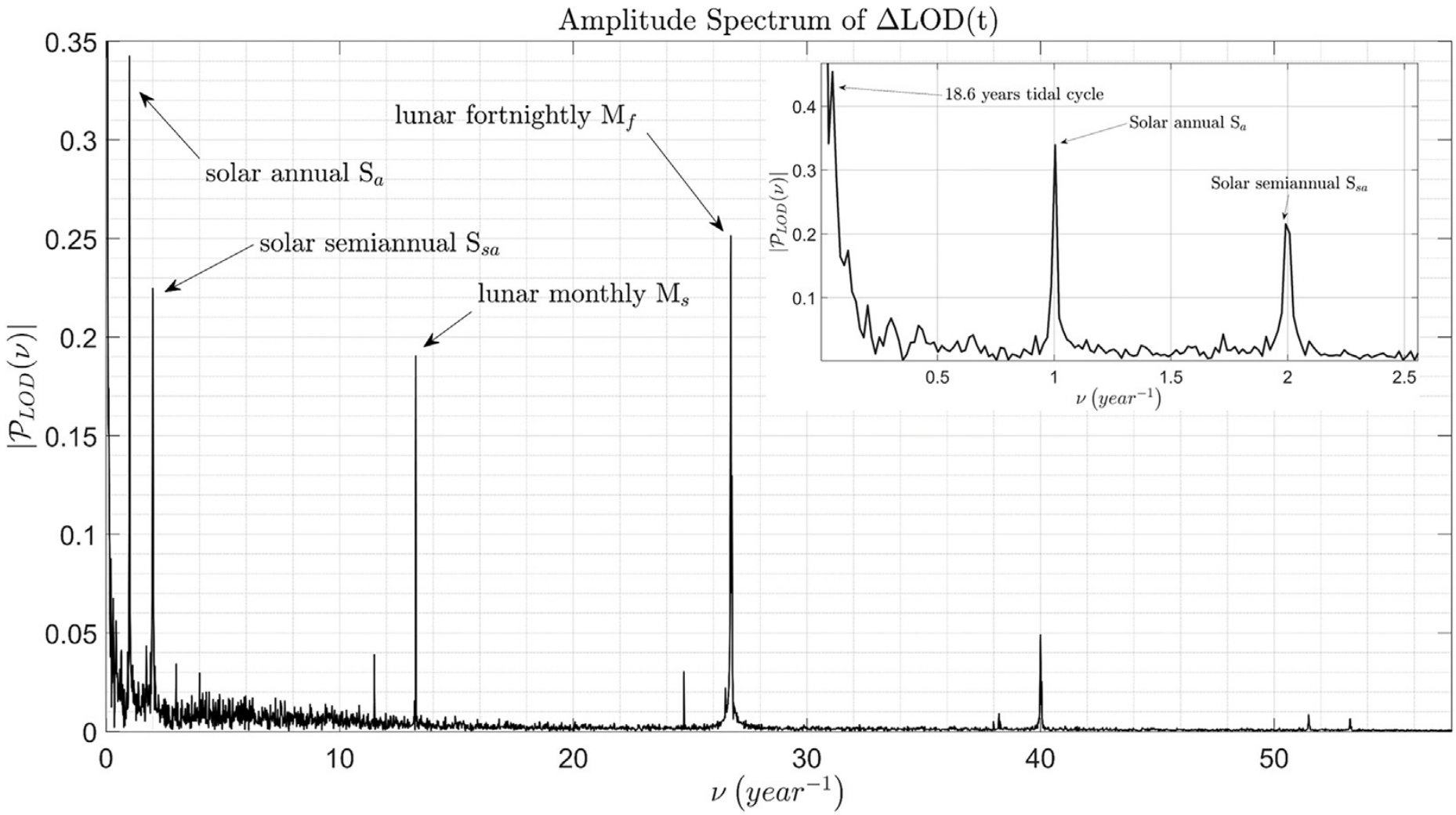

Nesi et al. 2023 GSF

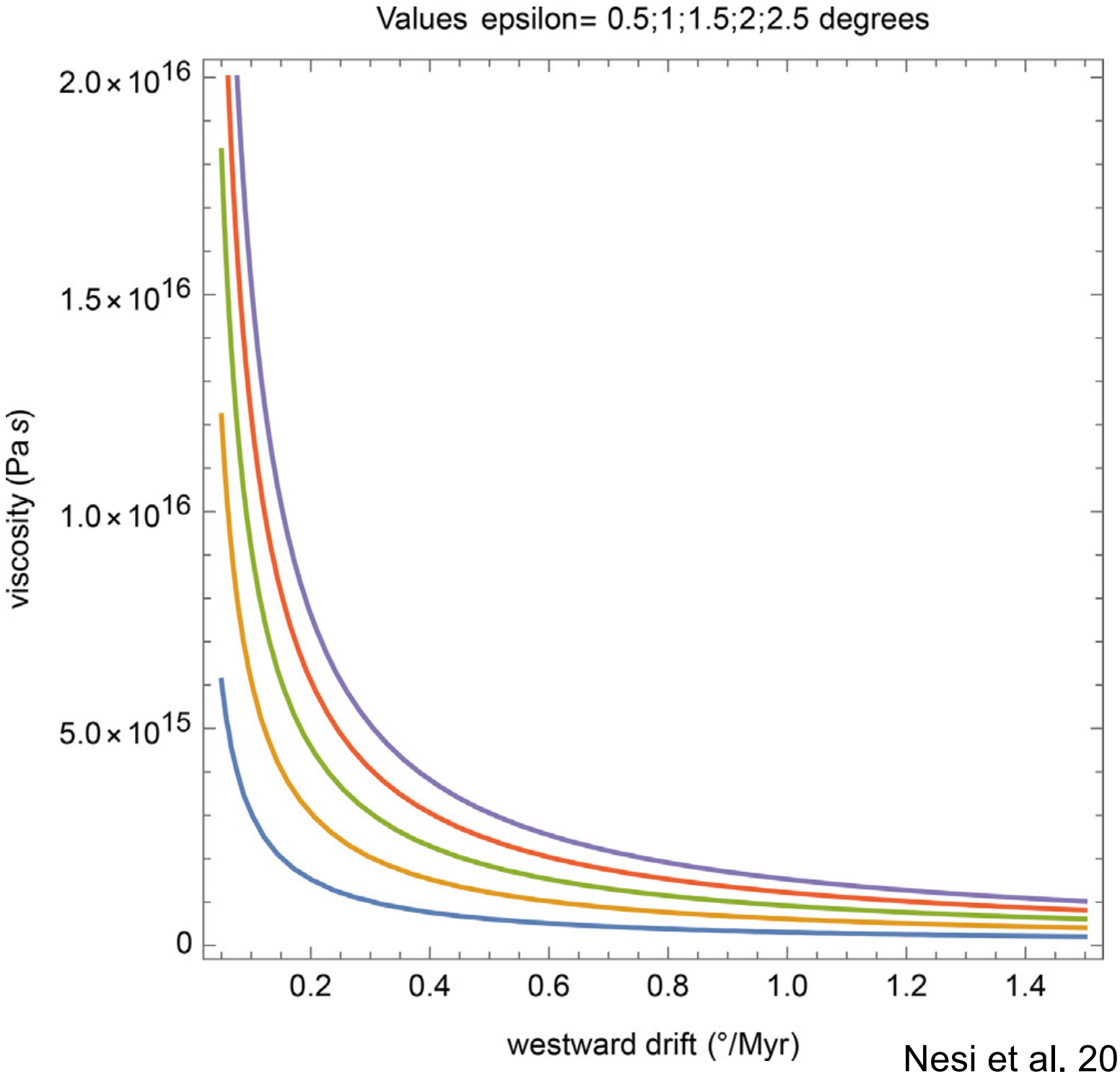

Nesi et al. 2023 GSF

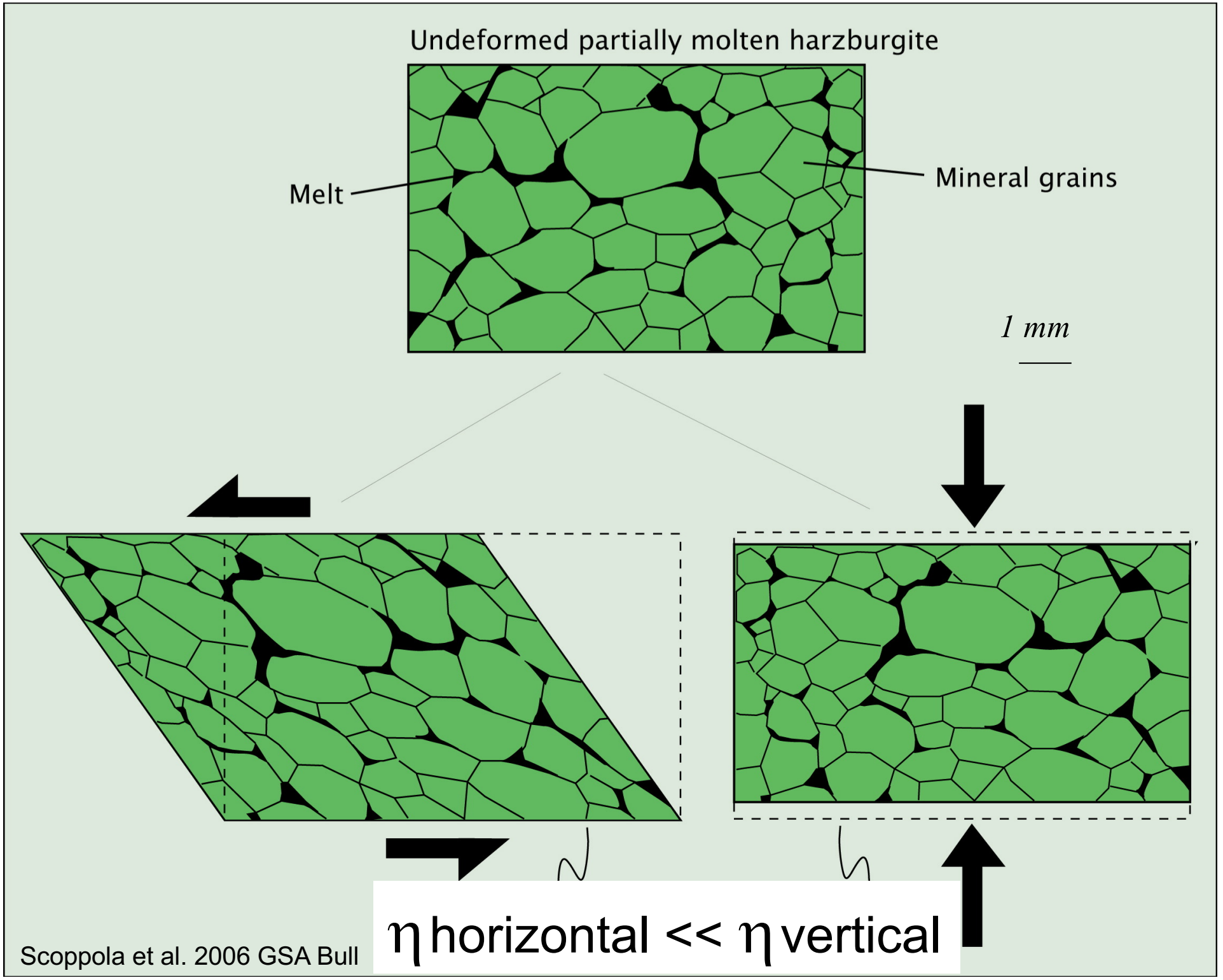
Undeformed partially molten harzburgite
Melt
Mineral grains
1 mm
η horizontal << η vertical
Scoppola et al. 2006 GSA Bull

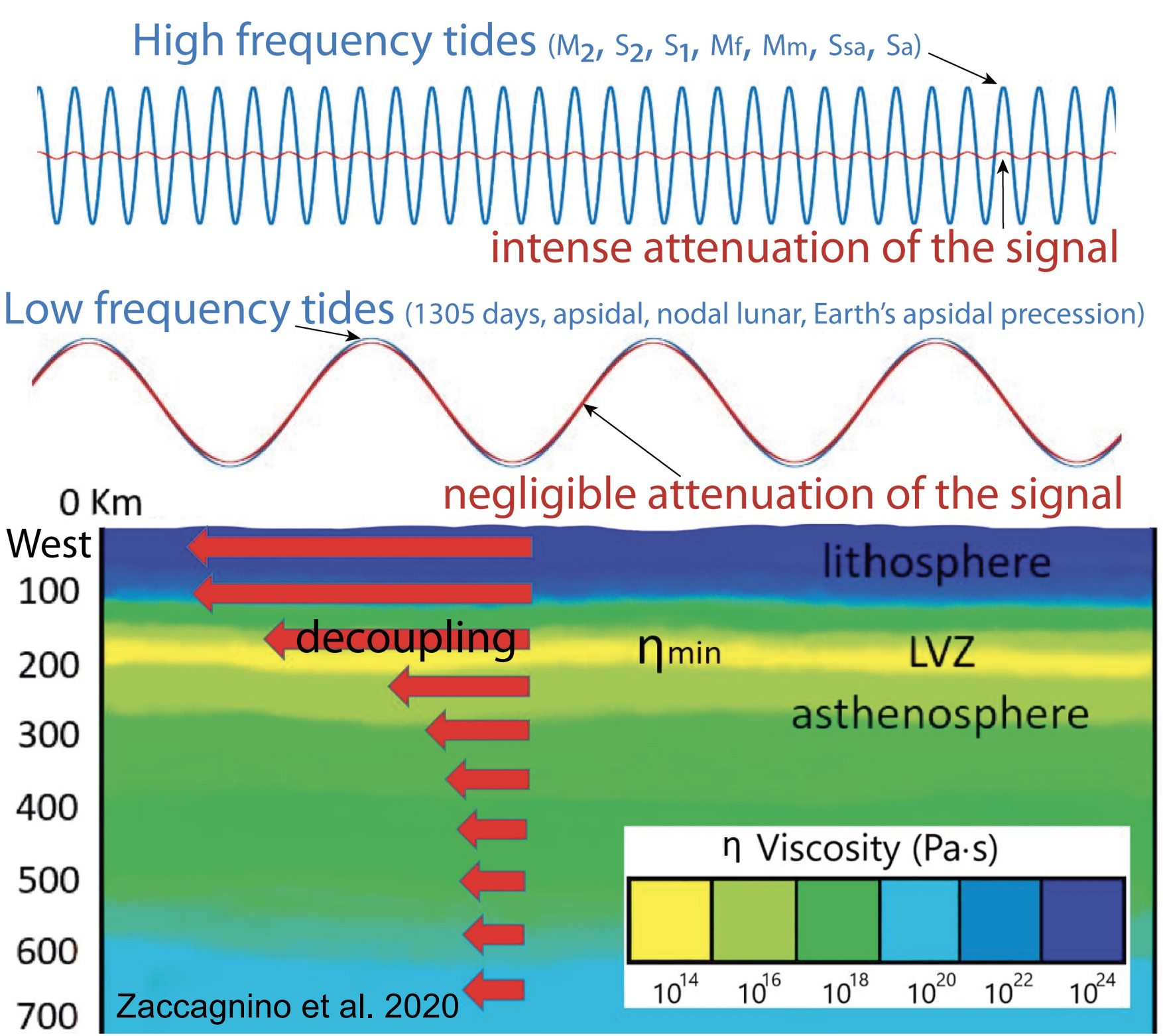
High frequency tides (M_2, S_2, S_1, Mf, Mm, Ssa, Sa)
intense attenuation of the signal
Low frequency tides (1305 days, apsidal, nodal lunar, Earth's apsidal precession)
negligible attenuation of the signal
0 Km
West
100
200
300
400
500
600
700
decoupling
lithosphere
η_{min}
LVZ
asthenosphere
η Viscosity (Pa·s)
10^{14} 10^{16} 10^{18} 10^{20} 10^{22} 10^{24}
Zaccagnino et al. 2020

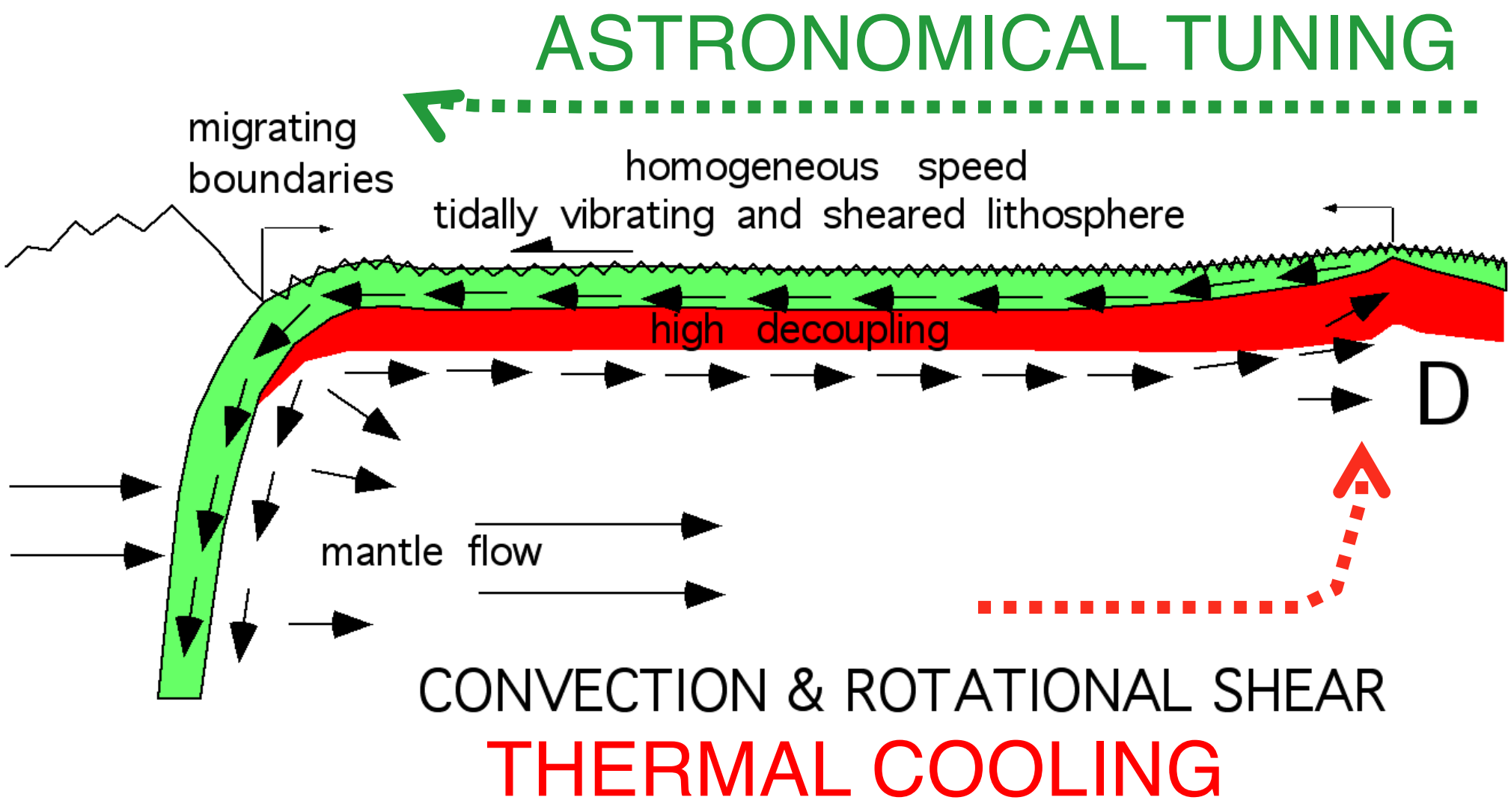

Self Organized Chaotic System

1) Orogens and Rifts show an “E-W” global asymmetry

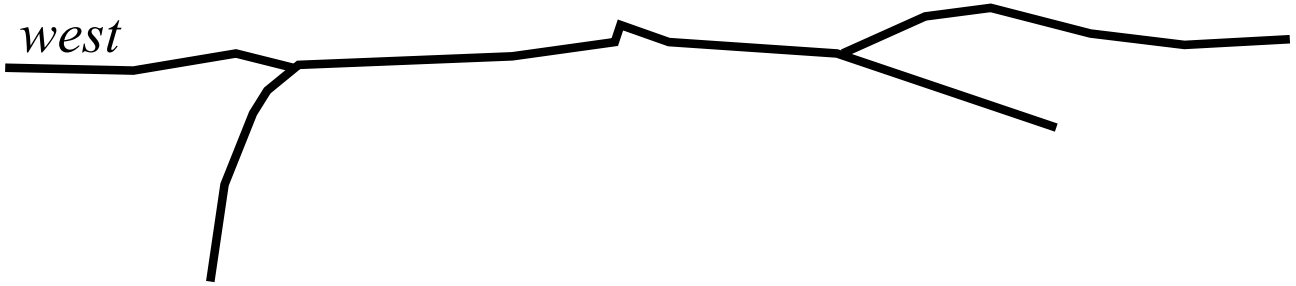

2) The lithosphere moves along a westerly polarized flow

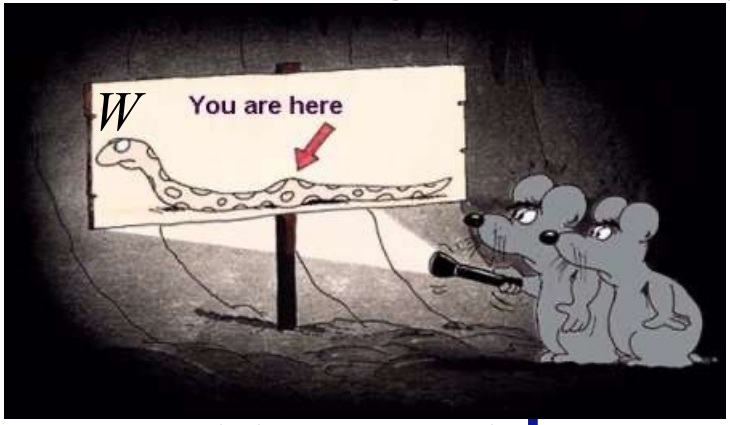

3) Plate tectonics is tuned by Earth’s rotation

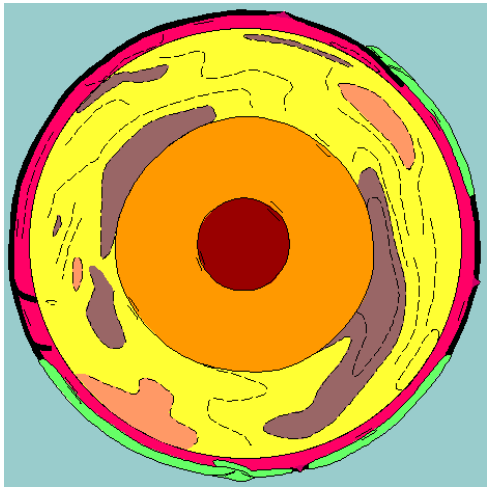

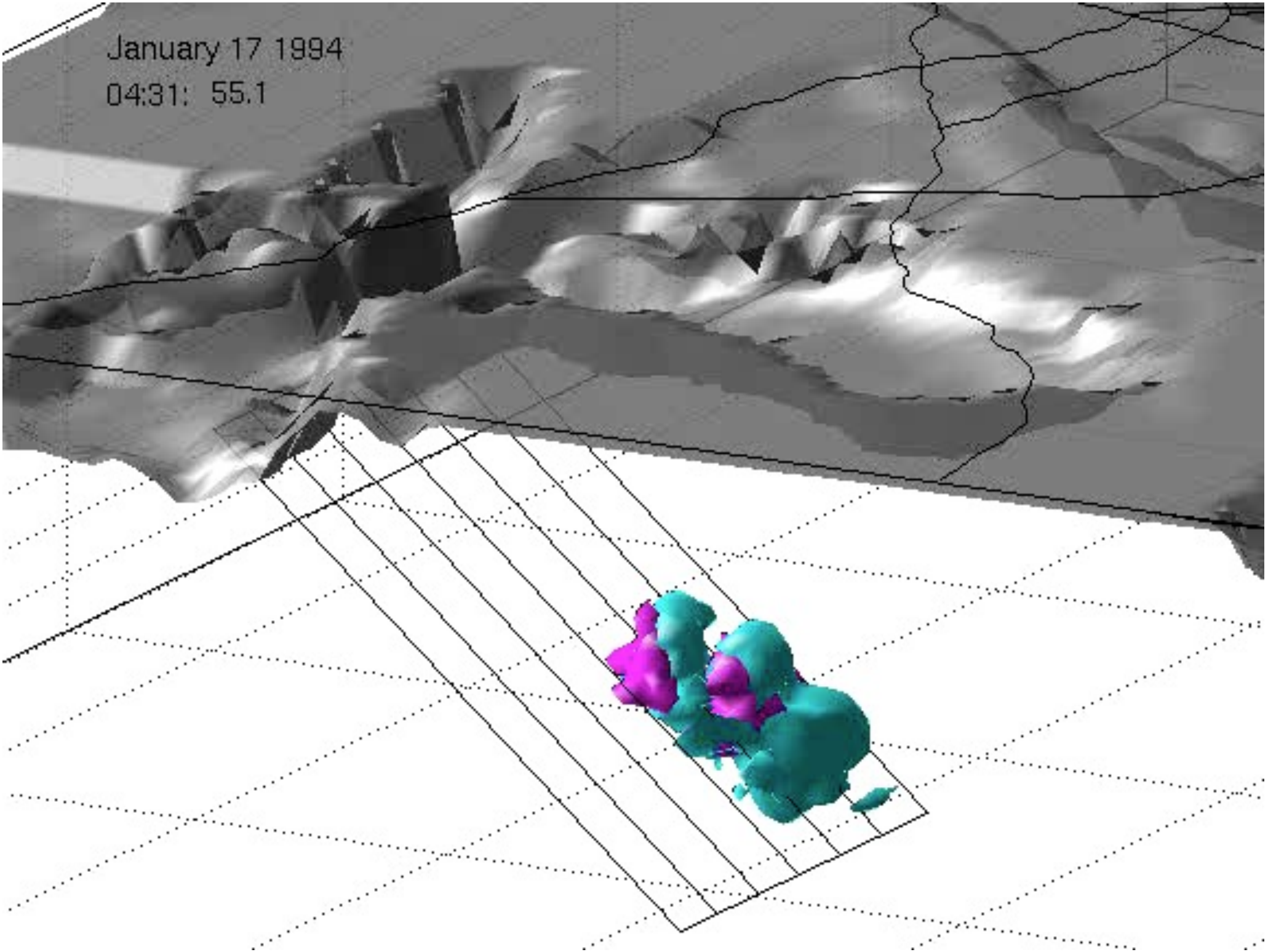
January 17 1994
04:31: 55.1

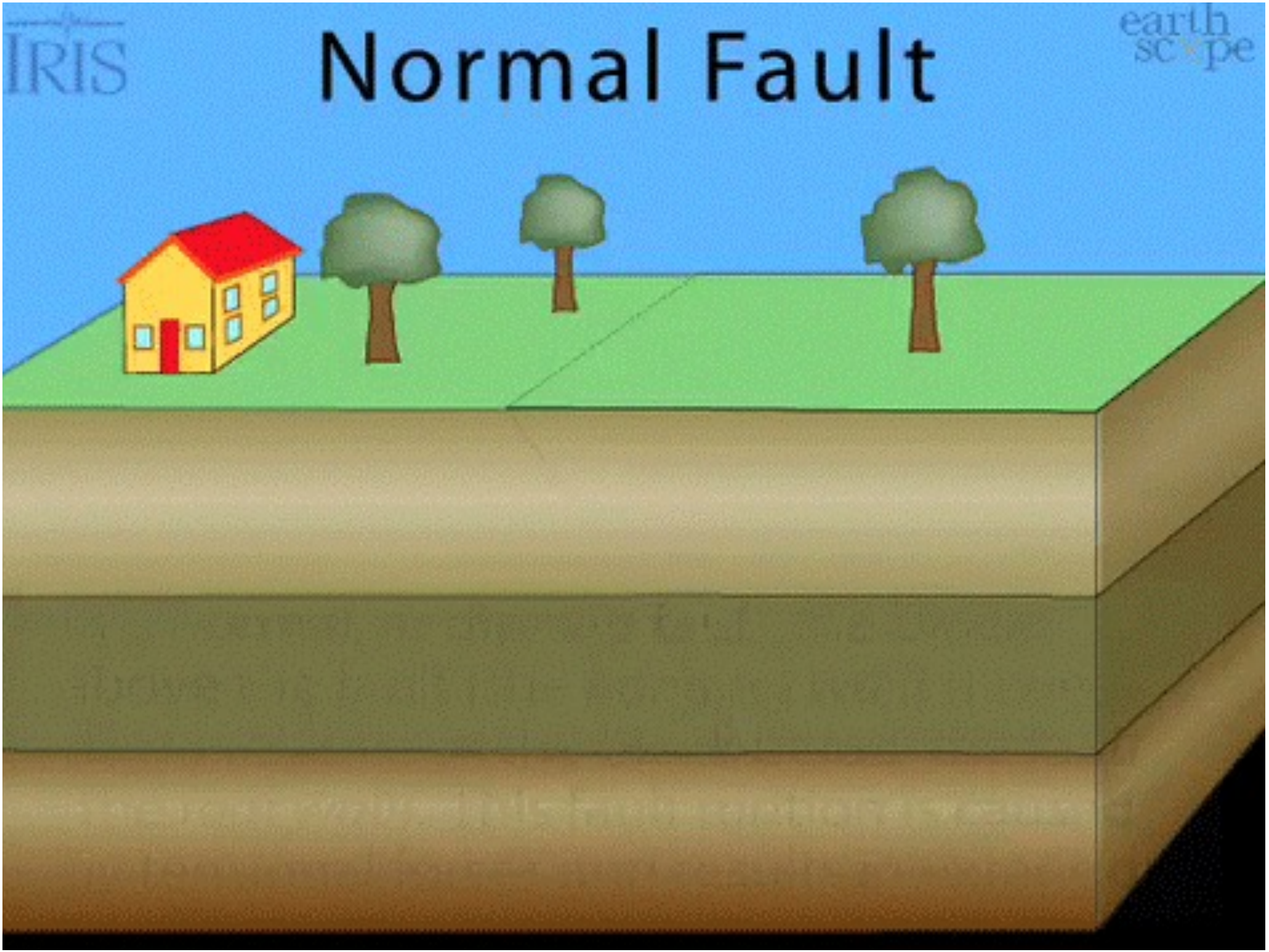
IRIS
Normal Fault
earth scope


06.02.2023
13:24, Mw=7.6
Malatya Fayı
Kayhan Engin
Kahramanmaraş, Nurhak, Tatlar köyü

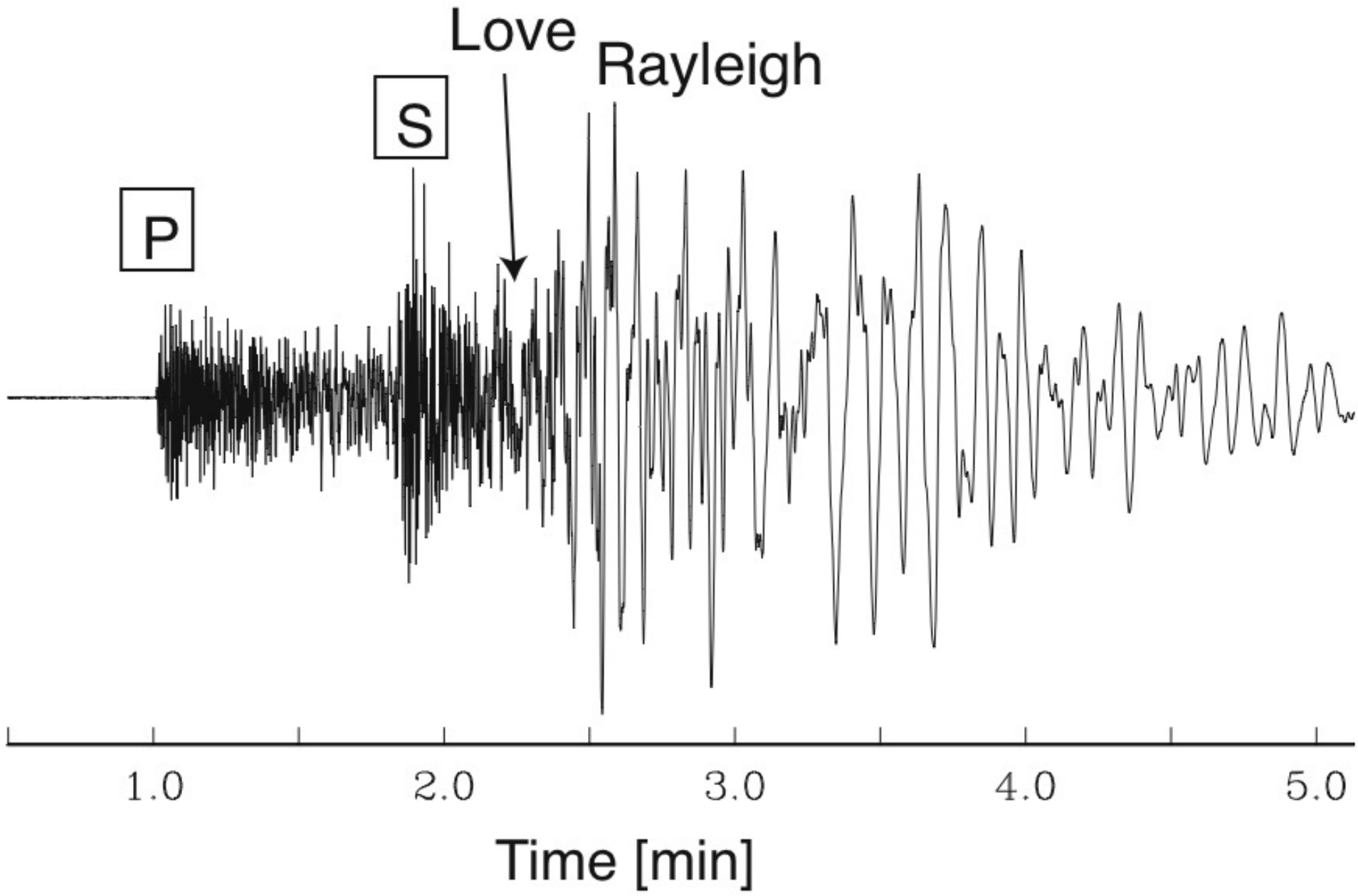
Love
Rayleigh
S
P
1.0
2.0
3.0
4.0
5.0
Time [min]

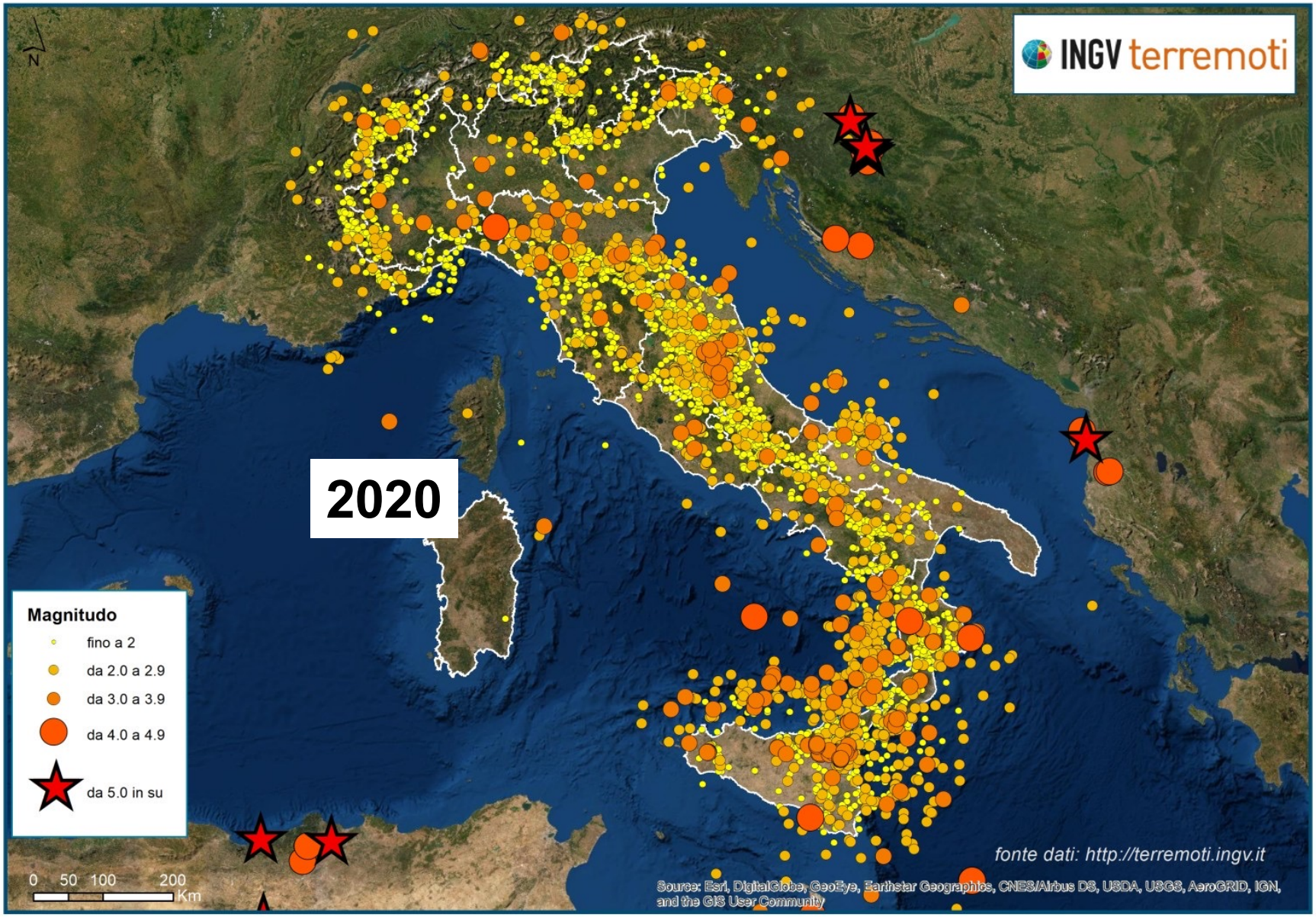
INGV terremoti
2020
Magnitudo
fino a 2
da 2.0 a 2.9
da 3.0 a 3.9
da 4.0 a 4.9
da 5.0 in su
0 50 100 200
Km
fonte dati: http://terremoti.ingv.it
Source: Esri, DigitalGlobe, GeoEye, Earthstar Geographics, CNES/Airbus DS, USDA, USGS, AeroGRID, IGN, and the GIS User Community

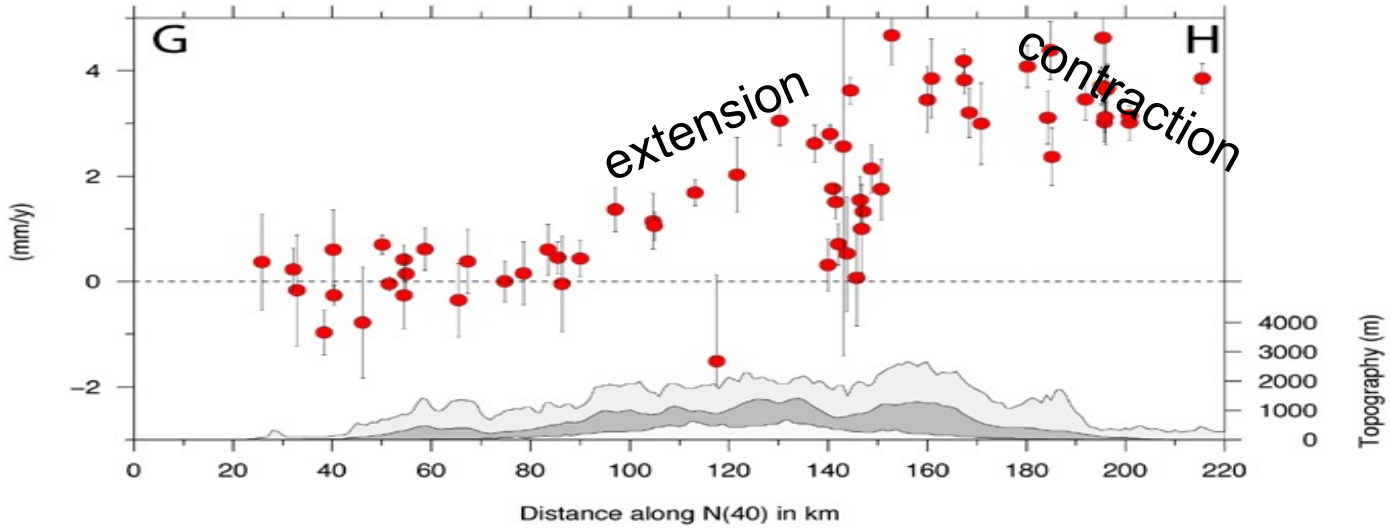
G
H
extension
contraction
(mm/y)
4
2
0
−2
0
20
40
60
80
100
120
140
160
180
200
220
Distance along N(40) in km
4000
3000
2000
1000
0
Topography (m)

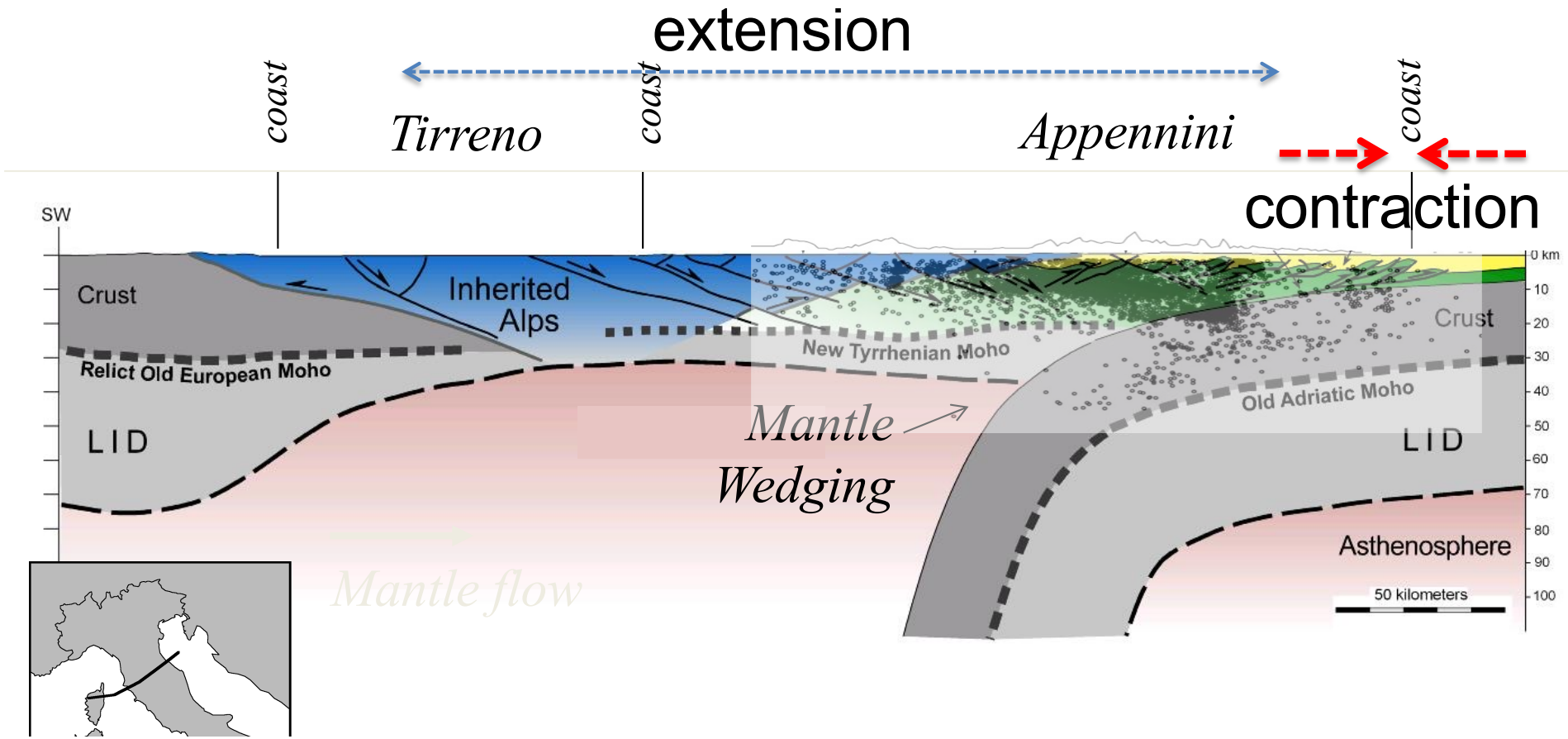
extension
coast
Tirreno
coast
Appennini
coast
contraction
SW
Crust
Inherited
Alps
Relict Old European Moho
LID
New Tyrrhenian Moho
Mantle
Wedging
Mantle flow
Crust
Old Adriatic Moho
LID
Asthenosphere
50 kilometers
0 km
10
20
30
40
50
60
70
80
90
100

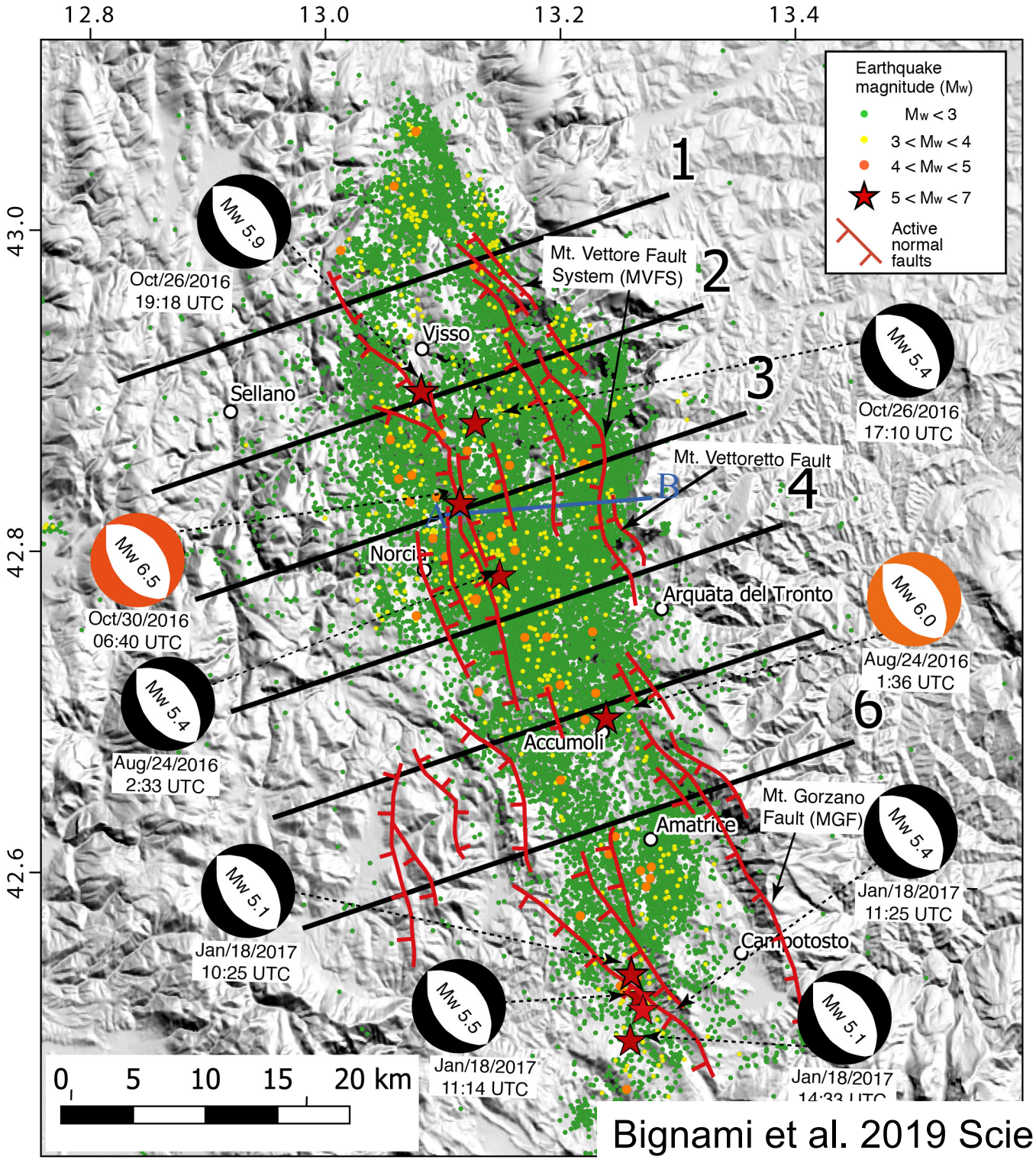

Bignami et al. 2019 Scientific Reports

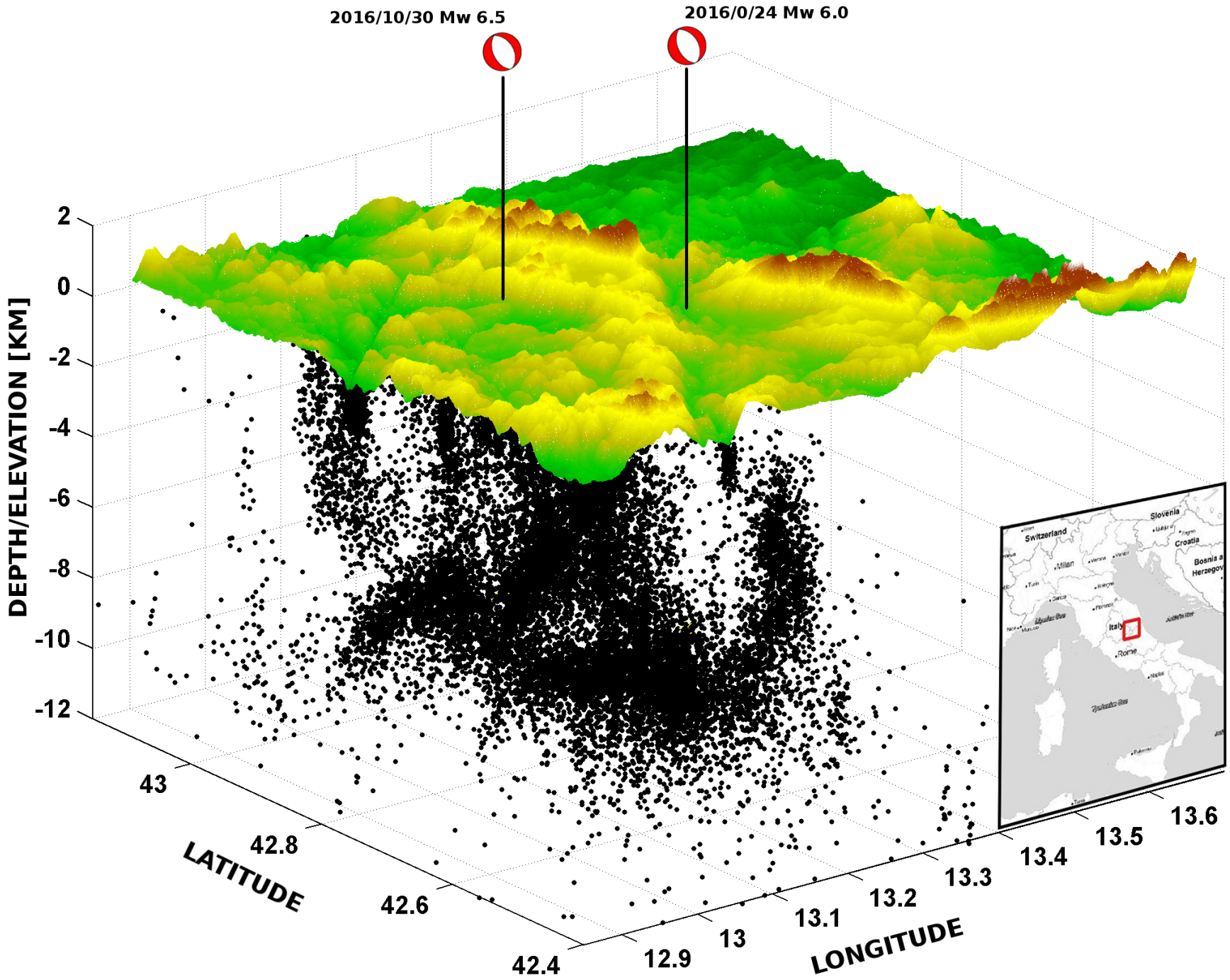

Bignami et al. 2019 Scientific Reports

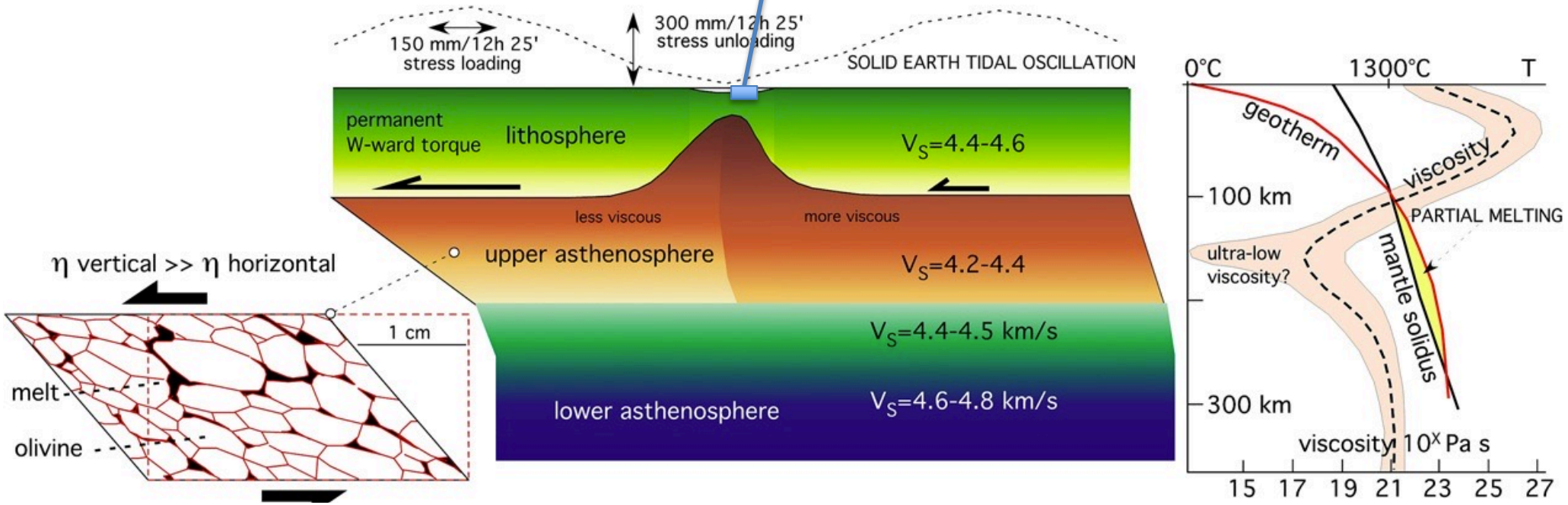
150 mm/12h 25'
stress loading
300 mm/12h 25'
stress unloading
SOLID EARTH TIDAL OSCILLATION
permanent
W-ward torque
lithosphere
V_S=4.4-4.6
less viscous
more viscous
upper asthenosphere
V_S=4.2-4.4
V_S=4.4-4.5 km/s
lower asthenosphere
V_S=4.6-4.8 km/s
η vertical >> η horizontal
1 cm
melt
olivine
0°C
1300°C
T
geotherm
viscosity
100 km
PARTIAL MELTING
ultra-low
viscosity?
mantle solidus
300 km
viscosity 10^X Pa s
15
17
19
21
23
25
27

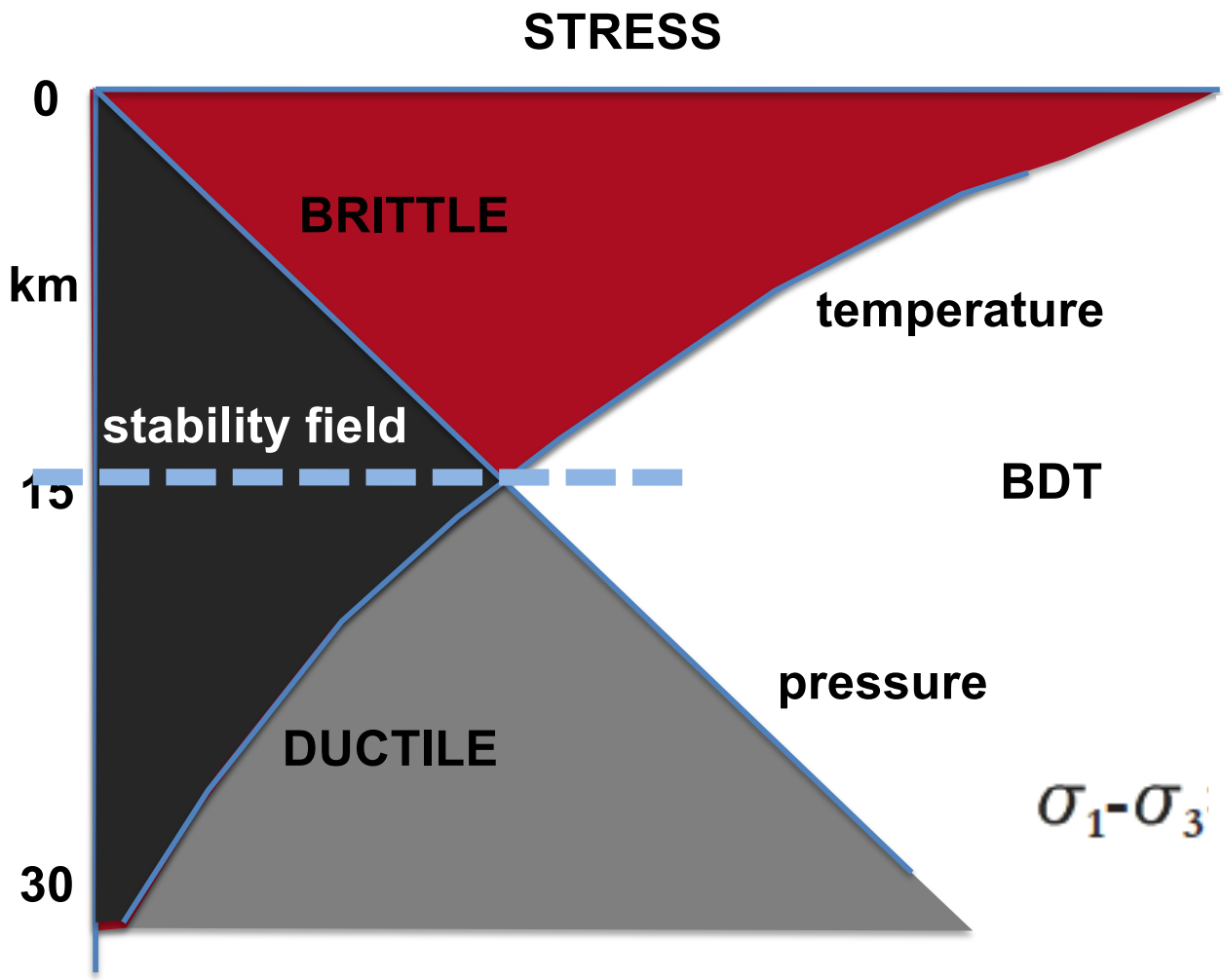

$$\sigma_1-\sigma_3=\beta\rho g z(1-\lambda)$$

λ, pore fluids
β, type of fault

$$\sigma_1-\sigma_3=\left(\frac{\dot{\varepsilon}}{A}\right)^{1/n}\exp\left(\frac{Q}{nRT}\right)$$

Q, activation energy
A, viscosity coefficient
ε, effective strain
n, stress power law

β=3 thrust, 1.2 strike-slip, 0.75 normal fault

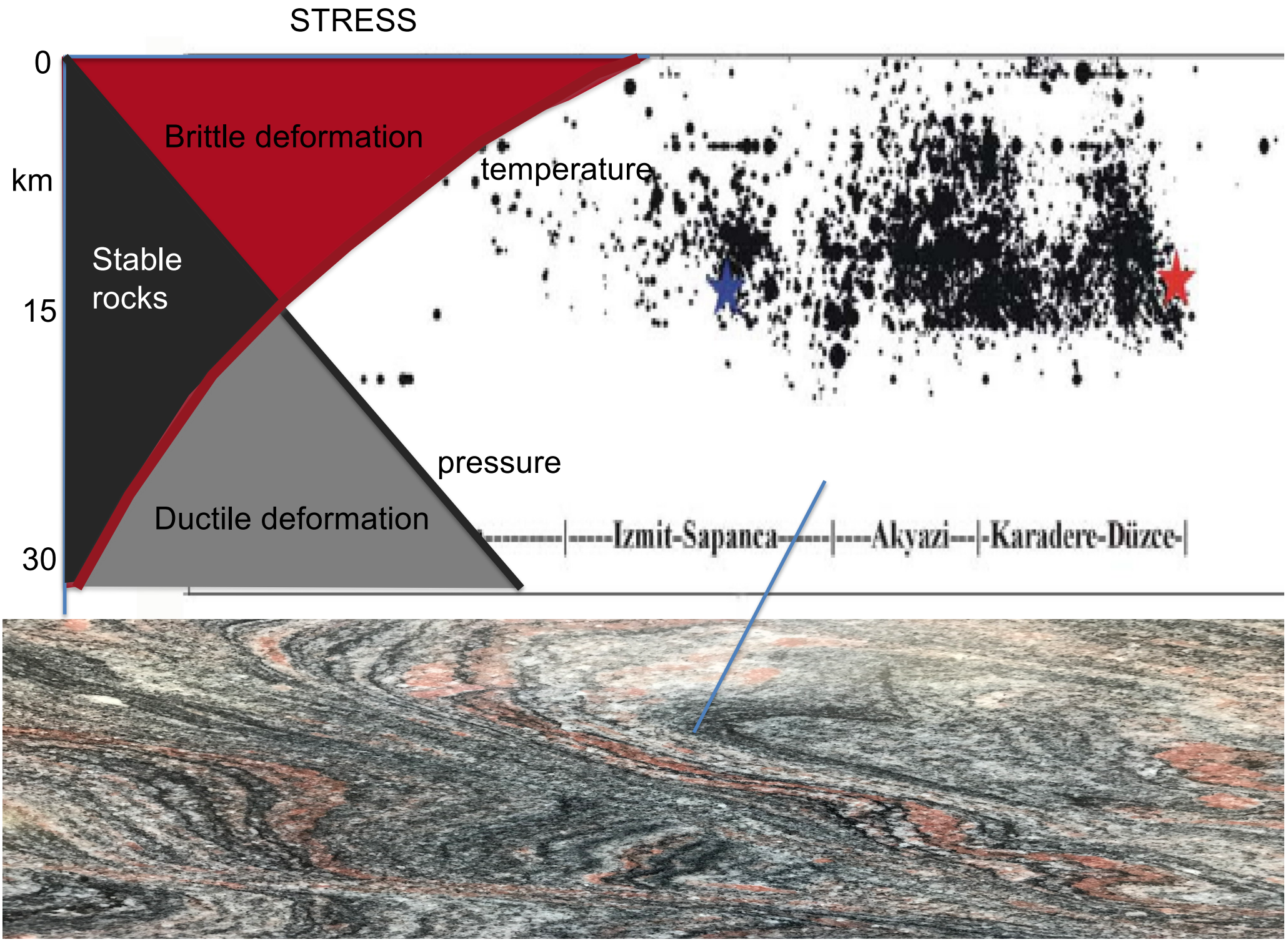
STRESS
0
km
15
30
Brittle deformation
Stable
rocks
Ductile deformation
temperature
pressure
Izmit-Sapanca
Akyazi
Karadere-Düzce

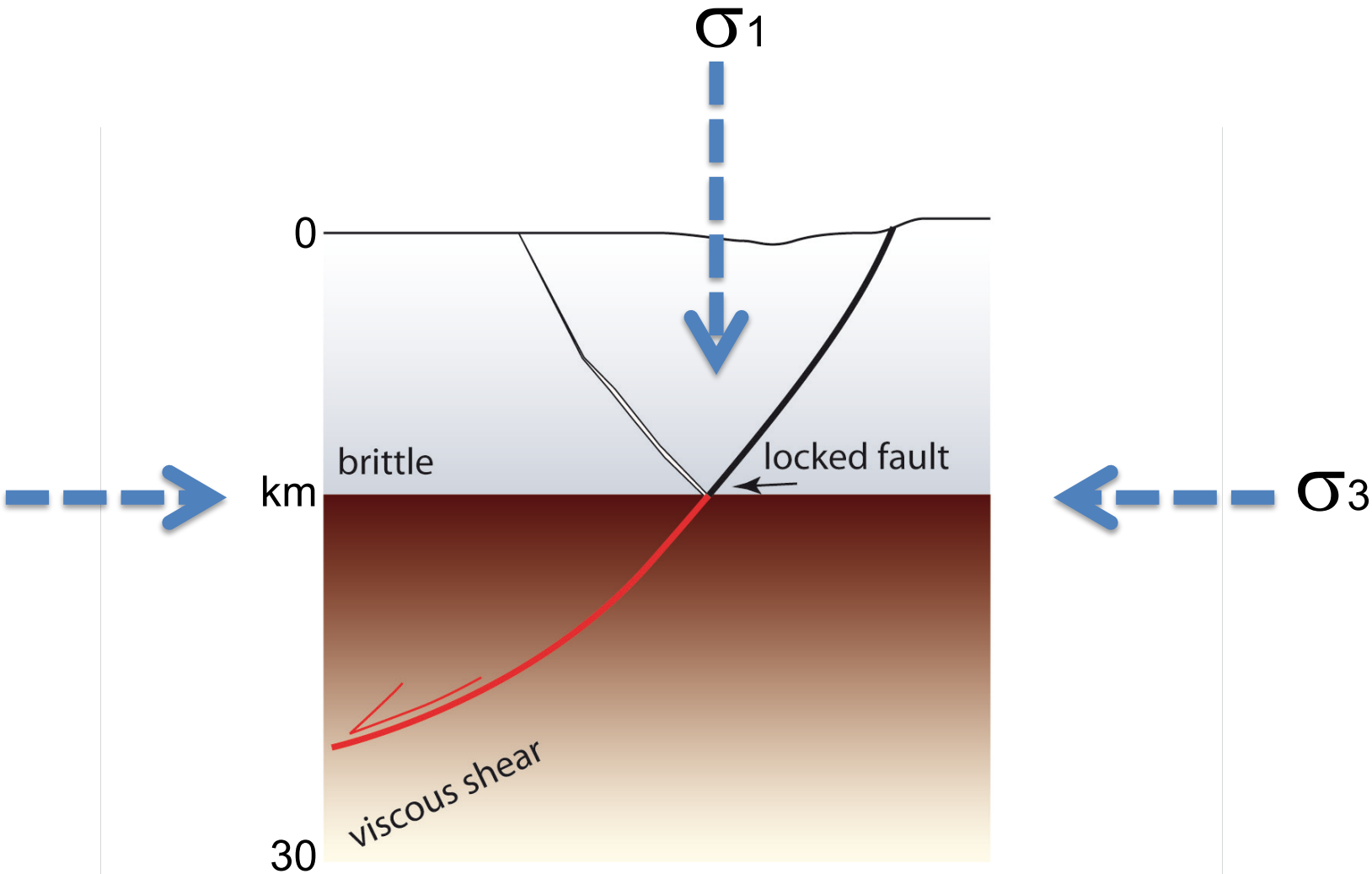
σ1
0
brittle
locked fault
km
σ3
viscous shear
30

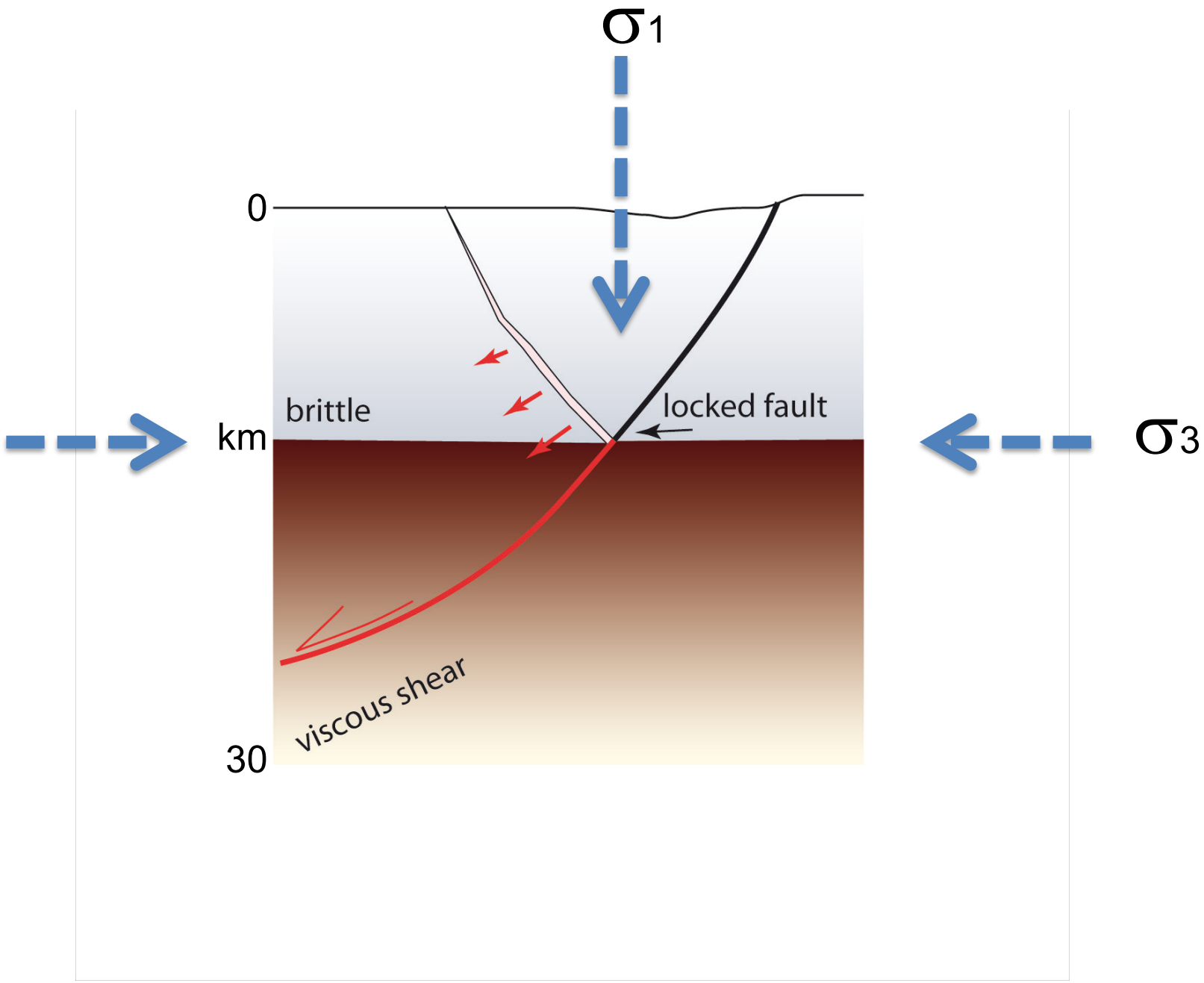
σ1
0
brittle
km
locked fault
σ3
viscous shear
30

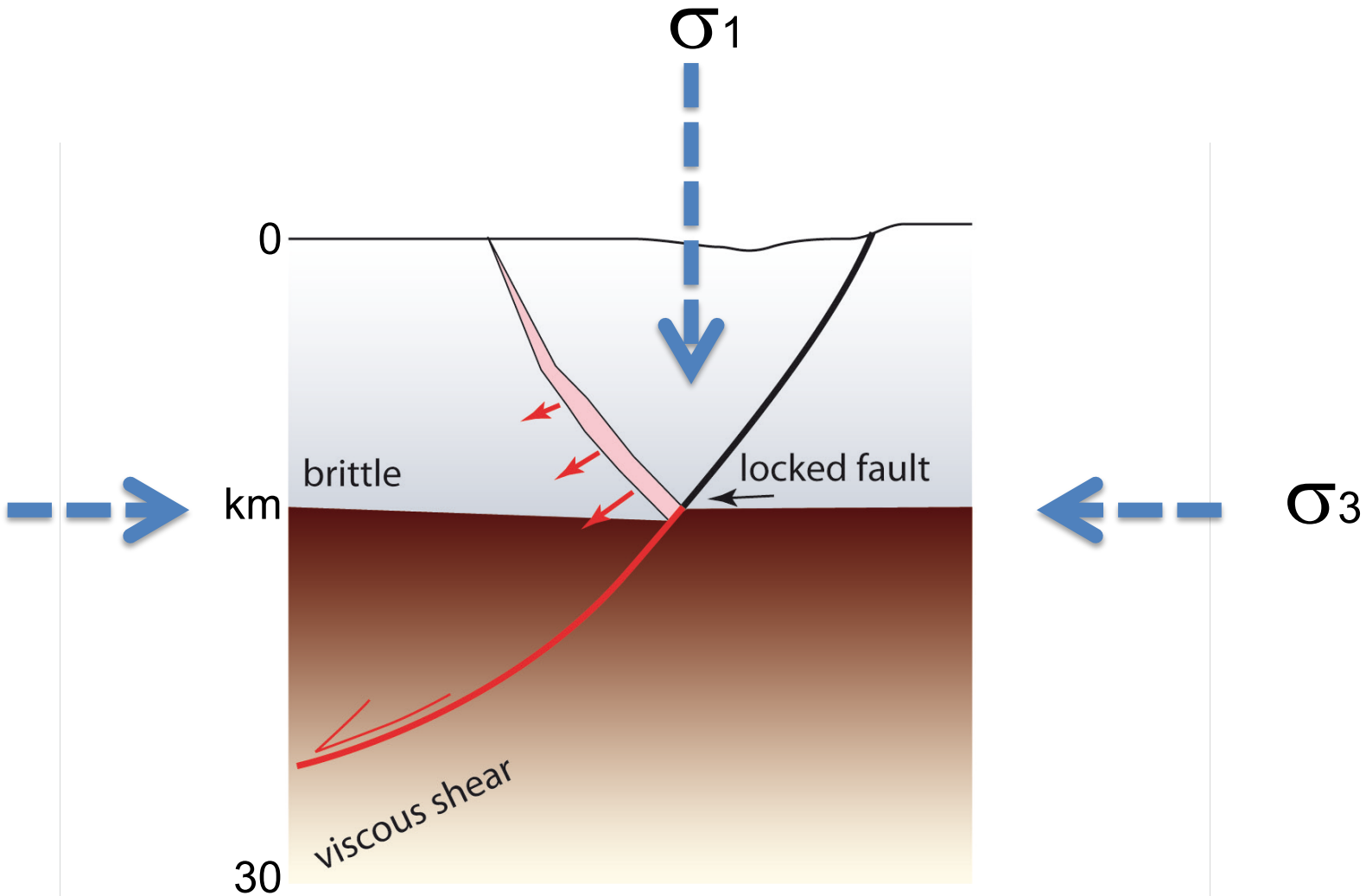
σ1
0
brittle
locked fault
km
σ3
viscous shear
30

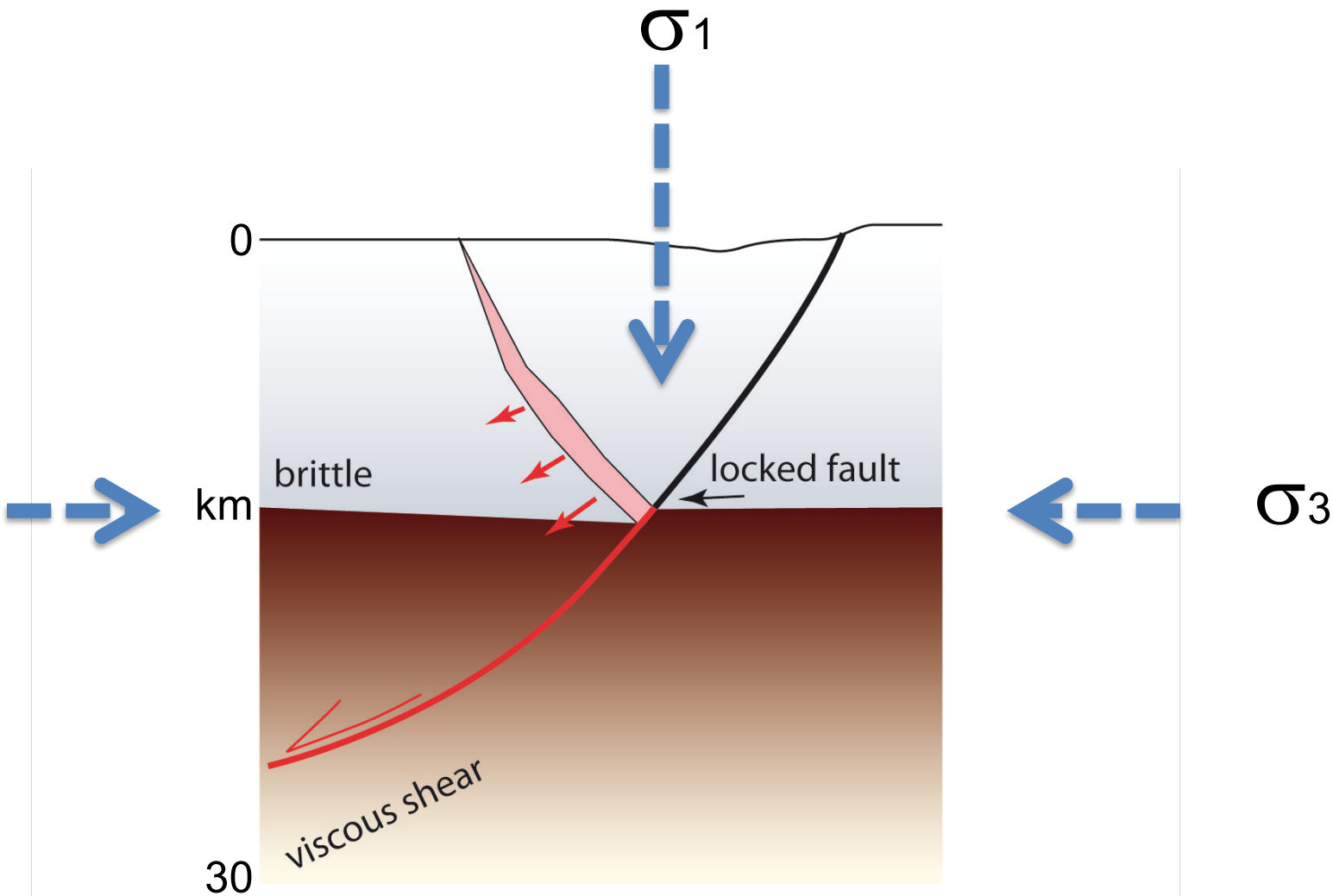
σ1
0
brittle
locked fault
km
σ3
viscous shear
30

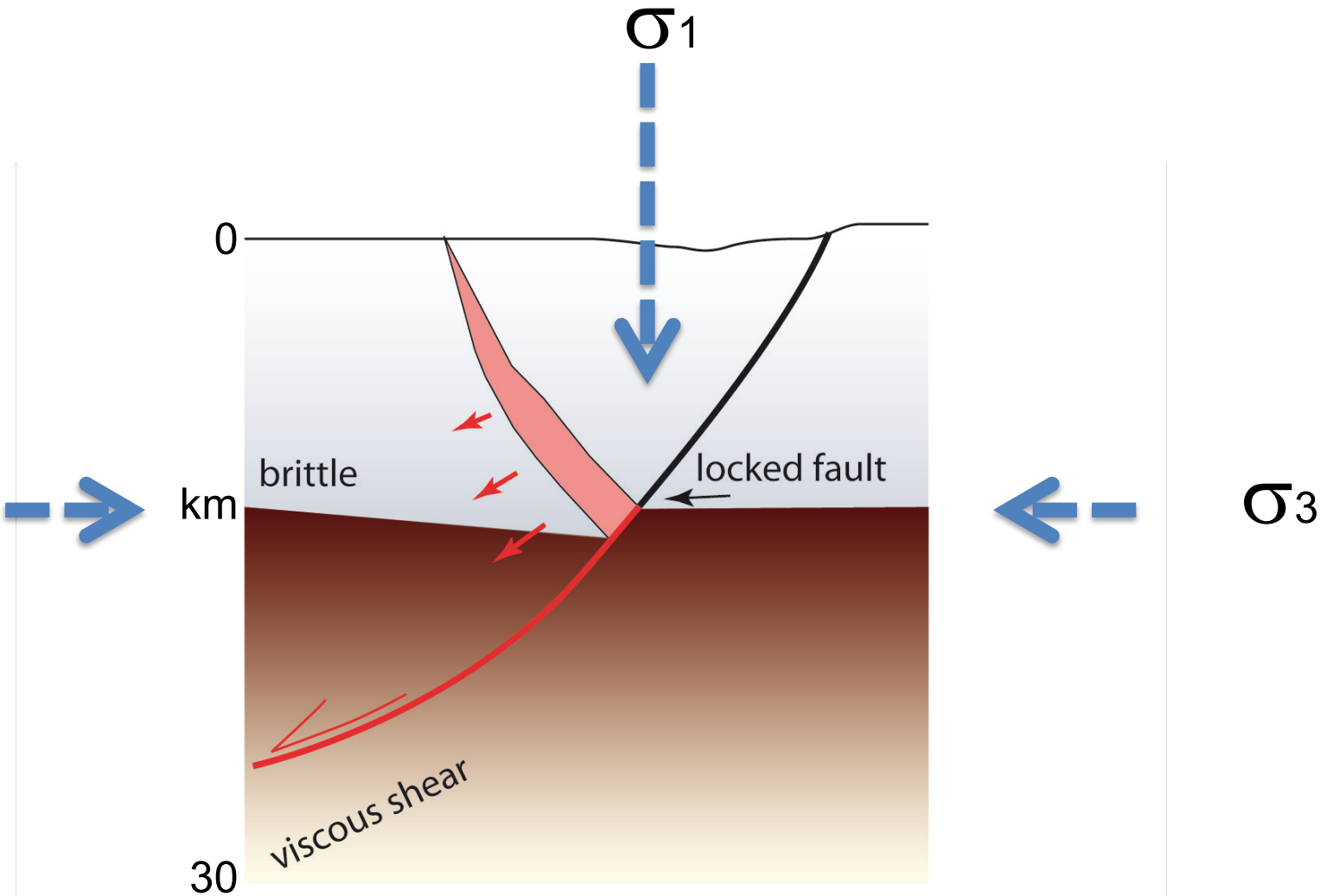
σ1
0
km
brittle
locked fault
σ3
viscous shear
30

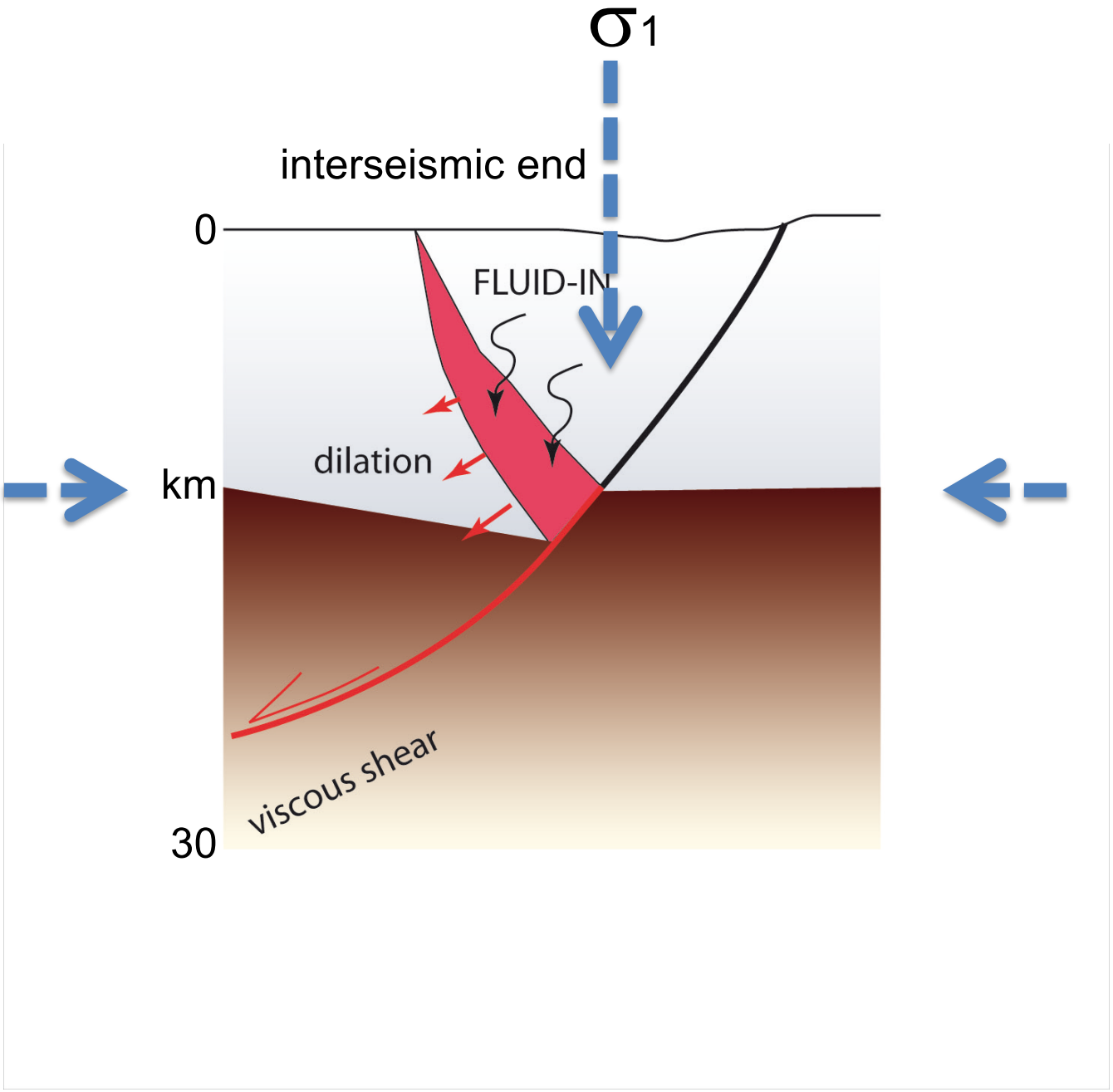
σ1
interseismic end
0
FLUID-IN
dilation
km
σ3
viscous shear
30

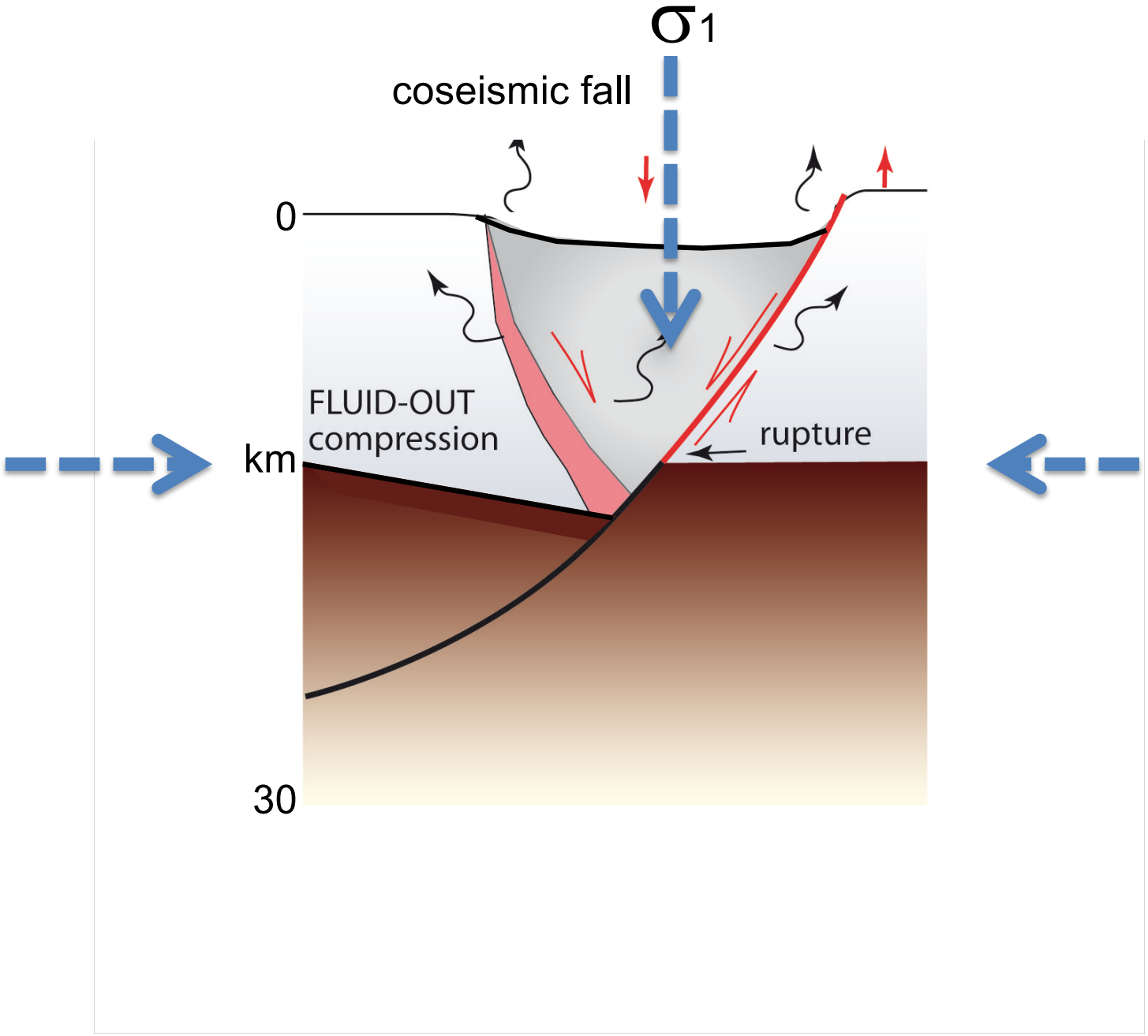
σ1
coseismic fall
0
FLUID-OUT
compression
rupture
km
σ3
30

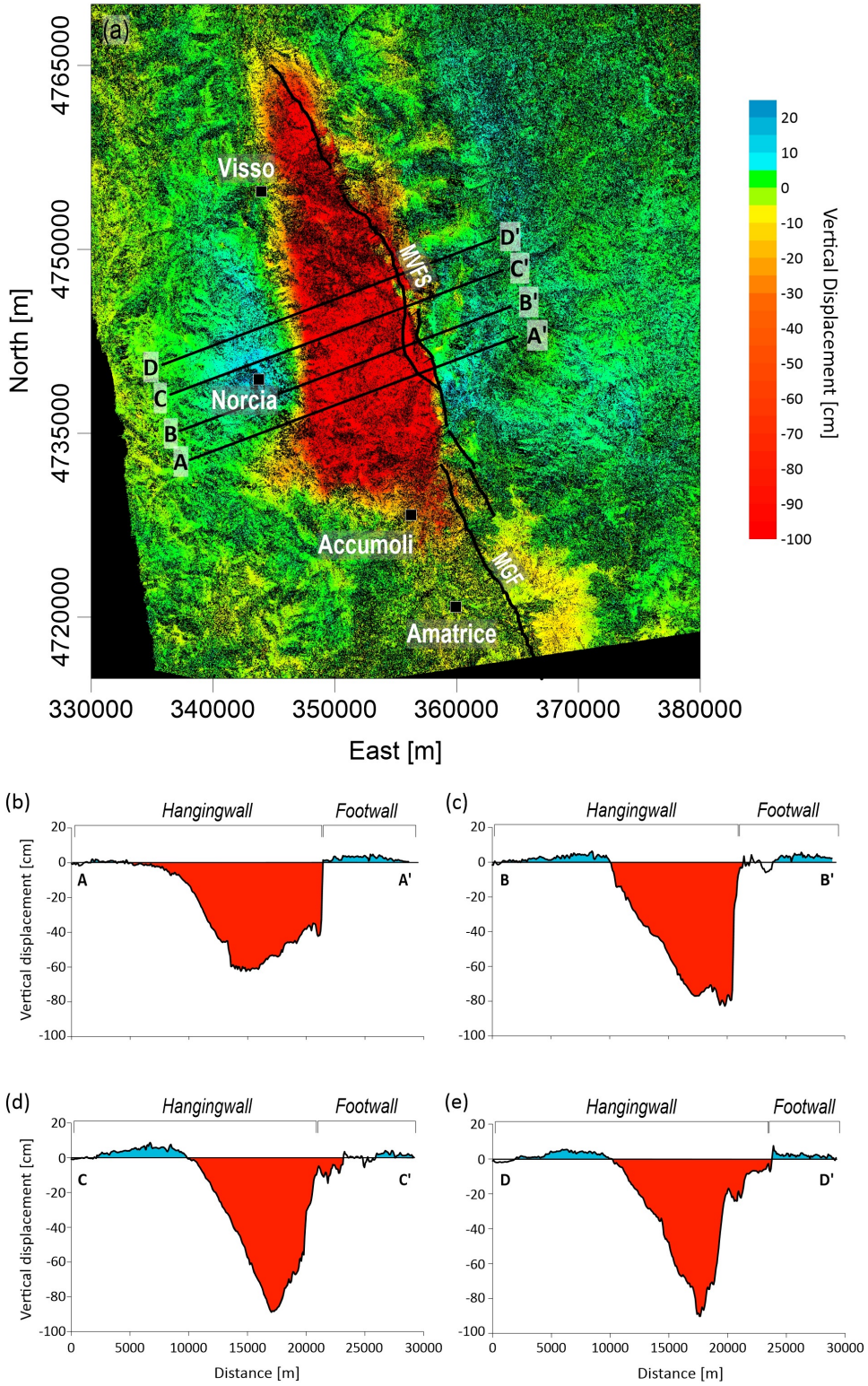

Valerio et al., 2018

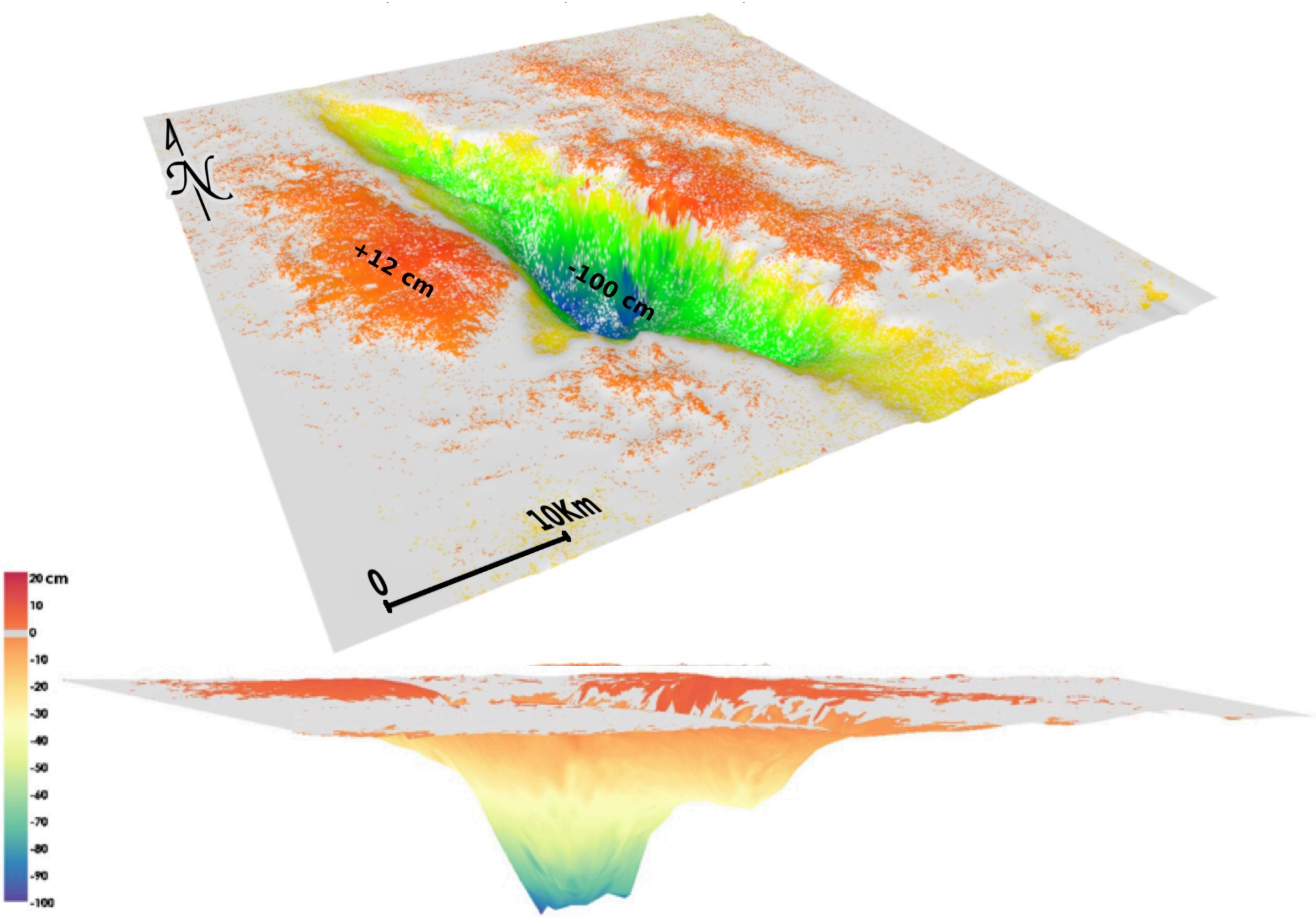

Bignami et al. 2019 Scientific Reports

VERTICAL COSEISMIC MOTION

$A \approx 7.5B$

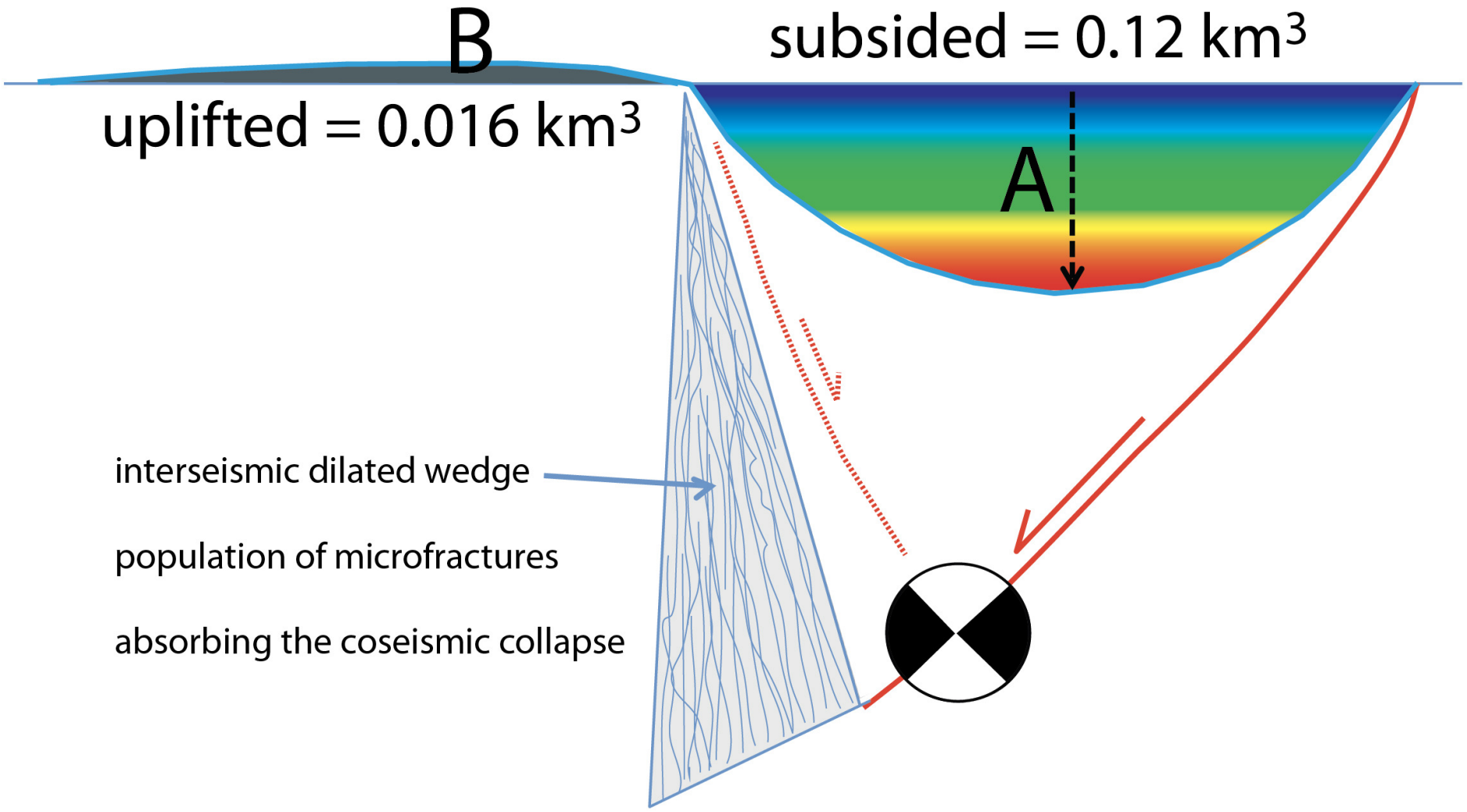

Bignami et al. 2019 Scientific Reports

normal fault seismic cycle

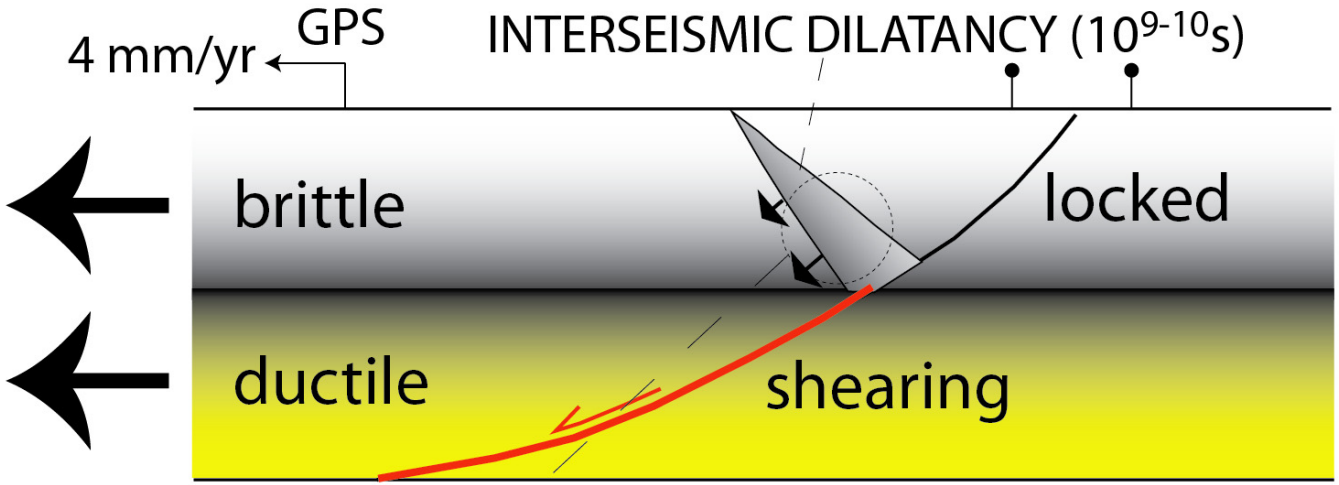

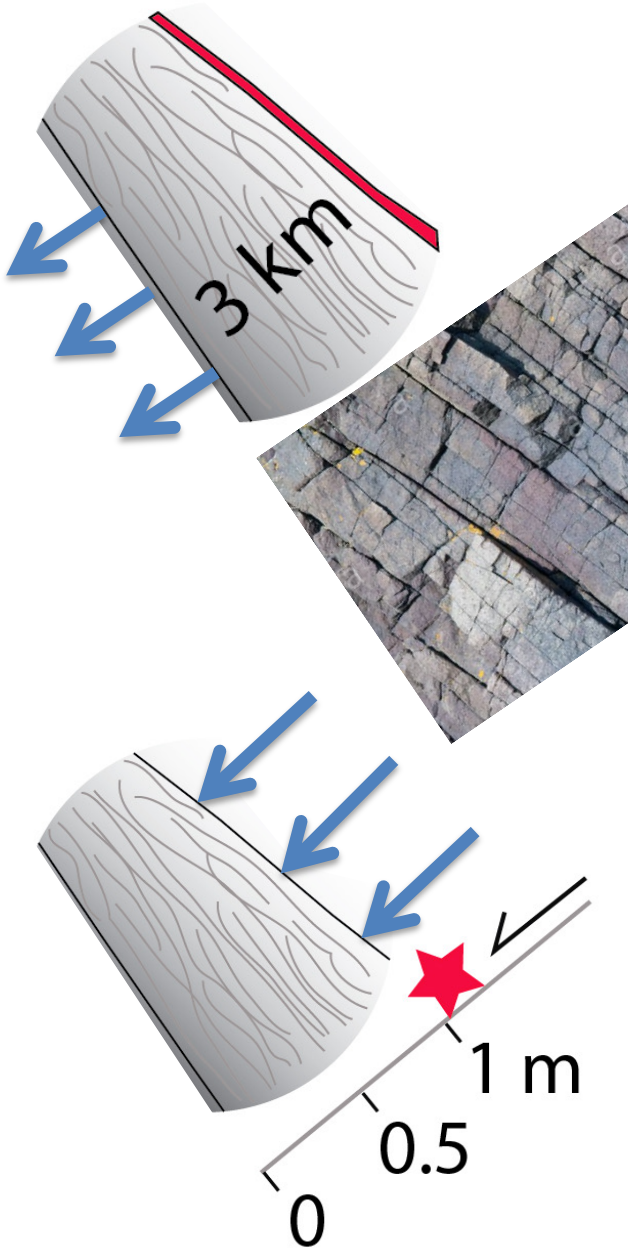

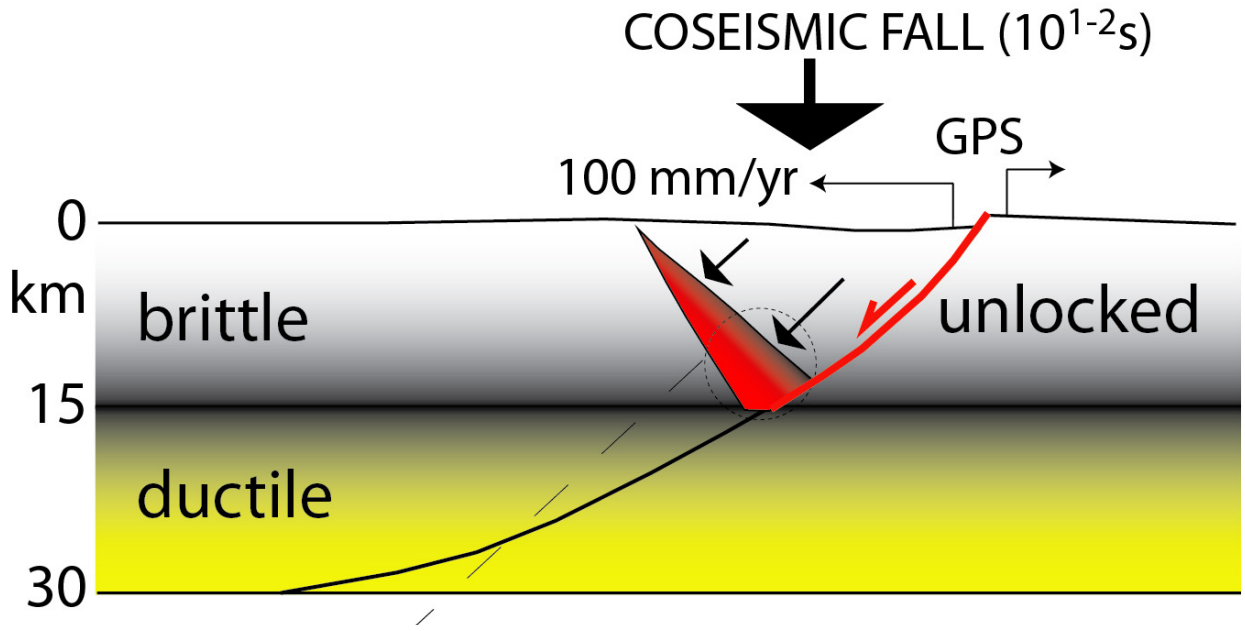


USGS

ESTENSION

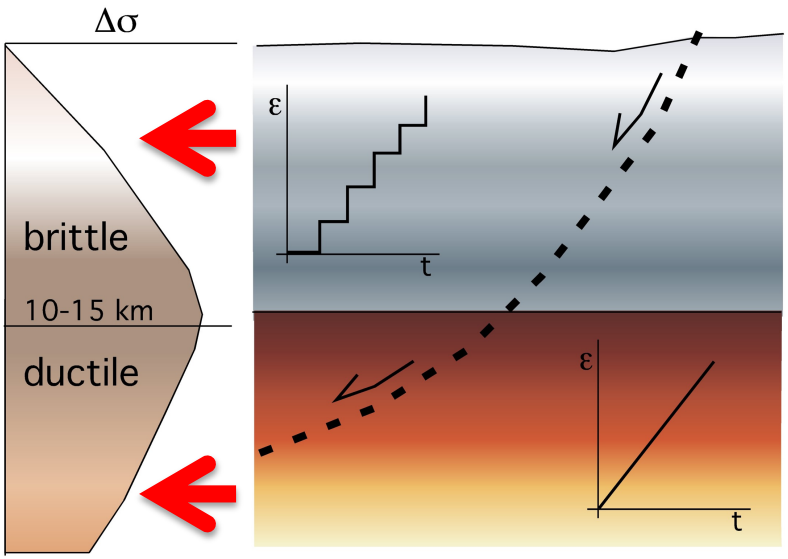

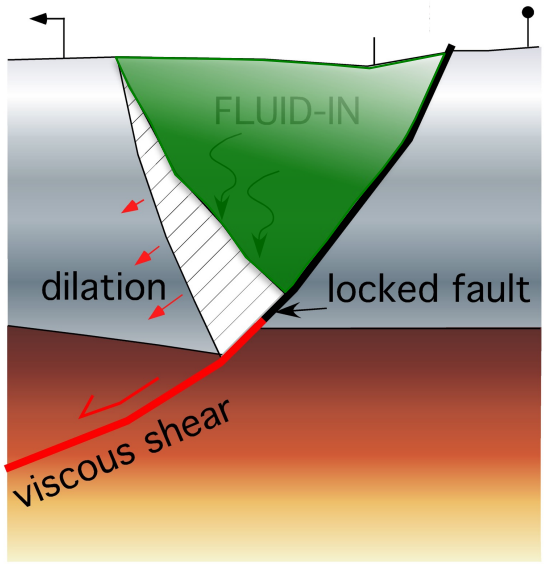

graviquake

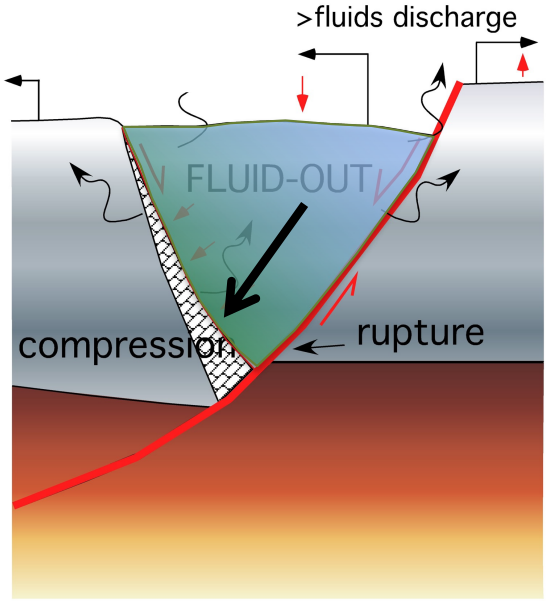

COMPRESSION

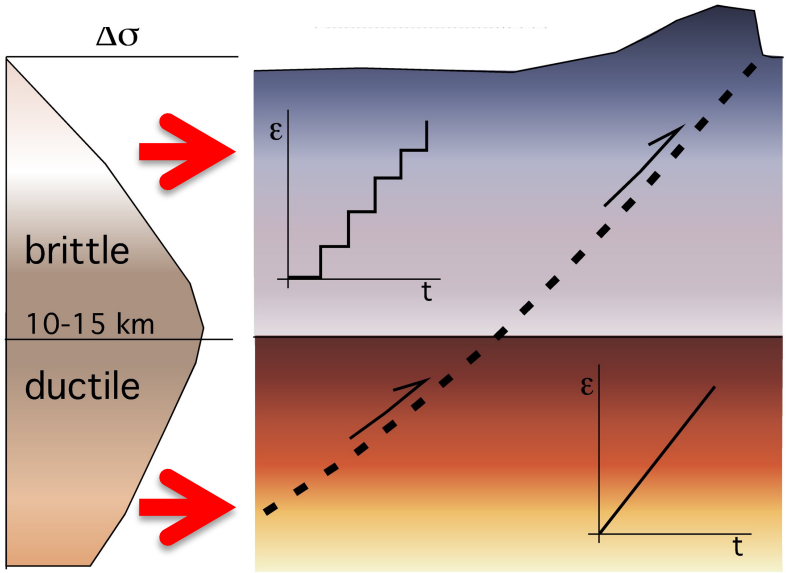

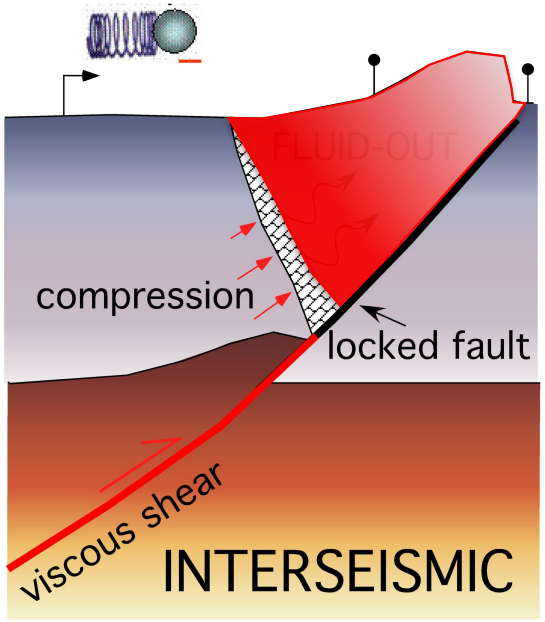

elastoquake

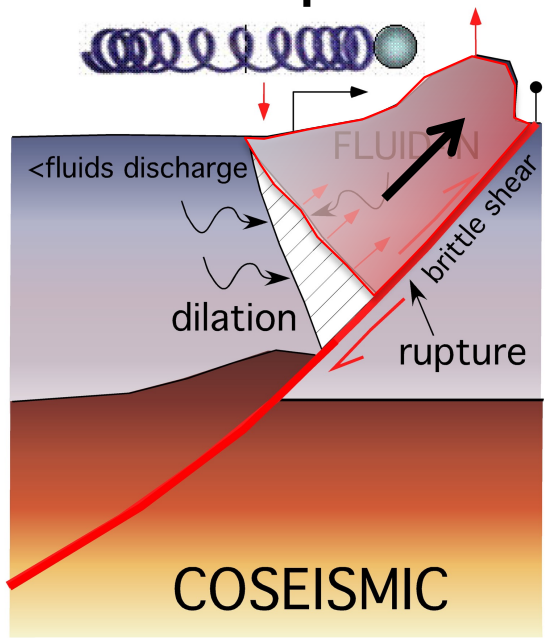

Doglioni et al. 2015 SREP

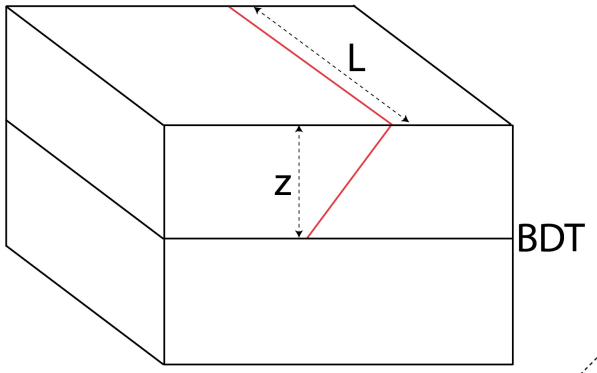

Fault type	Earthquake	M	Z (km)	L (km)	L/z
Normal fault	Pleasant Valley 1915	7.2	15-20	~60	3-4
Normal fault	Irpinia 1980		.5	~45	3
Normal fault	Corinth 1981		.3	~40	3
Normal fault	Edgecumbe 1987		.5	~50	3.3
Normal fault	L'Aquila 2009	6.3	10	~30	3
Strike slip	Macquarie Ridge 1989	8.1	12-15	~140	9.3-11.6
Strike slip	Luzon 1990		.5-20	~150	7.
Strike slip	Landers 1992		.2	~85	7
Strike slip	Izmit 1999		.5	~160	1(
Strike slip	Sumatra 2012	8.7	35-40	~400	10-11.4
Thrust	Chile 1960	9.5	30-40	~900	22.5-30
Thrust	Alaska 1964		0-40	~700-800	1
Thrust	Sumatra 2004		5-45	~1200	2(
Thrust	Maule 2010		5-30	~500	1(
Thrust	Tohoku 2011	9.0	30	~650	21.6

7.5

8.7

9.5

3

10

25

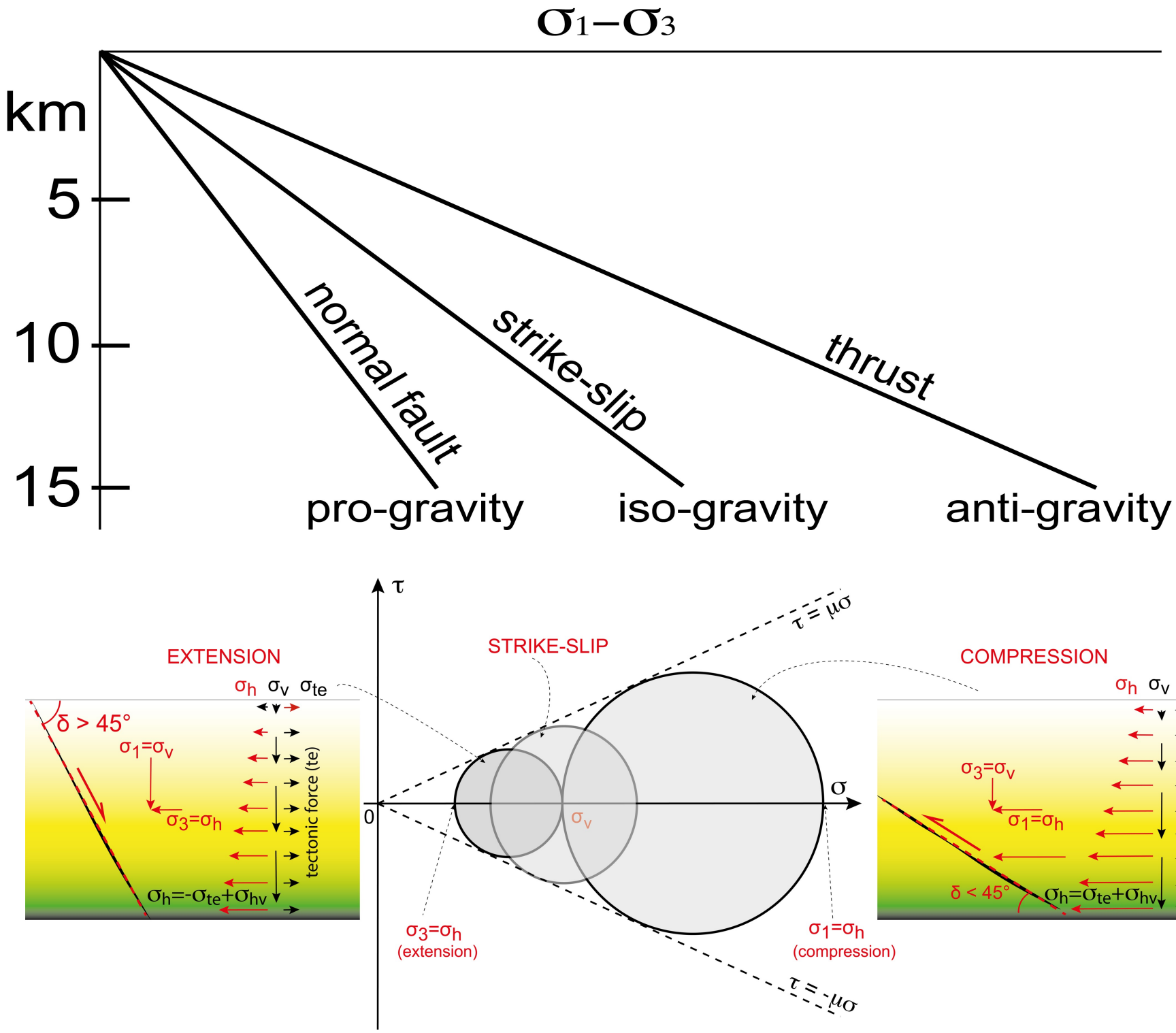
σ1−σ3
km
5
10
15
normal fault
strike-slip
thrust
pro-gravity
iso-gravity
anti-gravity
τ
σ
0
τ = μσ
τ = -μσ
EXTENSION
STRIKE-SLIP
COMPRESSION
σh σv σte
δ > 45°
σ1=σv
σ3=σh
σh=-σte+σhv
tectonic force (te)
σv
σ3=σh
(extension)
σ1=σh
(compression)
σ3=σv
σ1=σh
δ < 45°
σh=σte+σhv

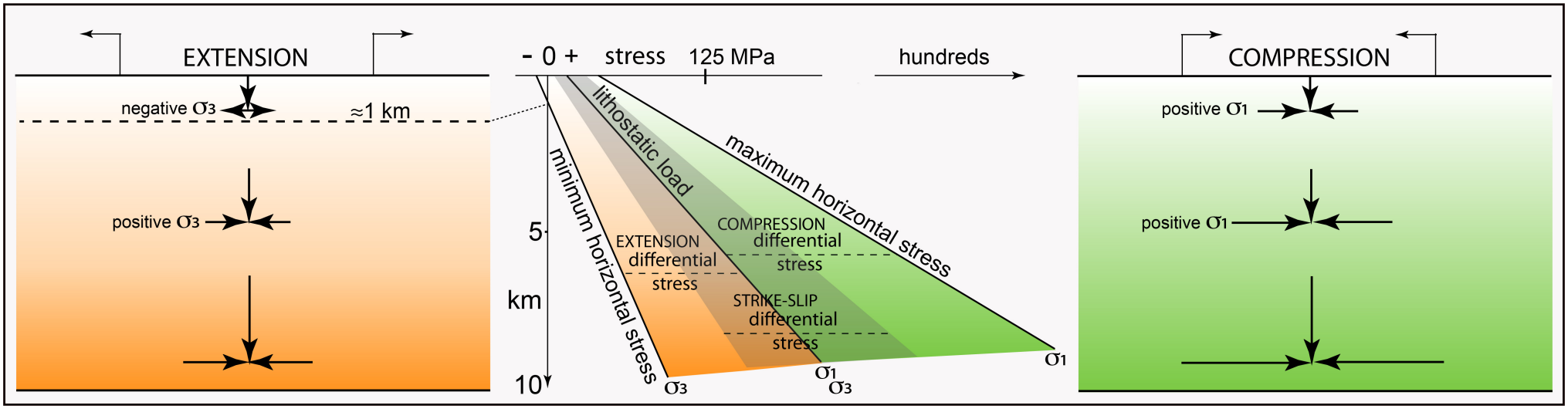
EXTENSION
negative σ3
≈1 km
positive σ3
- 0 + stress 125 MPa
hundreds
lithostatic load
maximum horizontal stress
minimum horizontal stress
5
km
10
EXTENSION differential stress
COMPRESSION differential stress
STRIKE-SLIP differential stress
σ3
σ1
σ1
σ3
COMPRESSION
positive σ1
positive σ1

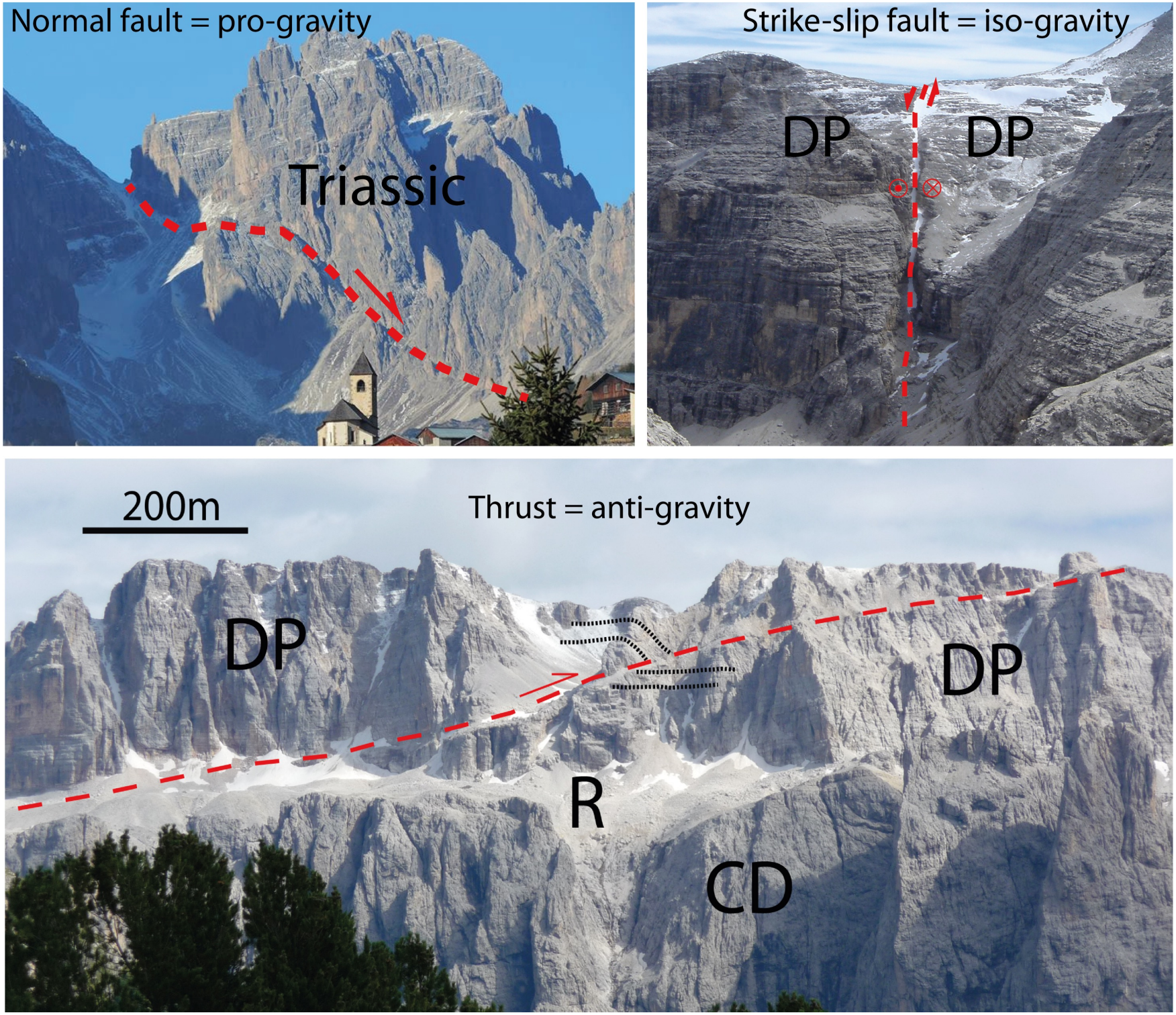
Normal fault = pro-gravity
Triassic
Strike-slip fault = iso-gravity
DP
DP
200m
Thrust = anti-gravity
DP
DP
R
CD

pro gravity

against gravity

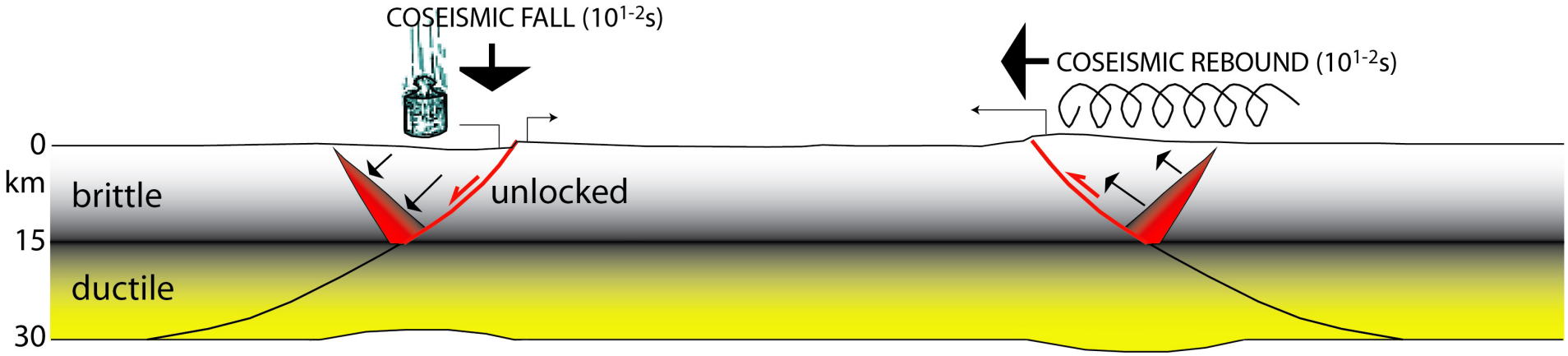

EARTHQUAKE ENERGY

GRAVIQUAKE

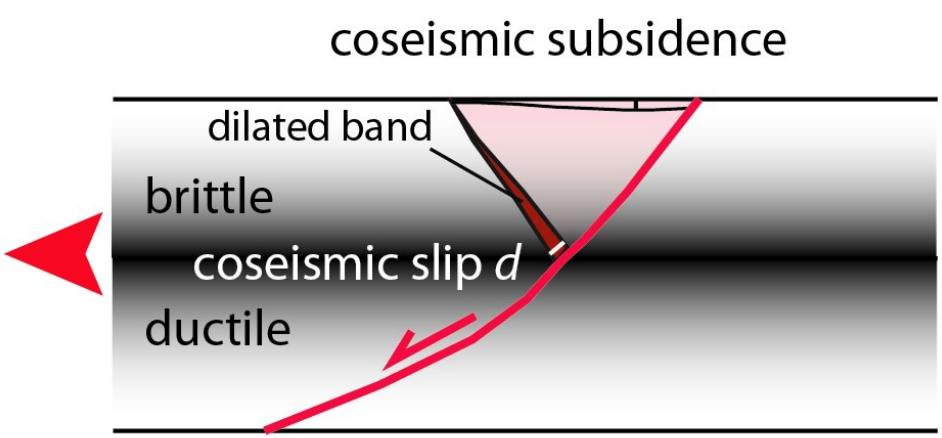

normal faulting

ELASTOQUAKE

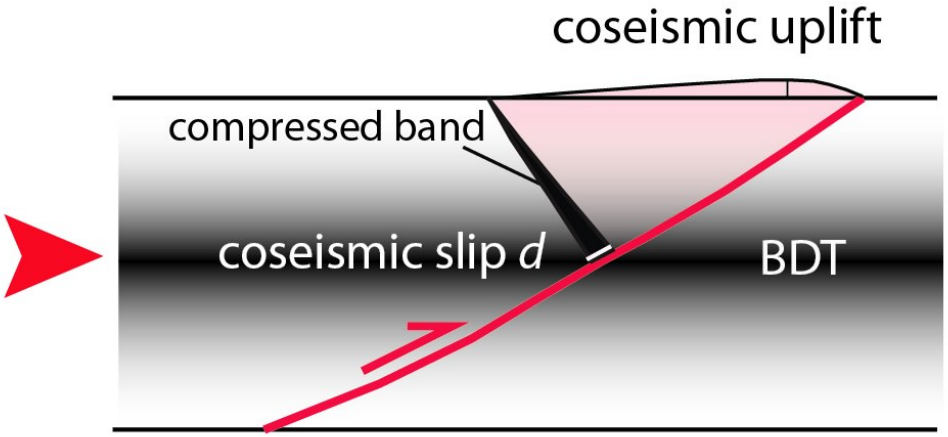

thrust faulting

$$E = mgh(\mu_s, \Theta)$$

$$E = \frac{1}{2} K \left(\frac{\Delta V(\mu_s, \Theta)}{V} \right)^2 \frac{m}{\rho}$$

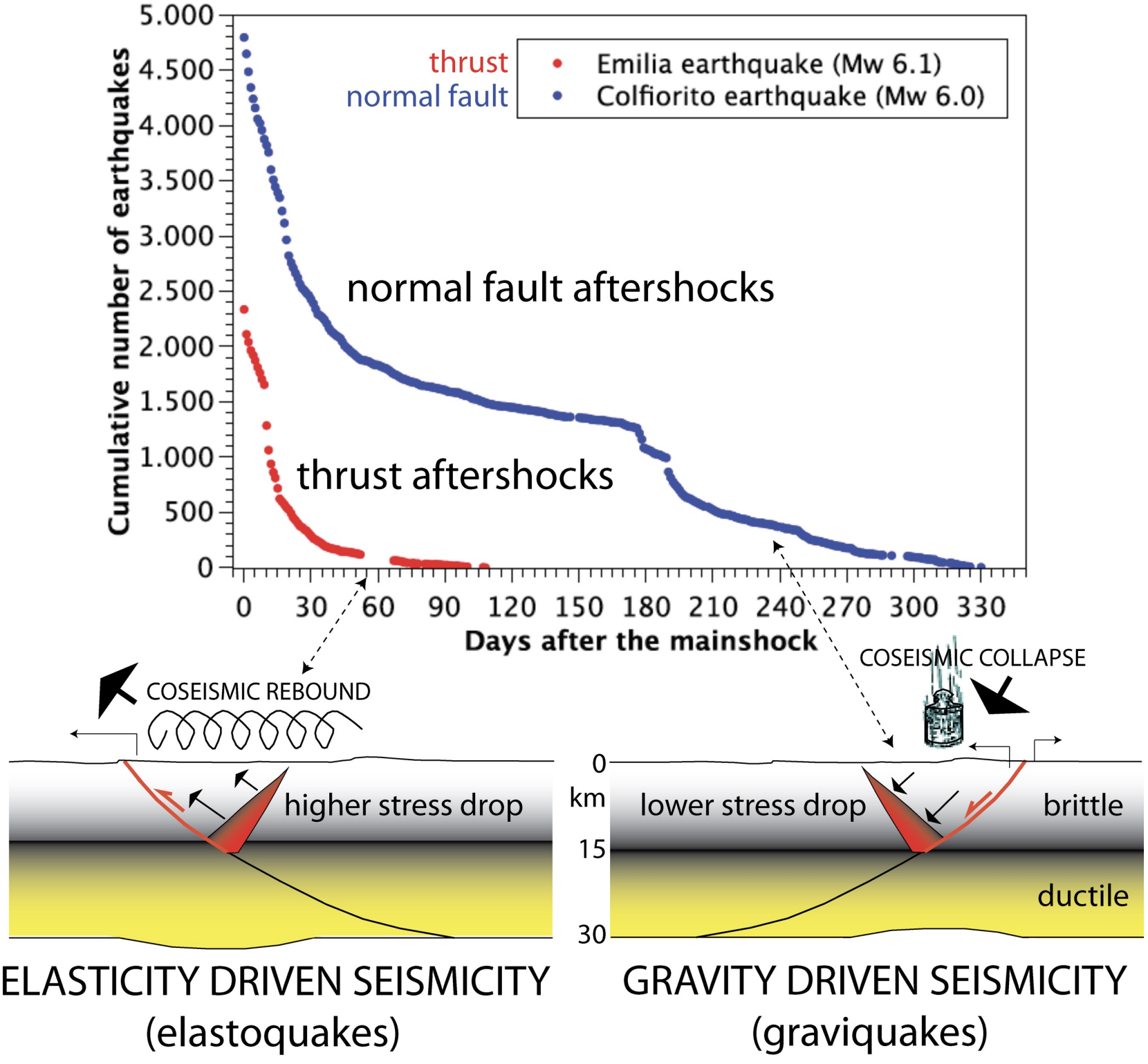
thrust
normal fault
Emilia earthquake (Mw 6.1)
Colfiorito earthquake (Mw 6.0)
Cumulative number of earthquakes
5.000
4.500
4.000
3.500
3.000
2.500
2.000
1.500
1.000
500
0
normal fault aftershocks
thrust aftershocks
0
30
60
90
120
150
180
210
240
270
300
330
Days after the mainshock
COSEISMIC REBOUND
higher stress drop
COSEISMIC COLLAPSE
0
km
15
30
lower stress drop
brittle
ductile
ELASTICITY DRIVEN SEISMICITY
(elastoquakes)
GRAVITY DRIVEN SEISMICITY
(graviquakes)

C

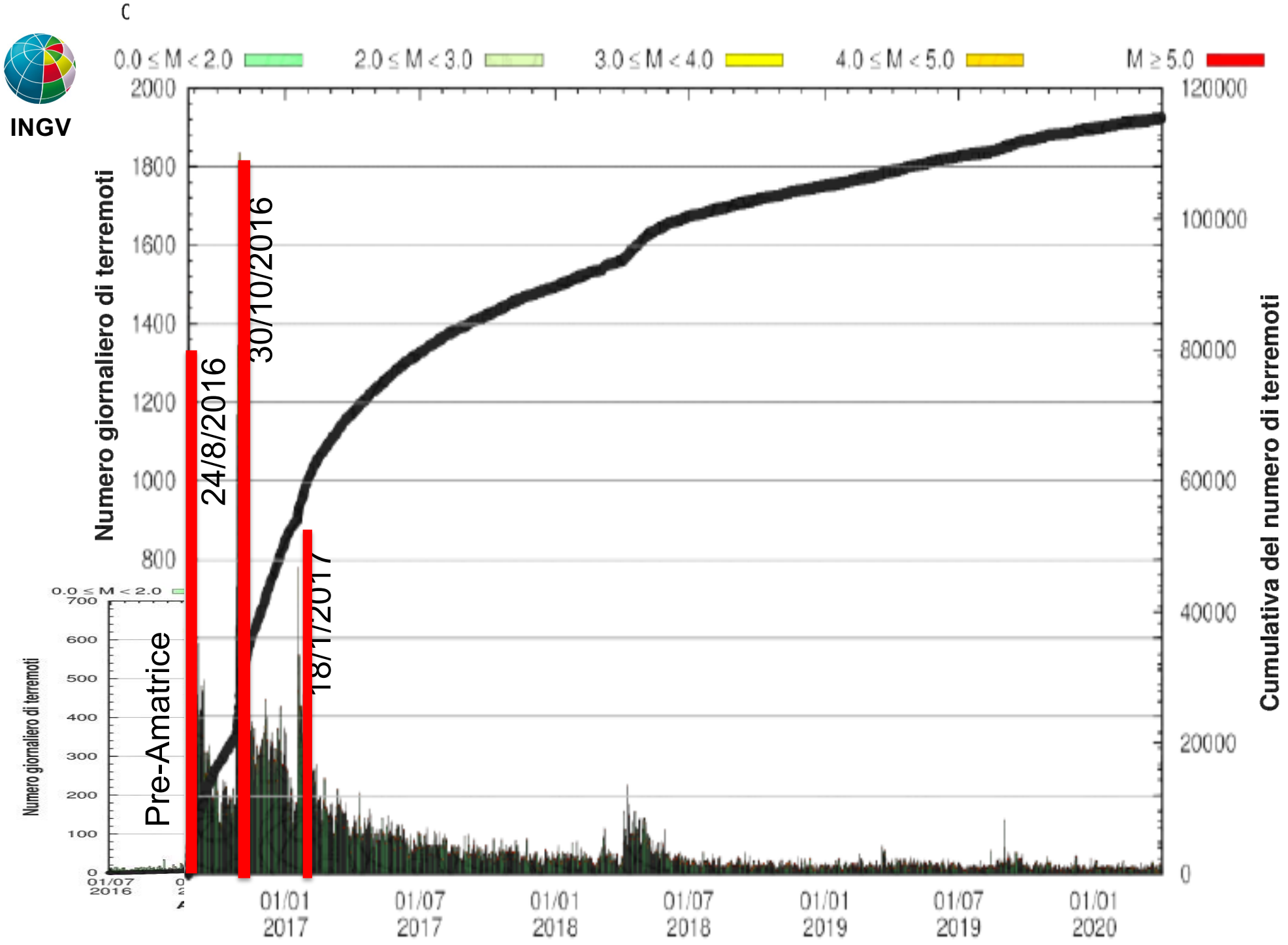
INGV
0.0 ≤ M < 2.0
2.0 ≤ M < 3.0
3.0 ≤ M < 4.0
4.0 ≤ M < 5.0
M ≥ 5.0
Numero giornaliero di terremoti
Cumulativa del numero di terremoti
24/8/2016
30/10/2016
18/1/2017
Pre-Amatrice
2000
1800
1600
1400
1200
1000
800
120000
100000
80000
60000
40000
20000
0
01/01 2017
01/07 2017
01/01 2018
01/07 2018
01/01 2019
01/07 2019
01/01 2020
01/07 2016
700
600
500
400
300
200
100

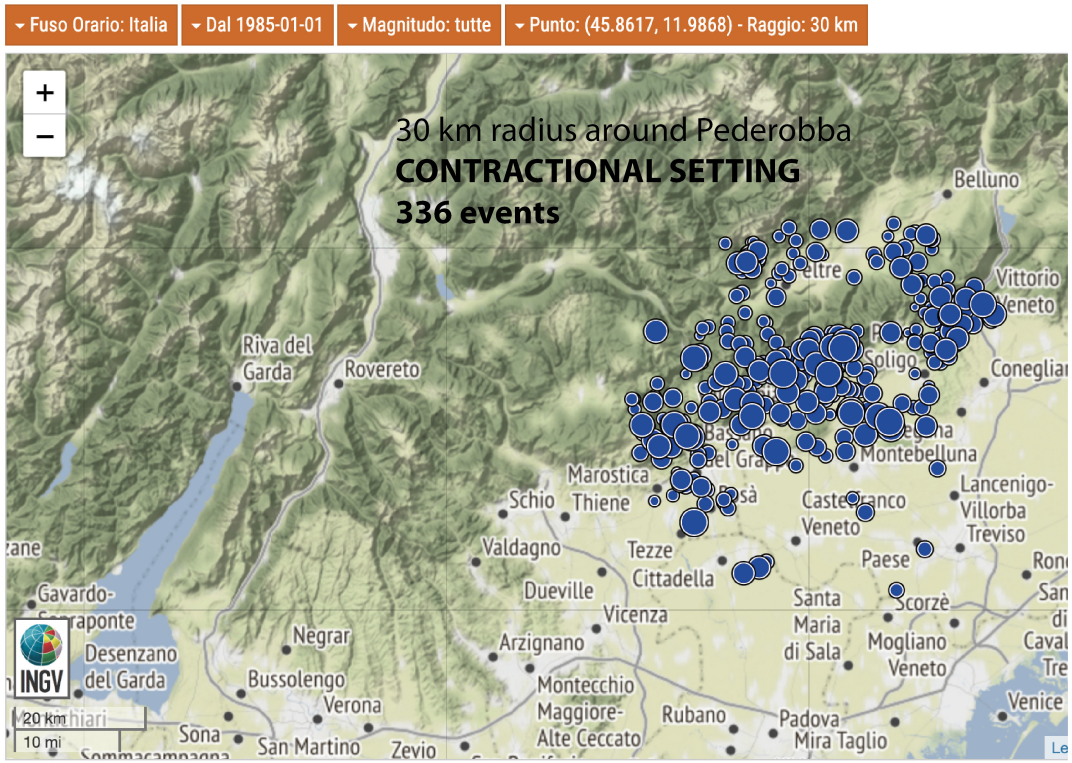

Earthquakes since January 1st 1985

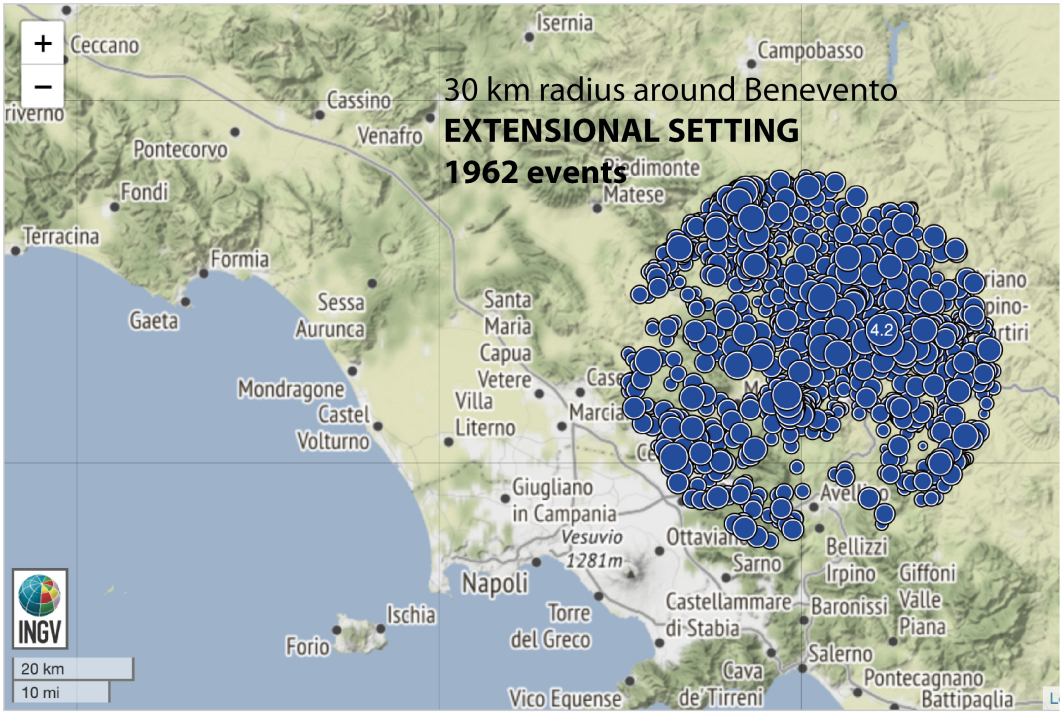

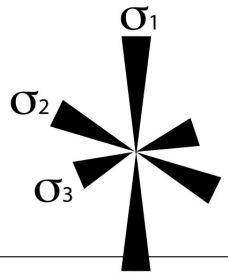

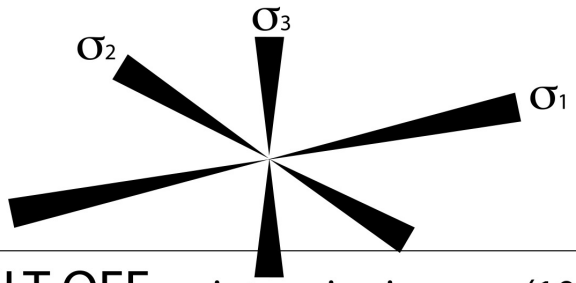

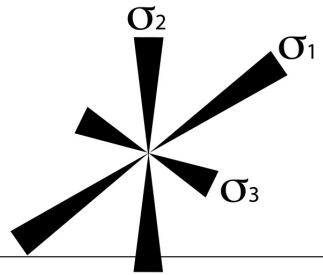

FAULT OFF - interseismic creep ($10^{9\text{-}10}$s)

normal

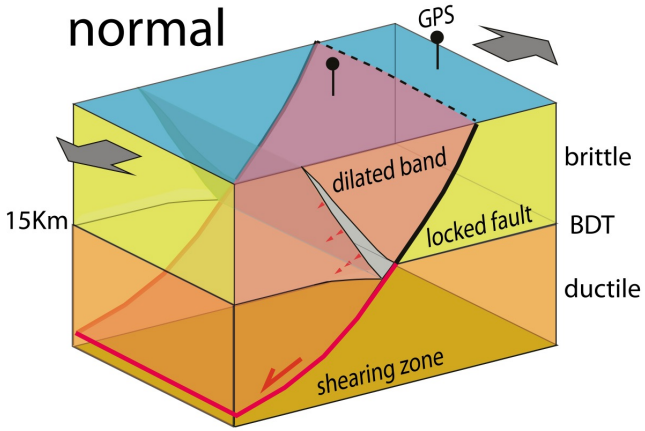

thrust

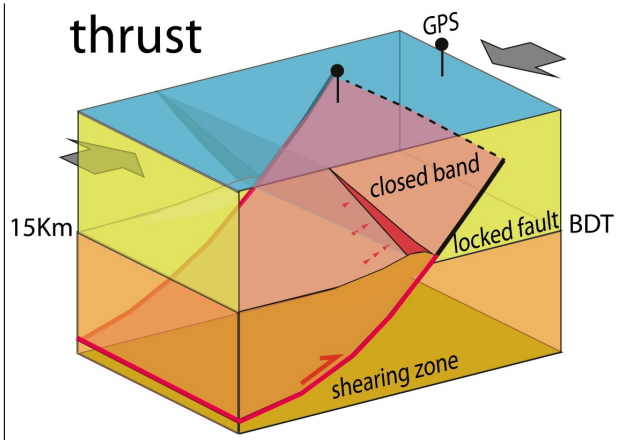

strike-slip

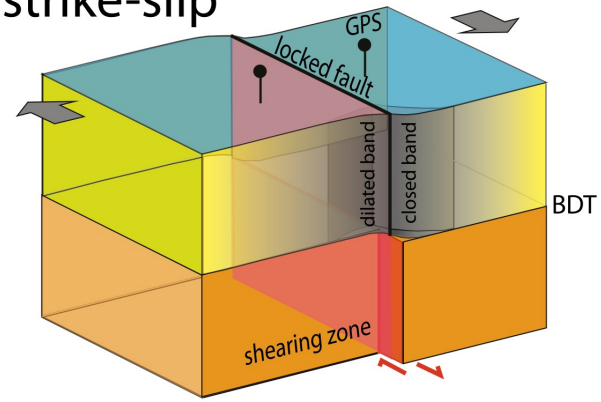

FAULT ON - coseismic creep (10^{2}s)

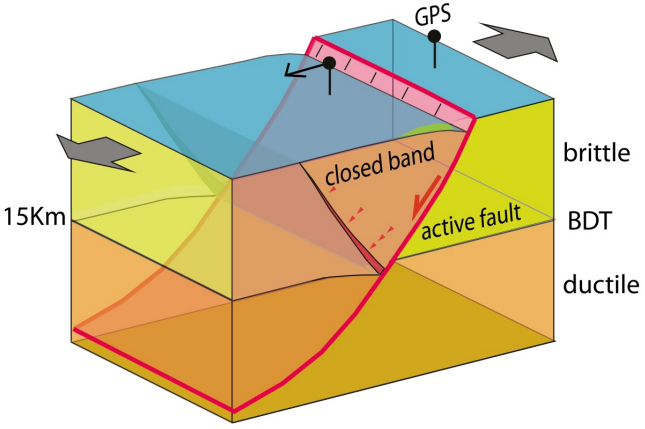

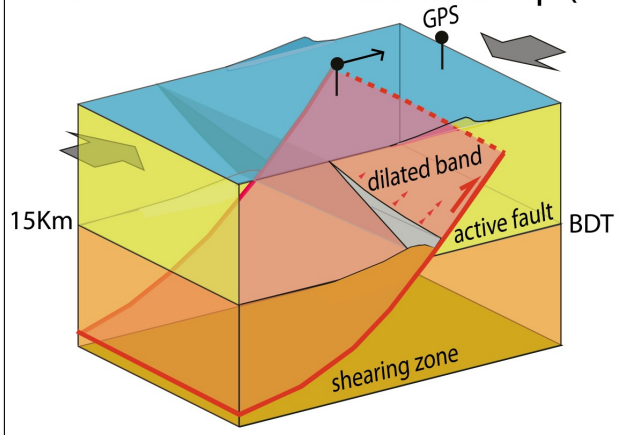

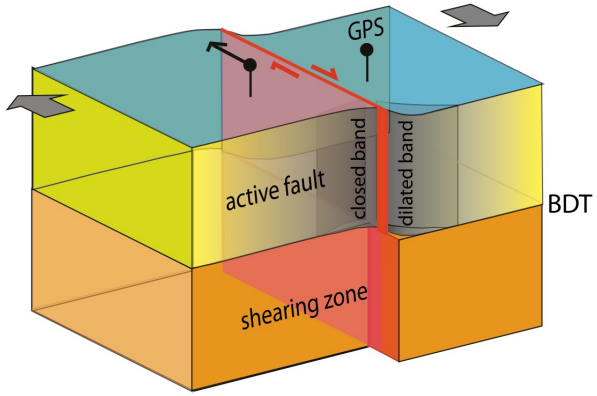

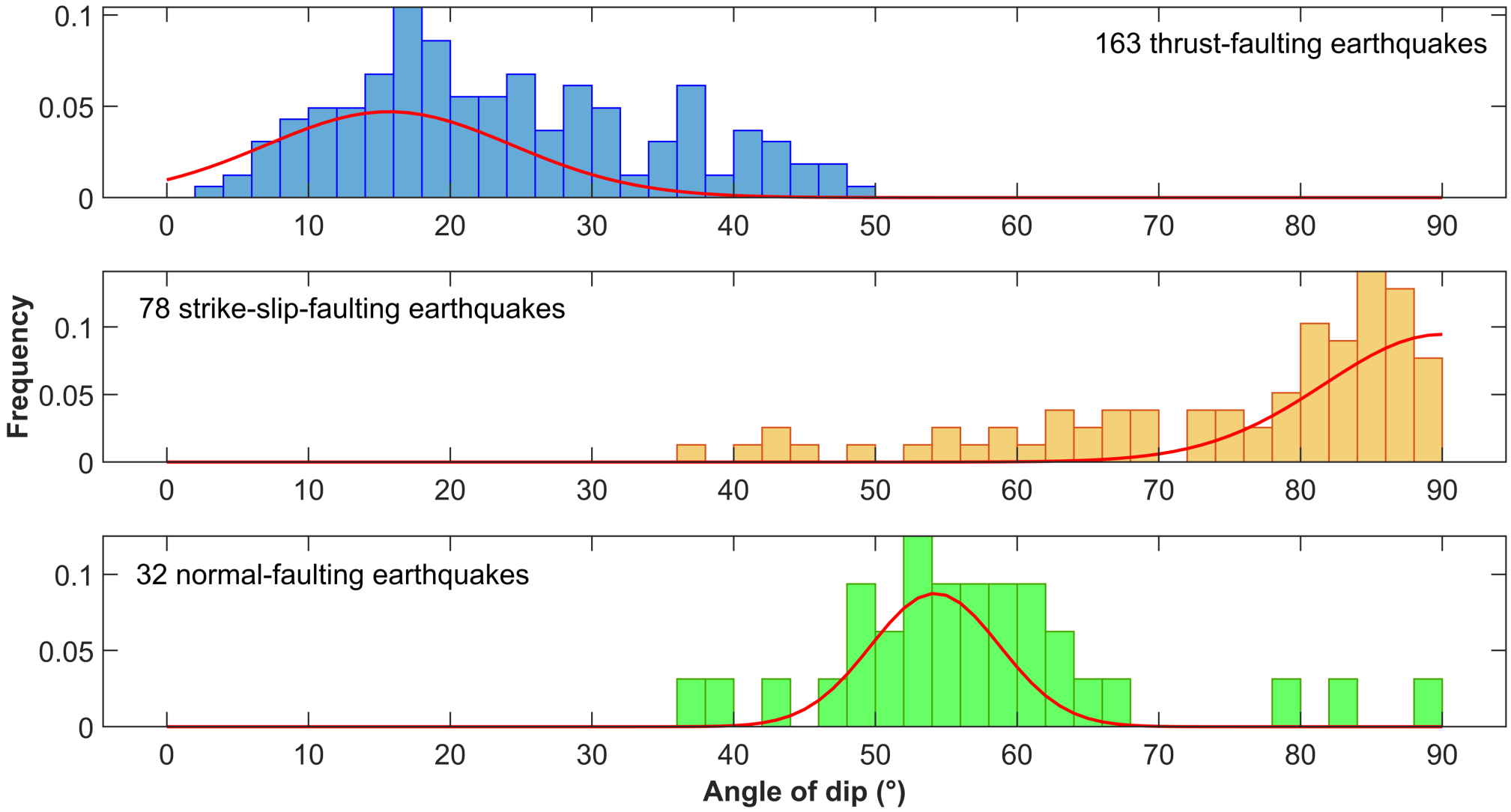
163 thrust-faulting earthquakes
78 strike-slip-faulting earthquakes
32 normal-faulting earthquakes
Frequency
0.1
0.05
0
0
10
20
30
40
50
60
70
80
90
Angle of dip (°)

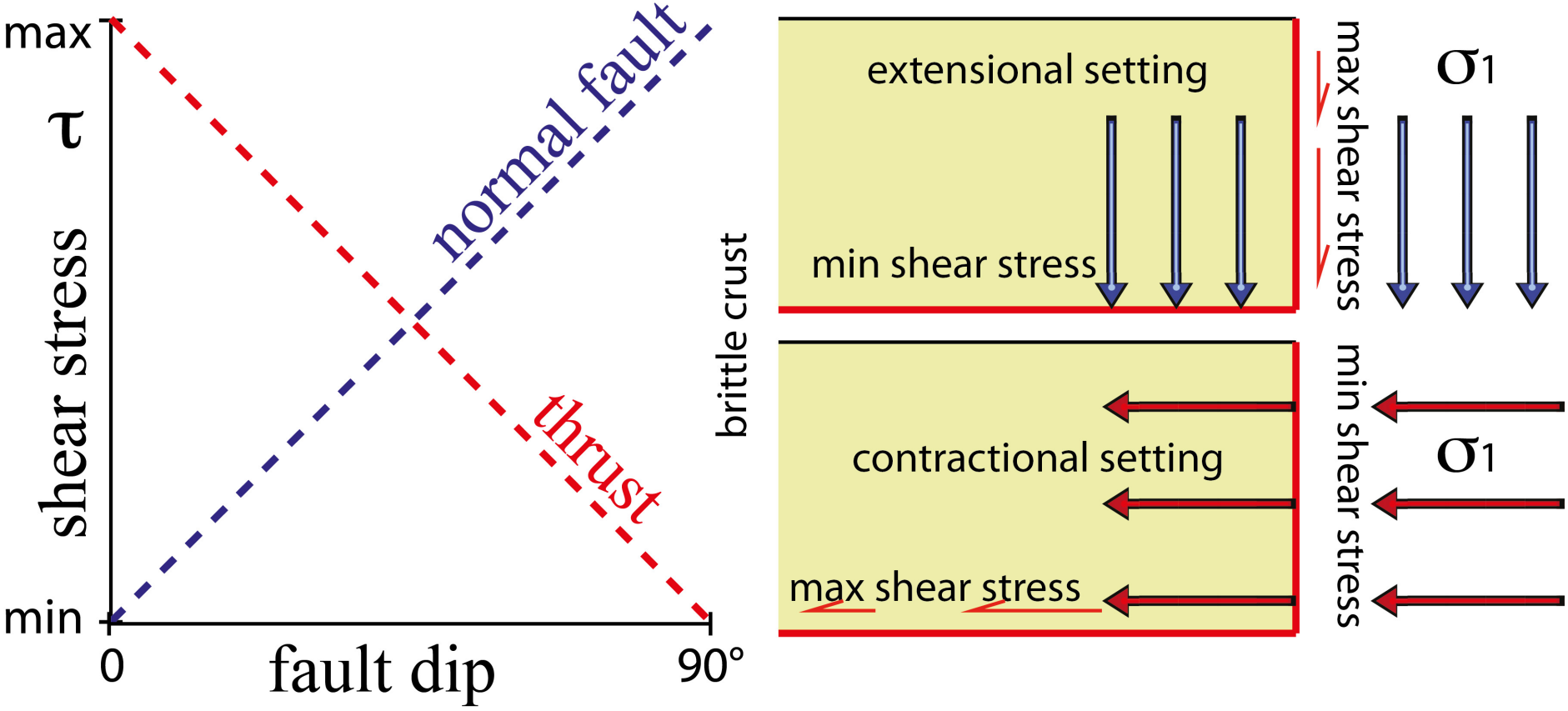
max
τ
shear stress
min
0
fault dip
90°
normal fault
thrust
brittle crust
extensional setting
min shear stress
max shear stress
σ1
contractional setting
max shear stress
min shear stress
σ1

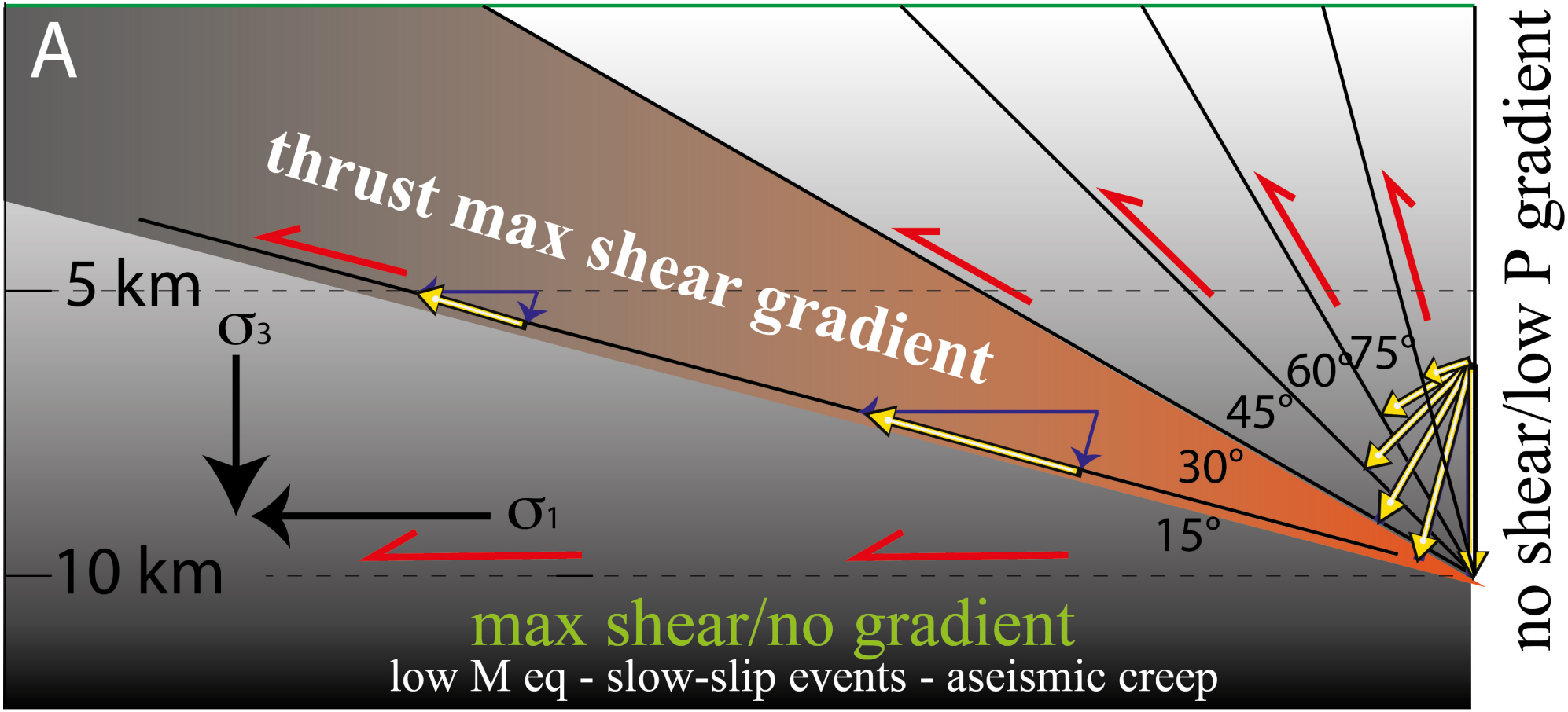
A
thrust max shear gradient
5 km
σ3
σ1
10 km
15°
30°
45°
60°
75°
max shear/no gradient
low M eq - slow-slip events - aseismic creep
no shear/low P gradient

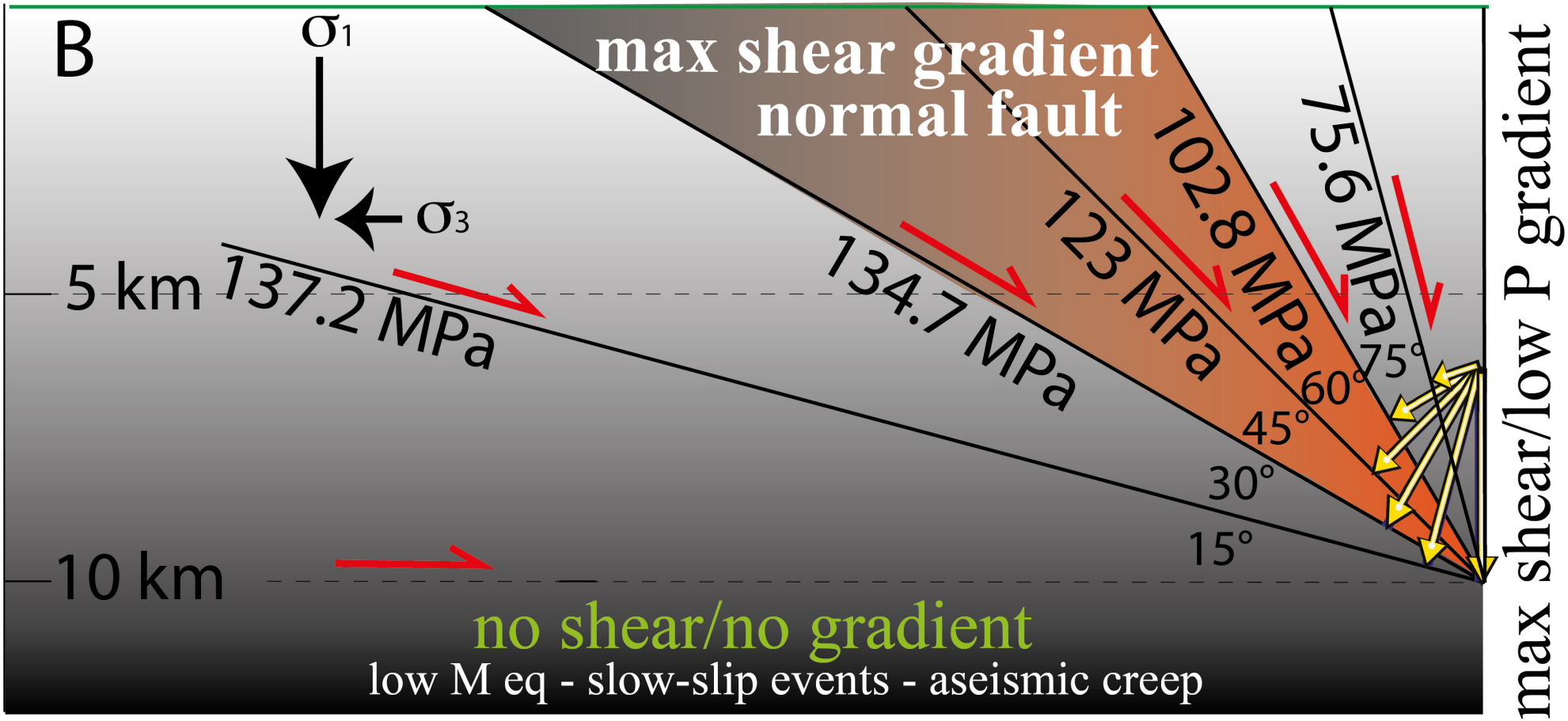
B
σ1
σ3
max shear gradient
normal fault
102.8 MPa
75.6 MPa
123 MPa
134.7 MPa
137.2 MPa
75°
60°
45°
30°
15°
5 km
10 km
no shear/no gradient
low M eq - slow-slip events - aseismic creep
max shear/low P gradient

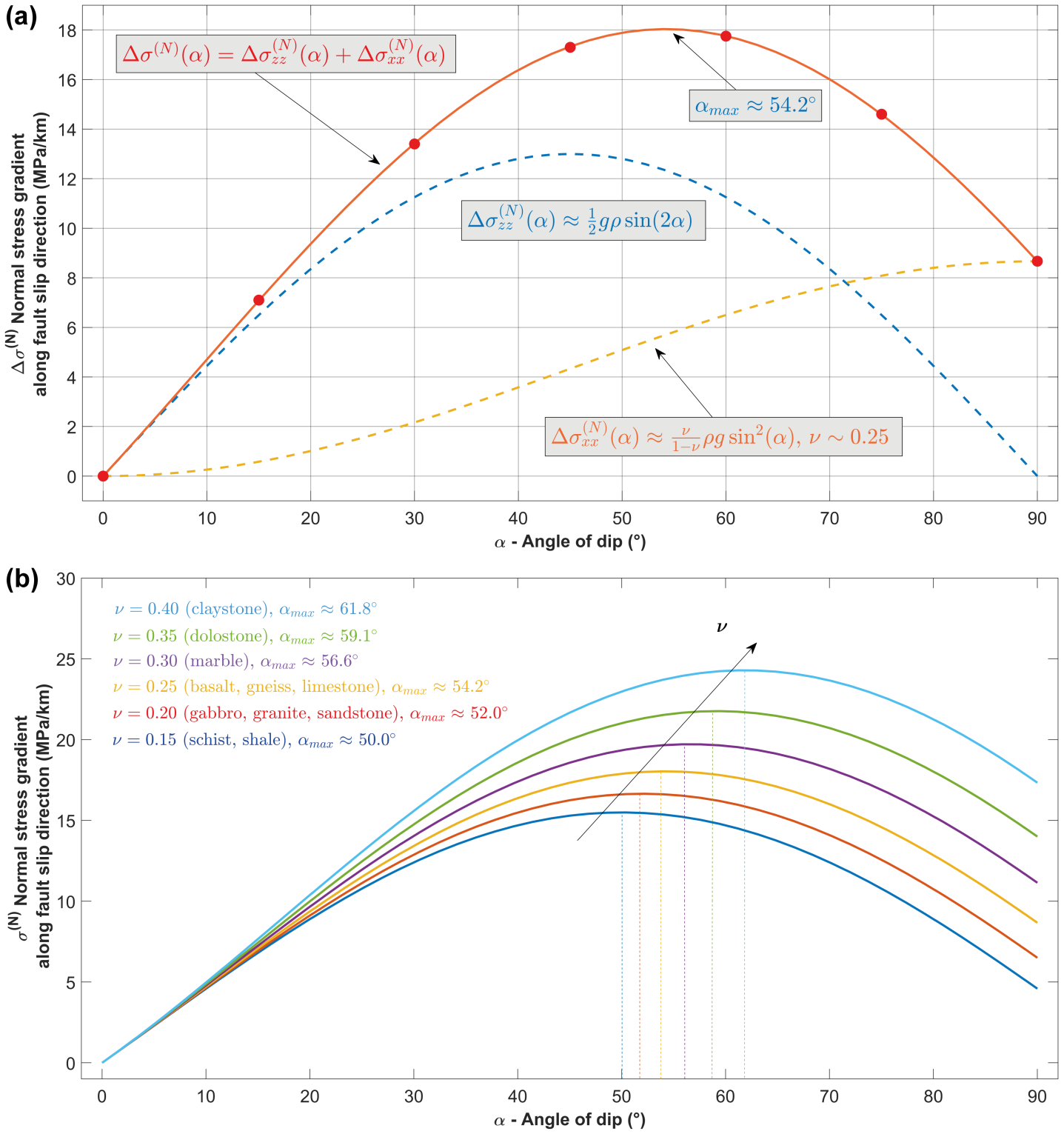
(a)
$\Delta\sigma^{(N)}(\alpha) = \Delta\sigma_{zz}^{(N)}(\alpha) + \Delta\sigma_{xx}^{(N)}(\alpha)$
$\alpha_{max} \approx 54.2°$
$\Delta\sigma_{zz}^{(N)}(\alpha) \approx \frac{1}{2} g\rho \sin(2\alpha)$
$\Delta\sigma_{xx}^{(N)}(\alpha) \approx \frac{\nu}{1-\nu} \rho g \sin^2(\alpha),\ \nu \sim 0.25$
$\Delta\sigma^{(N)}$ Normal stress gradient along fault slip direction (MPa/km)
α - Angle of dip (°)
(b)
$\nu = 0.40$ (claystone), $\alpha_{max} \approx 61.8°$
$\nu = 0.35$ (dolostone), $\alpha_{max} \approx 59.1°$
$\nu = 0.30$ (marble), $\alpha_{max} \approx 56.6°$
$\nu = 0.25$ (basalt, gneiss, limestone), $\alpha_{max} \approx 54.2°$
$\nu = 0.20$ (gabbro, granite, sandstone), $\alpha_{max} \approx 52.0°$
$\nu = 0.15$ (schist, shale), $\alpha_{max} \approx 50.0°$
ν
$\sigma^{(N)}$ Normal stress gradient along fault slip direction (MPa/km)
α - Angle of dip (°)

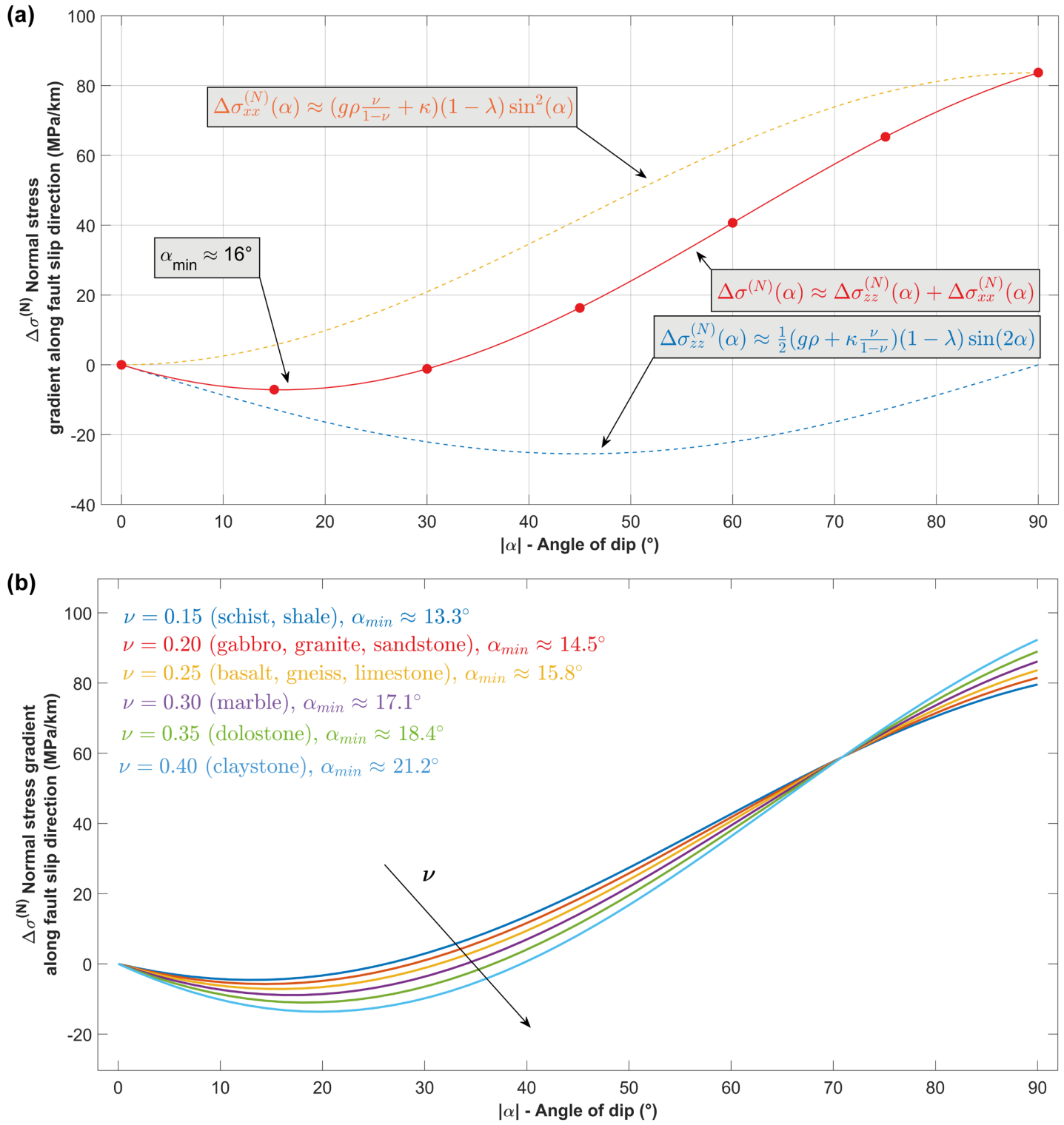
(a)
100
80
60
40
20
0
-20
-40
0
10
20
30
40
50
60
70
80
90
$\Delta\sigma^{(N)}$ Normal stress
gradient along fault slip direction (MPa/km)
|α| - Angle of dip (°)
$\Delta\sigma_{xx}^{(N)}(\alpha) \approx (g\rho\frac{\nu}{1-\nu} + \kappa)(1-\lambda)\sin^2(\alpha)$
$\alpha_{min} \approx 16°$
$\Delta\sigma^{(N)}(\alpha) \approx \Delta\sigma_{zz}^{(N)}(\alpha) + \Delta\sigma_{xx}^{(N)}(\alpha)$
$\Delta\sigma_{zz}^{(N)}(\alpha) \approx \frac{1}{2}(g\rho + \kappa\frac{\nu}{1-\nu})(1-\lambda)\sin(2\alpha)$
(b)
$\nu = 0.15$ (schist, shale), $\alpha_{min} \approx 13.3°$
$\nu = 0.20$ (gabbro, granite, sandstone), $\alpha_{min} \approx 14.5°$
$\nu = 0.25$ (basalt, gneiss, limestone), $\alpha_{min} \approx 15.8°$
$\nu = 0.30$ (marble), $\alpha_{min} \approx 17.1°$
$\nu = 0.35$ (dolostone), $\alpha_{min} \approx 18.4°$
$\nu = 0.40$ (claystone), $\alpha_{min} \approx 21.2°$
ν
100
80
60
40
20
0
-20
0
10
20
30
40
50
60
70
80
90
$\Delta\sigma^{(N)}$ Normal stress gradient
along fault slip direction (MPa/km)
|α| - Angle of dip (°)

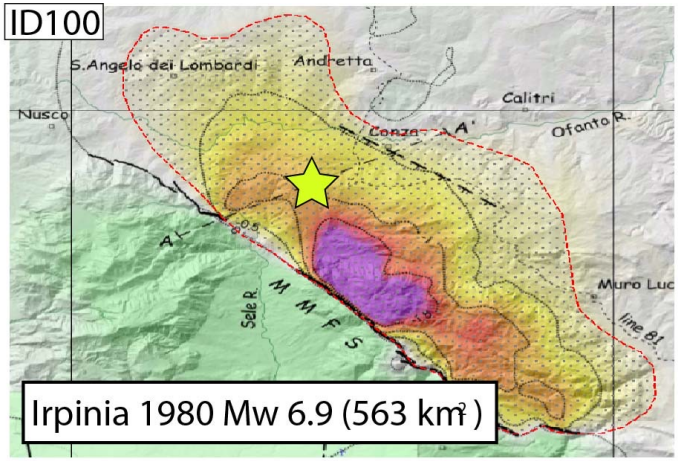

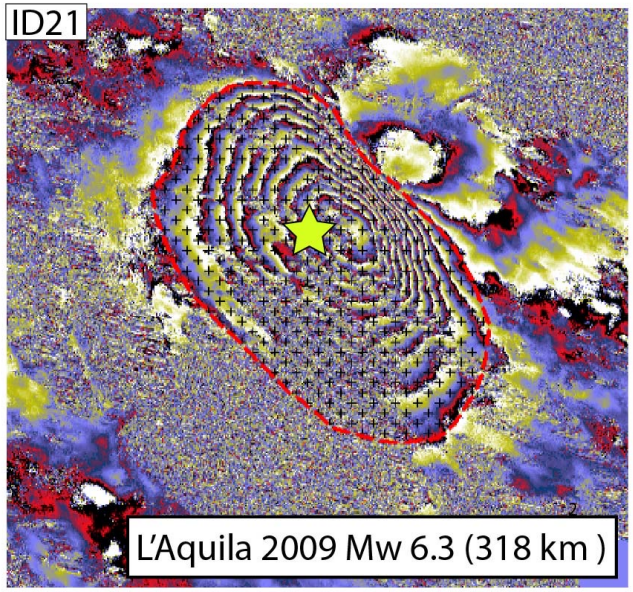

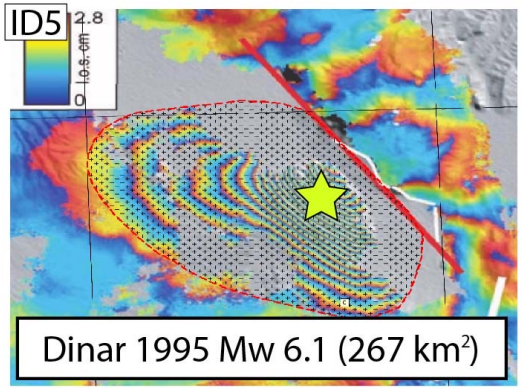

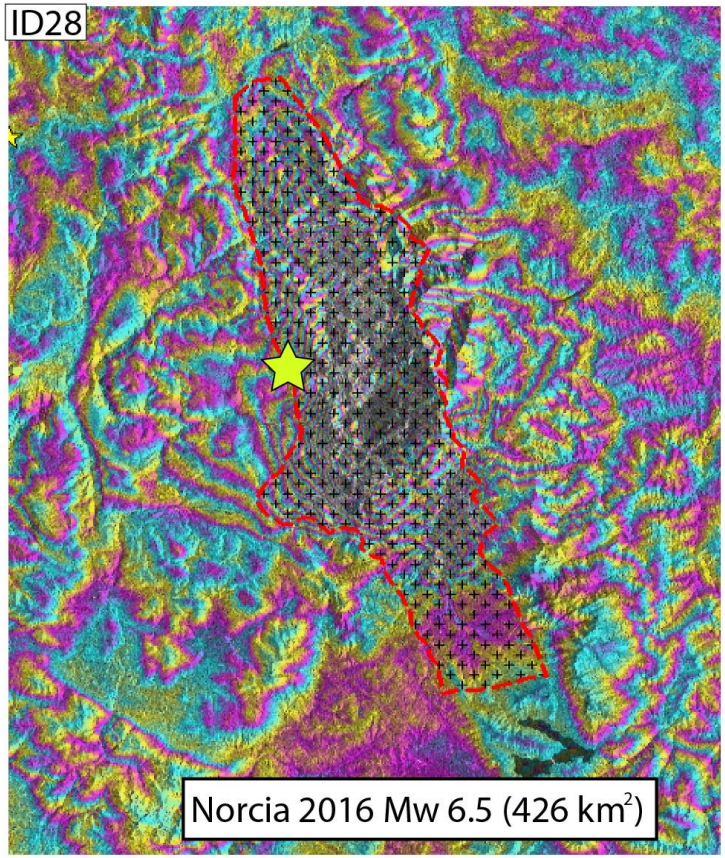

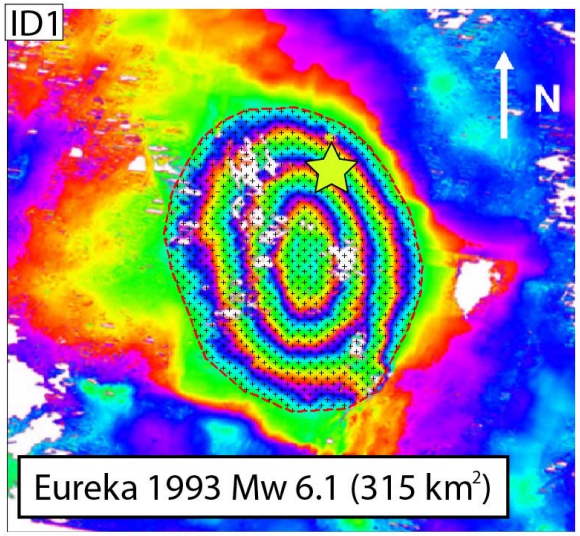

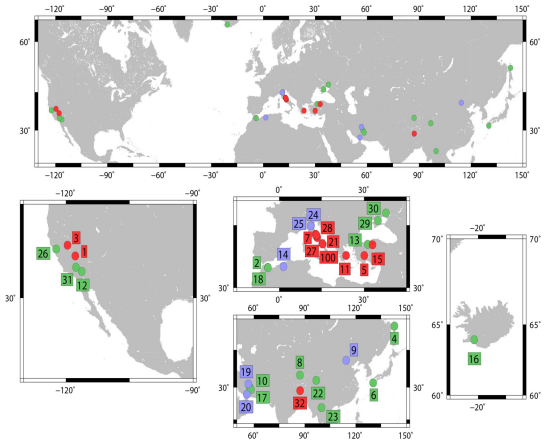

Petricca et al. 2021 ESR

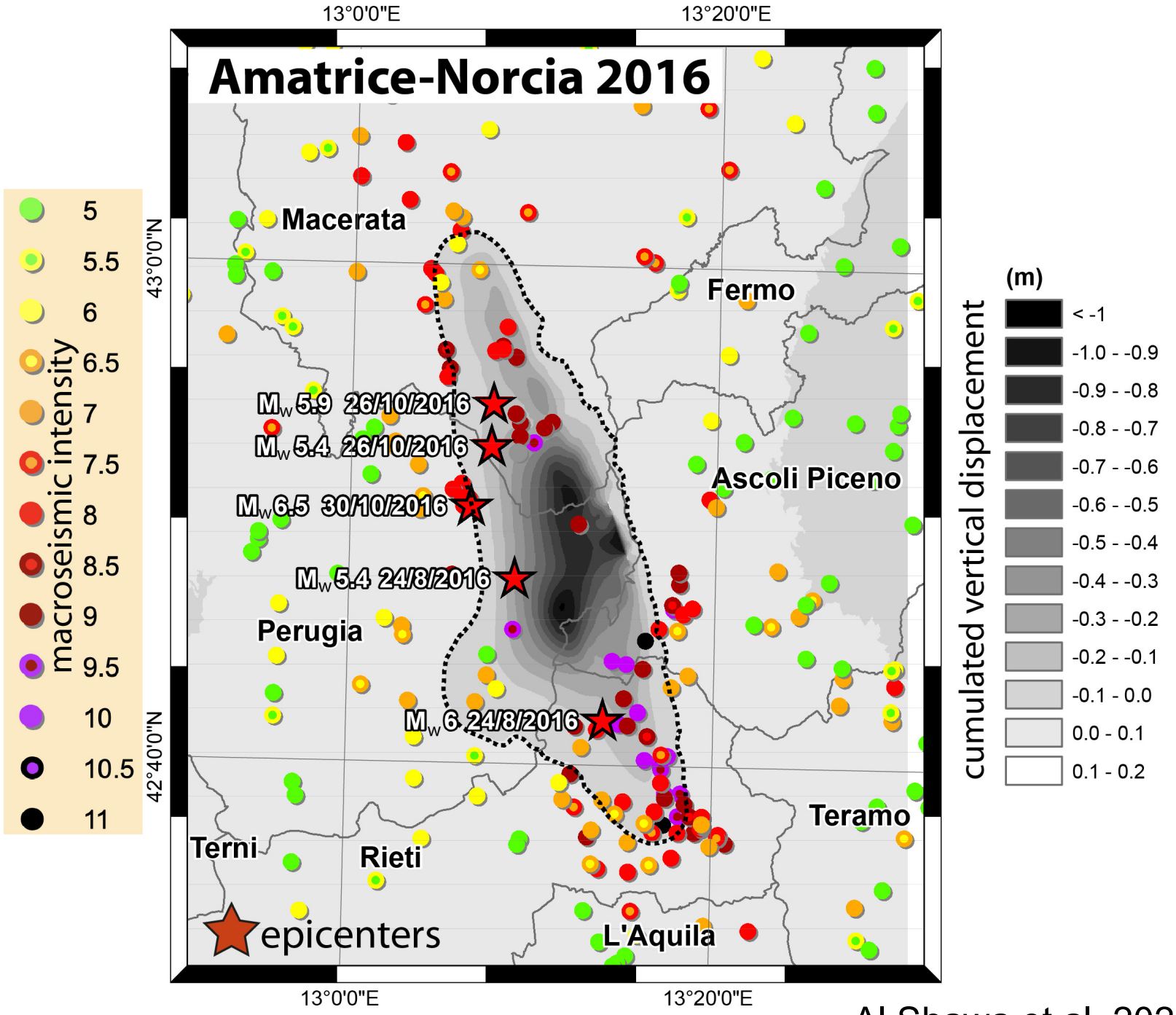

Al Shawa et al. 2021 Eng. Geol.

Mariani & Pugi 2019 Ingeni

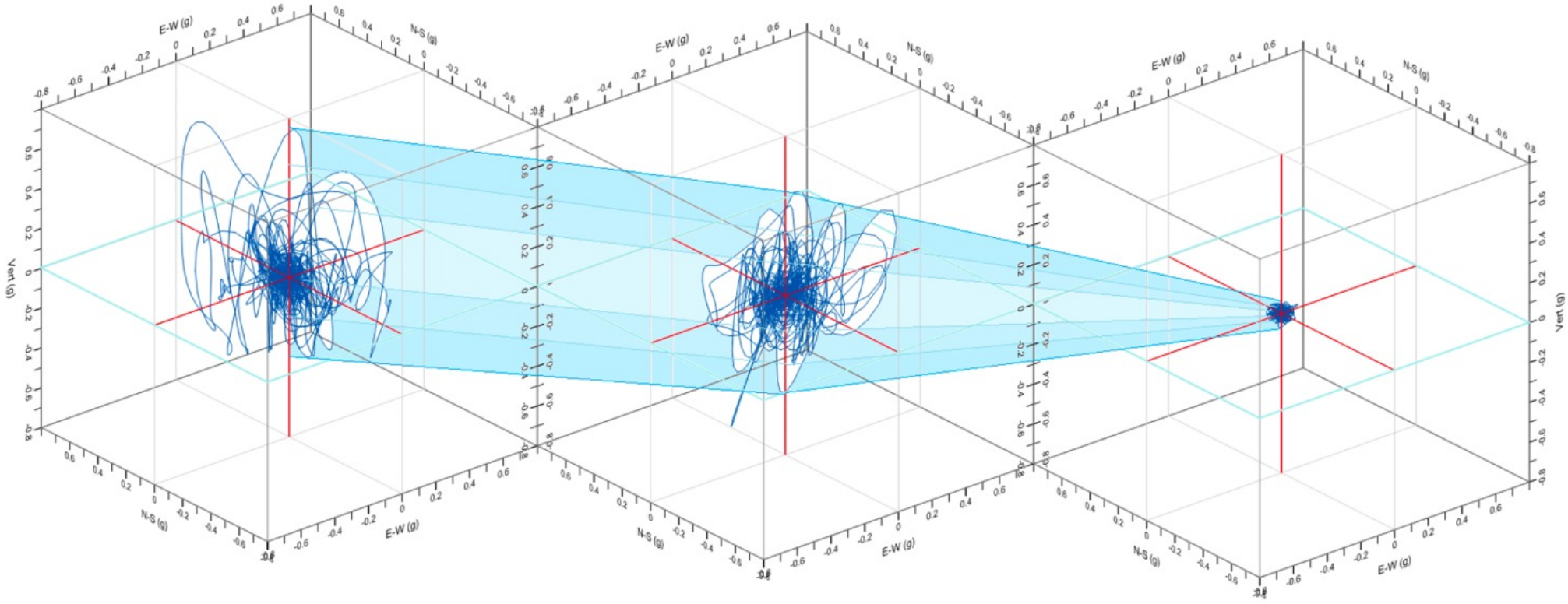

ITALIA CENTRALE, 30.10.2016

CASTELLUCCIO DI NORCIA CLO: 7.8 km → ACCUMULI ACC: 18.6 km → FABRIANO FBR: 59.1 km

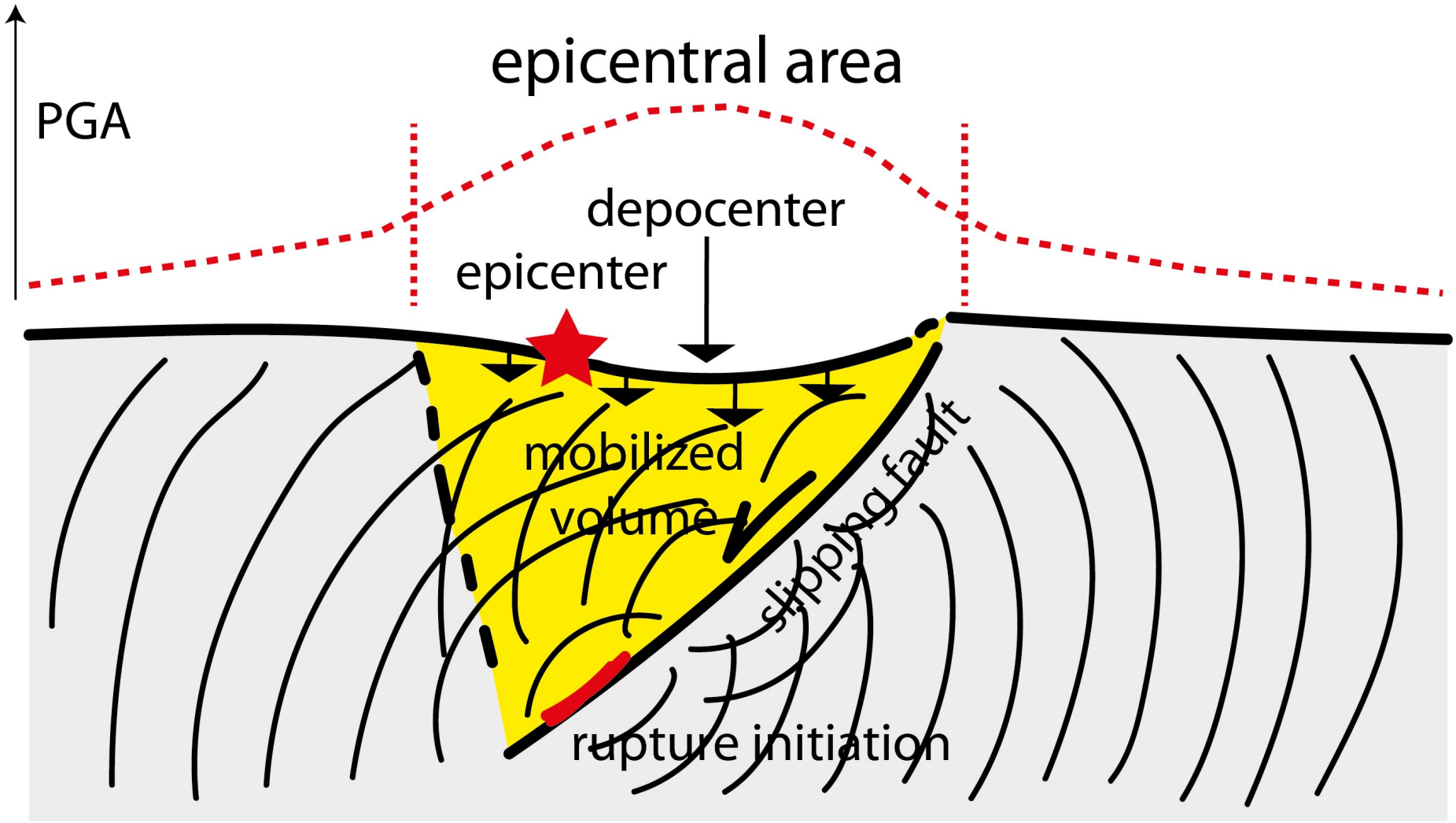

Al Shawa et al. 2021 Eng. Geol.

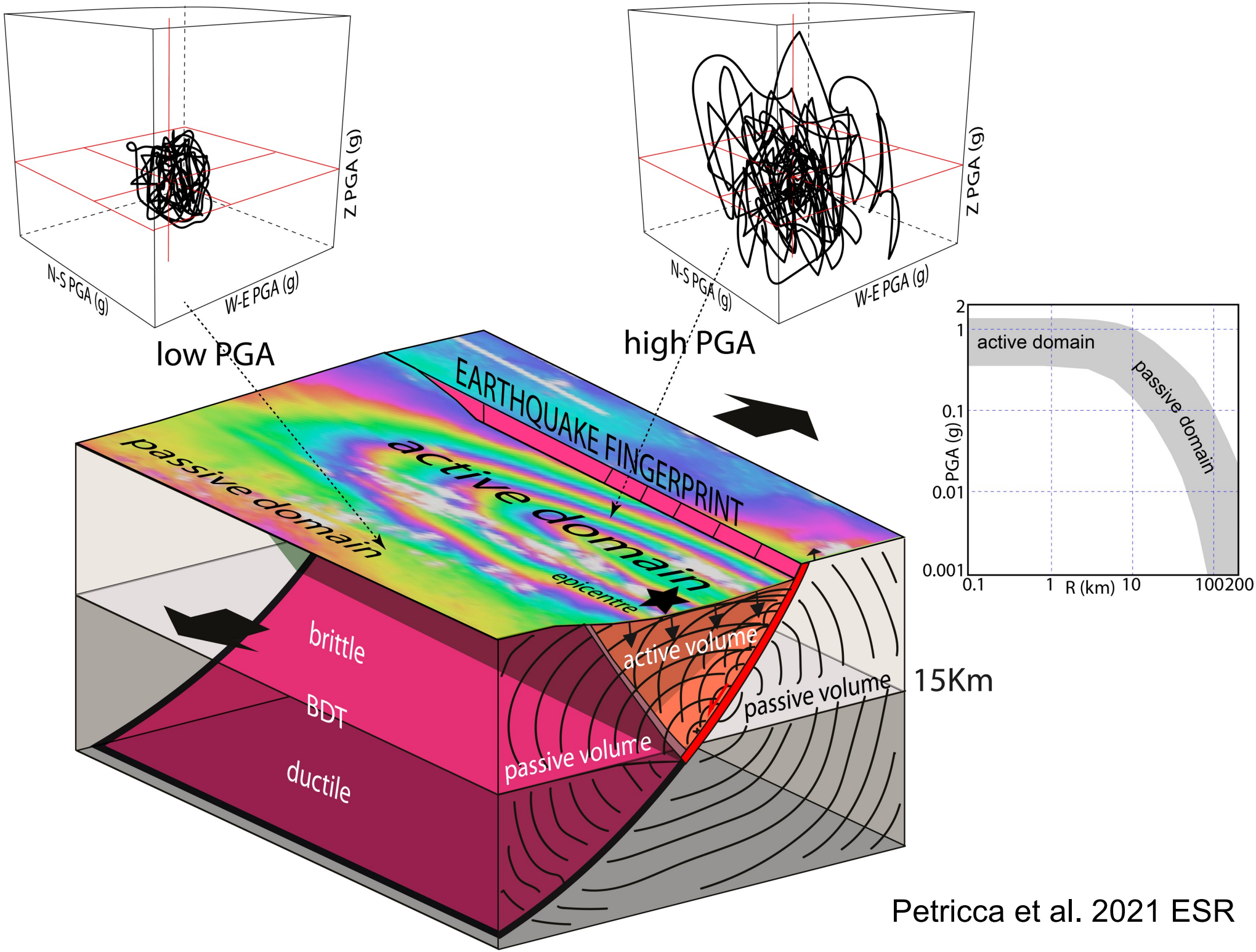

Petricca et al. 2021 ESR

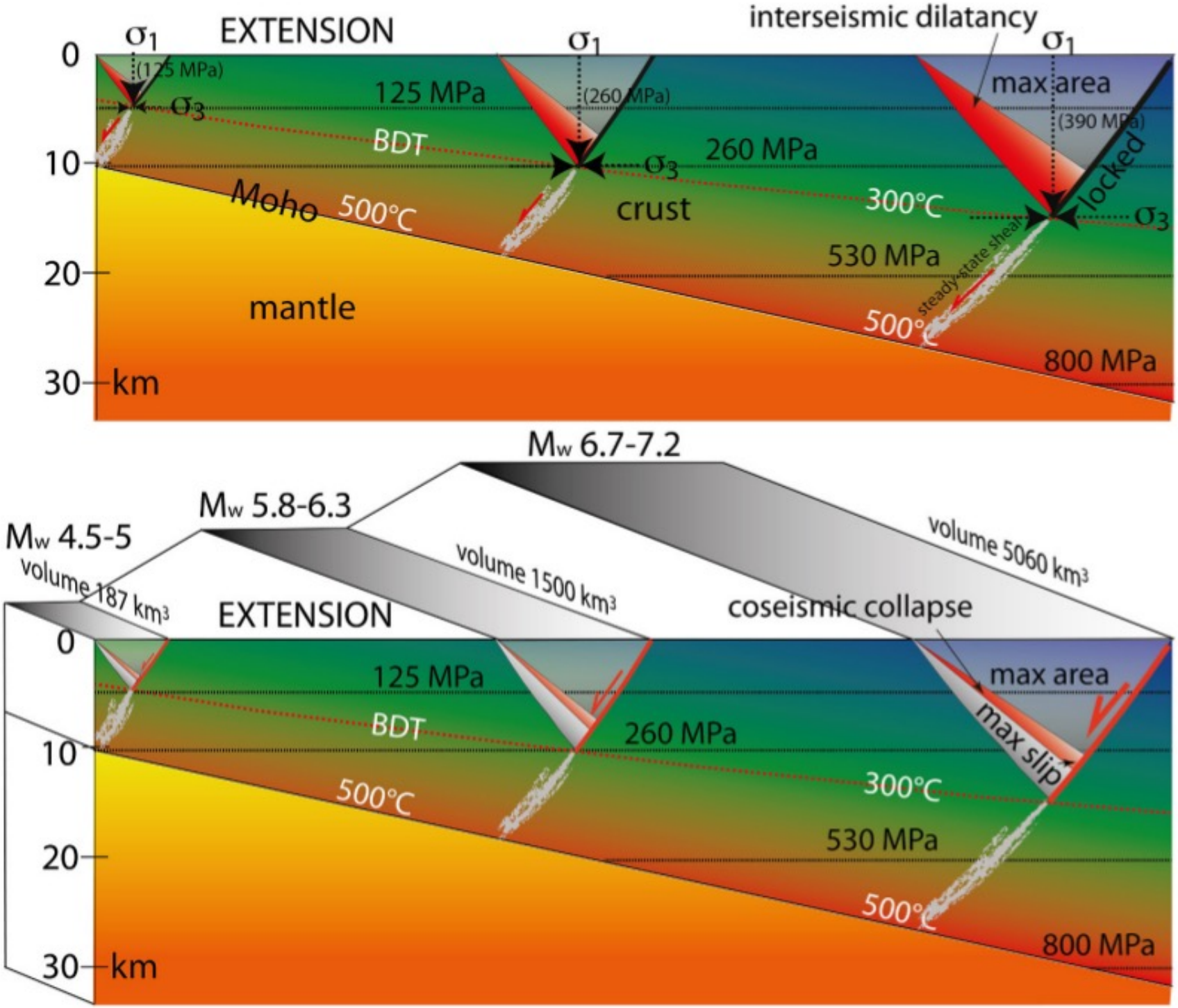

Bignami et *al.*, 2020

Mw normal –> Choy and Boatwright (1995)

Mw thrust –> Bath and Duda (1964)

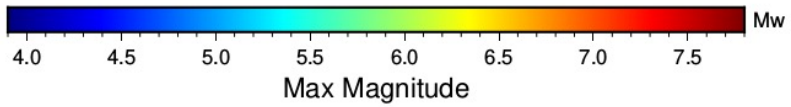

Fault dip: thrust=30 normal=45

W/z ratio: thrust=3 normal=2

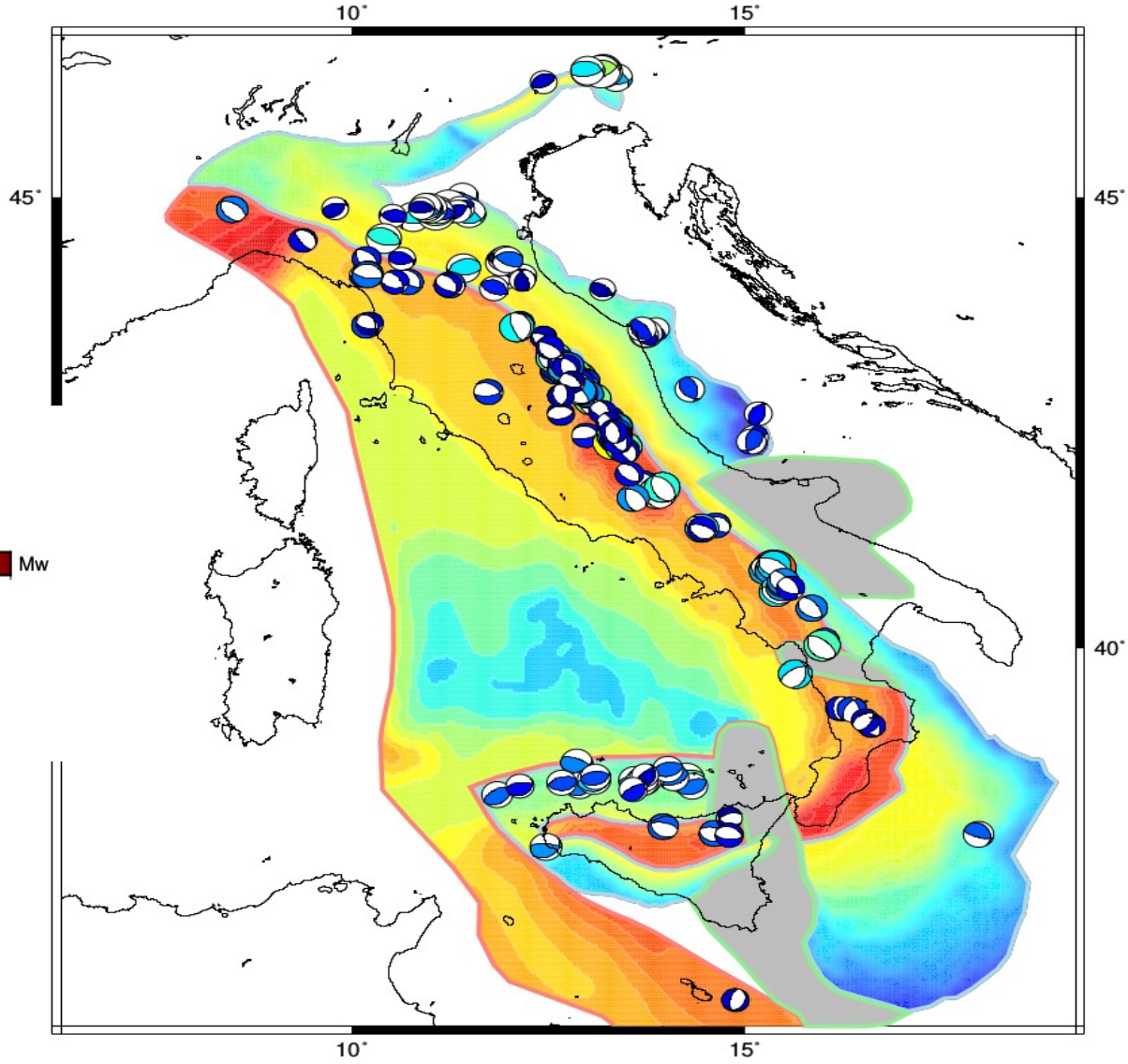

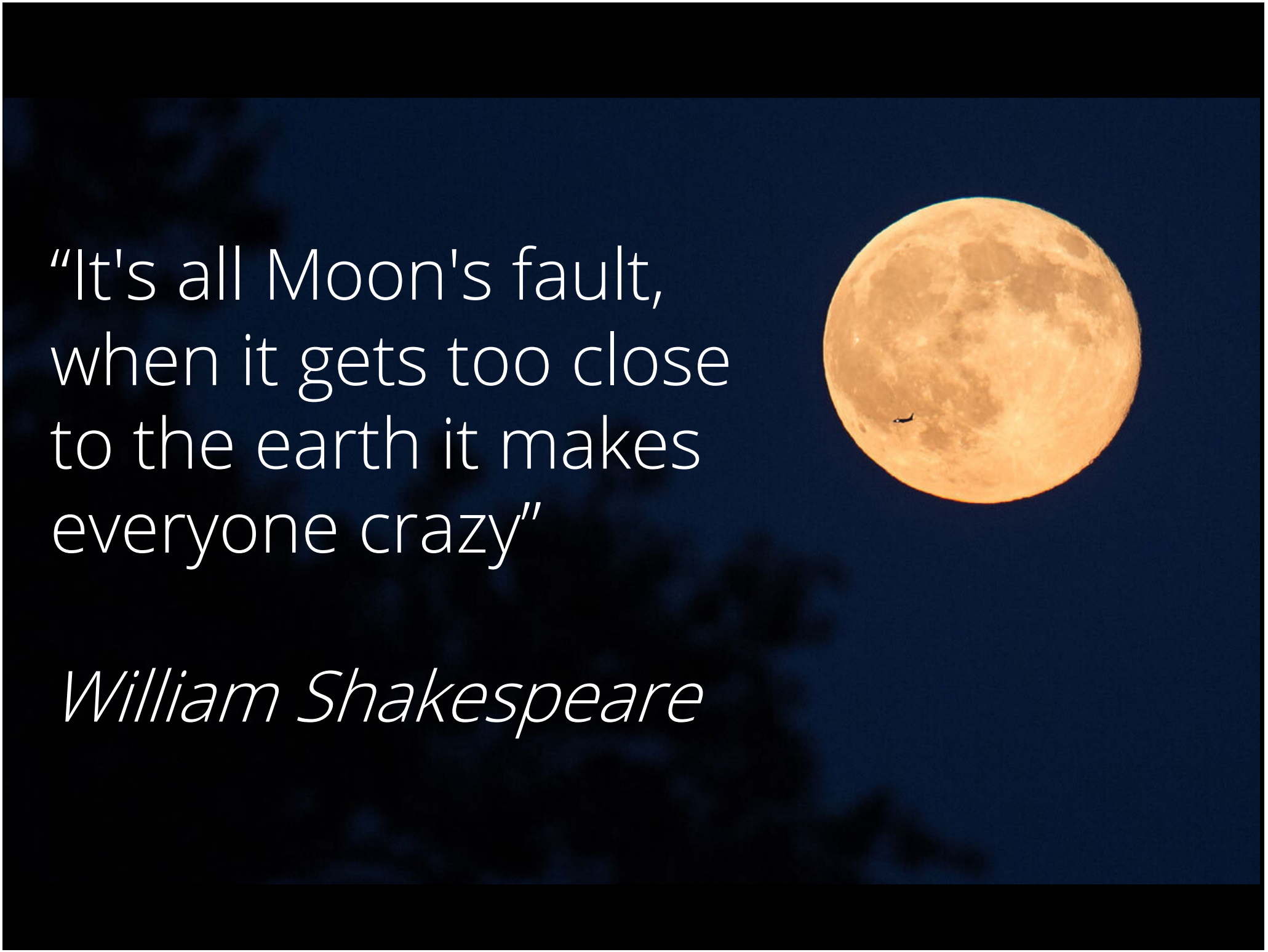
“It's all Moon's fault, when it gets too close to the earth it makes everyone crazy”
William Shakespeare

Piero: an hyperbolic gradient